Alternative Technologies for the Production of High Carbon Ferromanganese: A Techno-economic Evaluation

by

Ntokozo Aphelele Sithole

Thesis presented in fulfilment of the requirements for the degree of Master of Engineering (Engineering Management) in the Faculty of Engineering at Stellenbosch University

Supervisor: Dr. Wouter G. Bam

Co-supervisor: Dr. Joalet D. Steenkamp

December 2020

Declaration

By submitting this thesis electronically, I declare that the entirety of the work contained therein is my own, original work, that I am the sole author thereof (save to the extent explicitly otherwise stated), that reproduction and publication thereof by Stellenbosch University will not infringe any third party rights and that I have not previously in its entirety or in part submitted it for obtaining any qualification.

Date: 31 August 2020

Abstract

The manganese resource (land-based) in South Africa is currently the largest, accounting for 75% of the global resource. Ore exporting has increased from 50% of the total sales in 1997 to around 85% in 2016 and the trend seems to be increasing (Directorate Mineral Economics, 2017). Furthermore, manganese smelters have either reduced capacity or shut down completely due to operational costs. Van Zyl (2017) explored the various aspects that limit growth in the mineral value chain (Van Zyl, 2017). One of the barriers that were identified in the beneficiation of manganese is the high cost of electricity required for ore smelting. Ferromanganese in South Africa is produced using Submerged-arc furnace (SAF) technology which relies heavily on electricity during production

The current study aimed to identify and compare alternative furnace technologies that can or could produce HCFeMn. The main criterion is to substantially reduce the reliance on electricity during production. The objective of the study was to make use of a literature review in the ferromanganese industry and the ironmaking industry to identify suitable alternative furnace technologies. Alternative technologies will then be compared using a techno-economic evaluation to assess the financial performance of each furnace when compared to the current technology the SAF. The evaluation consisted of mass and energy balances of the HCFeMn process and economic models. Furthermore, the sensitivity of the economic model results in response to deviations in CAPEX and OPEX estimates was investigated.

The SAF was compared to the BF that was identified in the ferromanganese industry and the COREX® that was identified in the ironmaking industry. Both technologies commercially produce FeMn and/or pig iron. The BF relies on coke and the COREX® relies on coal. Mass and energy balance model results indicate that SAF recovers the least amount of manganese at 82.8% and the COREX® recovers the most at 84.1%. Fixed capital costs make the SAF the most attractive, the COREX® and BF cost 35% and 37% more, respectively. Annual production costs per ton of alloy for the COREX® on average over the project life are over 26% lower than both furnaces. The COREX® had the highest NPV (R 11 430.46) and IRR (33.11%) with the lowest discounted payback period of 7 years. The SAF NPV was 33% lower, IRR 5.04% lower, and DPBP 1 year longer than the COREX®. The BF performed the worst financially. In all three scenarios, the COREX® yielded a positive NPV, meaning the probability of a 15% return is 1. Furthermore, manganese recoveries as low as 79.7% still yield an NPV 38% higher than the SAF base case.

Sourcing of technical and economic data was a challenge, the BF model had outdated HCFeMn process data available. The COREX® has no data published for the HCFeMn process, data can be obtained from thermochemical modelling, laboratory or pilot plant scale tests.

Process data specific for the COREX® could improve the quality of the model outcomes of the. Collaborations with Mintek and industry partners are recommended to obtain better quality technical and economic data.

Opsomming

Die mangaanhulpbron in Suid-Afrika (landgebaseerde) is volgens berigte die grootste en is verantwoordelik vir 75% van die wêreld se bronne. Ertsuitvoere het toegeneem van 50% van totale produksie in 1997 tot ongeveer 85% in 2016 en dit blyk asof die neiging toeneem (Directorate Mineral Economics, 2017). Verder het die smelters met mangaanlegerings óf die kapasiteit verlaag óf, weens die toename in bedryfskoste, heeltemal gesluit. Van Zyl (2017) het die verskillende aspekte ondersoek wat groei in die minerale waardeketting beperk. Een van die hindernisse wat identifiseer is vir die veredeling van mangaan, is die koste van elektrisiteit wat benodig word vir die smelt van erts. Ferromangaanlegerings in Suid-Afrika word vervaardig met behulp van dompelboog-oondtegnologie wat tydens produksie baie afhanklik is van elektrisiteit.

Die doel van die huidige studie was om alternatiewe oondtegnologieë te identifiseer en te vergelyk wat FeMn moontlik kan produseer. Die belangrikste kriteria is om die afhanklikheid van elektrisiteit tydens produksie aansienlik te verminder. Die doel van die studie was om gebruik te maak van 'n literatuuroorsig van die ferromangaan-industrie en die ysterbedryf om geskikte alternatiewe oondtegnologieë te identifiseer. Alternatiewe tegnologieë word dan met behulp van 'n tegno-ekonomiese evaluering vergelyk om die finansiële prestasie van elke oond te beoordeel in vergelyking met die huidige dompelboogoond tegnologie. Die evaluering het bestaan uit massa- en energiebalanse van die proses vir die produksie van hoëkoolstof ferromangaanlegerings, en 'n ekonomiese model.

Die dompelboogoond is vergelyk met die hoogoond wat in die ferromangaan-industrie geïdentifiseer is, en die COREX® wat in die ysterbedryf geïdentifiseer is. Beide tegnologieë produseer ferromangaanleregings en/of ruyster. Die hoogoond maak staat op kooks en die COREX® maak staat op steenkool. Die resultate van die massa- en energiebalansmodel dui aan dat die dompelboogoond die kleinste hoeveelheid mangaan op 82.8% herwin en dat die COREX® die meeste op 84.1%. Kapitaalkoste maak die dompelboogoond die aantreklikste; die COREX® en hoogoond kos onderskeidelik 35% en 37% meer. Die jaarlikse produksiekoste per ton legering vir die COREX® is gemiddeld 26% laer as vir die ander twee oonde. Die COREX® die hoogste netto huidigewaarde (R 11 430.46) en interne rendement (33.11%) met die laagste terugbetalingstydperk van 7 jaar. Die dompelboogoond se netto huidigewaarde was 33% laer, interne rendement 5.04% laer en met ‘n terugbetalingstydperk 1 jaar langer as dié van die COREX®. Die hoogoond het finansieël die slegste gevaar. Die COREX® 'n positiewe NPV gelewer in alle scenario's, wat impliseer dat die waarskynlikheid van 15% opbrengs 1 is. Verder lewer mangaan verhaling so laag as 79.7% steeds 'n netto huidigewaarde wat 38% hoër is as die dompelboogoond op die basis geval.

Die verkrying van tegniese en ekonomiese insette tot hierdie modelle was 'n uitdaging. Die hoogoond-model het gebruik gemaak van effens verouderde prosesdata vir die produksie van hoëkoolstof ferromangaanlegerings. Die COREX® het geen data wat vir die produksie van hoëkoolstof ferromangaanlegerings-publiseer is nie. Die verkryging van hierdie data deur middel van termodinamiese modellering, laboratorium- of loodsaanlegte, kan die kwaliteit van die modeluitkomste verbeter. Samewerking tussen Mintek en bedrysvennote word aanbeveel om tegniese en ekonomiese data van beter gehalte te bekom.

Acknowledgements

Through this piece of work I have not only gone through an academic journey but a personal and vocational journey as well. I feel honoured to express my immense gratitude to the individuals and institutions that contributed to the successful journey. First and foremost, I would like to thank God for consistently reminding me to be teachable in all situations whether good or bad and strive to be the best version of myself. I would like to thank:

- My Stellenbosch University supervisor, Dr. Wouter Bam, for his consistent support and guidance in getting this project completed. Having you as a study leader made the process very manageable
- Mintek co-supervisor, Dr. Joalet Steenkamp, for being a valuable source of ideas, resources, and opportunities. I got more than a qualification from this project.
- Mintek represented by my manager, Isabel Geldenhuys, for the financial assistance which translated to believing in my capabilities as a young engineer.
- Mintek colleague, Angus Auchterlonie (retiree from MESU), for providing me with a significant amount of data I used in my calculations.
- Stellenbosch University postgraduate manager, Melinda Rust, for making the postgraduate system efficient enough for me to complete my studies remotely.
- Mintek colleague, Markus Erwee, for supporting me during my early phases of getting into modelling. I initially found it daunting, but the more I spoke to you the better my understanding became.
- Mintek former colleague, Kabikwa Bisaka, for sharing parts of his journey with me and how to gain different perspectives on seemingly challenging tasks.
- Daniel Bopape for taking the time to give me candid feedback and confidence in the calculations I have worked on for over 2 years.
- Family for always supporting me, my Mom (Nosipho Sithole), and Sister (Zamajobe Sithole) have never failed to be there when I needed them. My late Dad Thandabantu Sithole would be proud of our unity. Thank you for understanding why I had to be absent at times and I love you.
- Friends and colleagues who allowed me to go on endless monologues about my struggles and also became valuable sounding boards when I had a lot of decisions to sort through in my head.

Table of Contents

List of Figures

List of Tables

Abbreviations

Al_2O_3	Aluminium Oxide
BF	Blast Furnace
BFD	Block Flow Diagram
CaO	Calcium Oxide
CAPEX	Capital Expenditure
C	Carbon
CF	After Tax Cash Flow
CO_2	Carbon Dioxide
CO	Carbon Monoxide
D	Depreciation
DOF	Degrees of Freedom
DPBP	Discounted Pay Back Period
FBR	Fluidised Bed Reactor
FeO	Iron oxide
FeMn	Ferromanganese
FOB	Free On Board
FV	Future Value
GHG	Green House Gas
HCFeMn	High carbon ferromanganese
IRR	Internal Rate of Return
MgO	Magnesium oxide
Mn/Fe	Manganese to Iron mass ratio
MnO	Manganese Oxide
N_2	Nitrogen
NO_x	Nitrogen oxides
NPV	Net Present Value
O_2	Oxygen
OE	Operating Expenses
OPEX	Operational Expenditure
PFD	Process Flow Diagram
PV	Present Value
R	Revenue
SA	Sensitivity Analysis
SAF	Submerged Arc Furnace
SARS	South African Revenue Services
SiO_2	Silicon Oxide
SiMn	Silicomanganese
SR	Smelting Reduction
t	Tax
TM	Total Module
TRL	Technology Readiness Level

USD	United States Dollar
VOC	Volatile Organic Compounds
ZAR	South African Rand

Symbols

Symbol	Description	Units
$\boldsymbol{\delta}$	Secant method perturbation fraction	-
$\boldsymbol{\Delta \mathbf{q}}$	Simulated change in variable to estimate the sensitivity coefficient	-
Δw_i	Actual change in the variable of interest in sensitivity analysis	-
C_T	Calculated cost of equipment after cost factors are accounted	USD
C_0	Cost of equipment before cost factors are accounted	USD
C_1	Cost of equipment in reference year or capacity	USD
C_2	Calculated cost of equipment in current year or capacity	USD
f	Woods estimation method for cost factors	-
I_t	Cost index in current year	-
I_o	Cost index in reference year	-
L_1	Cost of labour in reference year	USD
L_2	Calculated cost of labour	USD
m_T	Total stream mass	kg
$\mathrm{N_d}$	Number of the degrees of freedom	-
$\mathrm{N_e}$	Number of independent variables in a system	-
$\mathrm{N_{sp}}$	Number of specified variables in a stream	-
$\mathrm{N_v}$	Number of variables in a system	-
n	Number of years	-
n_T	Total moles in stream	mole
P	Pressure of stream	atm
Q_1	Annual plant capacity of reference plant	-
Q_2	Annual plant capacity of plant under investigation	-
S_j	Sensitivity coefficient	-
T	Temperature of stream	℃
x_i	Mass fraction of solid stream	-
y_i	Mole fraction of gaseous stream	-
z_i	Secant method previously iterated value	-
z_{i+1}	Secant method next iteration value	-

Chapter 1

Introduction

1.1. Background

Ferromanganese (FeMn) alloys are utilised by the steel industry to manufacture various grades of steel to improve alloy properties (Gasik, 2013). Market trends of FeMn alloys are closely related to those of steel since approximately 90% of the demand is from the steel industry (S.E. Olsen *et al*., 2007). For several important applications, there is no adequate replacement for the manganese element (George *et al*., 2015), and this currently ensures the existence of the global manganese industry. Manganese is introduced into steel processing in the form of FeMn or silicomanganese (SiMn) alloys (S.E. Olsen *et al*., 2007). Various grades of FeMn alloys are produced and consumed globally. Table 1-1 lists the ASTM standards (ASTM Standards A99-03, 2009) and (ASTM Standards A483 / A483M - 10, 2010) of each grade.

Table 1-1: Grades of ferromanganese and silicomanganese products (ASTM Standards A99-03, 2009; ASTM Standards A483 / A483M - 10, 2010).

	Mn % **(spec)**	**C %** (max)	**Si %** (max)	**P %** (max)	**S %** (max)	**Fe %** (estimated)	**Mn/Fe** (estimated)
Grade A	78.0– 82.0	7.5	1.2	0.35	0.050	12.03– 8.03	6.48– 10.2
Grade B	76.0– 78.0	7.5	1.2	0.35	0.050	14.03– 12.03	5.42– 6.48
Grade C	74.0– 76.0	7.5	1.2	0.35	0.050	16.03– 14.03	4.62– 5.42
Grade A	80.0– 85.0	1.5	1.5	0.3	0.020	15.97– 10.97	5.00– 7.75
Grade B	80.0– 85.0	1.5	1.0	0.3	0.020	16.47– 11.47	4.86– 7.41
Grade C	80.0– 85.0	1.5	0.70	0.3	0.020	16.77– 11.77	4.77– 7.22
Grade D	80.0– 85.0	1.5	0.35	0.3	0.020	17.12– 12.12	4.67– 7.01
Nitrided	75– 80ɣ	1.5ɣ	1.5ɣ	0.3	0.020	16.97– 11.97	4.42– 6.68
Grade A	85.0– 90.0	spec*	2.0	0.2	0.020	11.45– 6.45	7.42– 13.9
Grade B	80.0– 85.0	0.75	5.0– 7.0	0.3	0.020	13.30– 6.30	6.02– 13.5
Grade A	65.0– 68.0	1.5	18.5– 21.0	0.2	0.04	13.82– 8.32	4.07– 8.17
Grade B	65.0– 68.0	2.0	16.0– 18.5	0.2	0.04	15.82– 10.32	4.11– 6.59
Grade C	65.0– 68.0	3.0	12.5– 16.0	0.2	0.04	18.32– 11.82	3.55– 5.75

* As specified

ɣ The specification is based on the metal content.

Raw materials required for FeMn and SiMn production can be broadly classified under the following: manganese source (may contain iron), carbon source, and fluxing agent (for SiMn it can also be the silicon source) (Tangstad *et al*., 2004). Many manganese ore deposits exist in the world, but the ore grade and the resources required to extract the ore reduces the economic return for some deposits. South Africa has the largest known land-based manganese source in the world, the identified resource accounts for about 78% of the ore with 29% being the reserve (Steenkamp, 2020). This is followed by Ukraine contributing an extra 10% (George *et al*., 2015). South Africa's manganese source is mined in the Kalahari Manganese Field located in the Northern Cape (Steenkamp & Basson, 2013).

Pyrometallurgical process routes are used to make FeMn alloys. The net endothermic carbothermic reduction of manganese ore is commercially executed in either submerged arc furnaces (SAFs) or blast furnaces (BFs) (S.E. Olsen *et al*., 2007). Most countries that produce FeMn alloys use SAF technology, but the BF is still applied in China, Russia, and Ukraine (Çardaklı, 2010). The process consists of raw materials being fed into a furnace and a heat source being used to raise the temperature in the furnace to facilitate reduction (Gasik, 2013). Materials in the furnace undergo physical and chemical changes to produce a molten alloy, slag, and off-gas (S.E. Olsen *et al*., 2007). Two process routes exist when using SAFs namely; the waste slag route and the duplex route (S.E. Olsen *et al*., 2007). The duplex route requires a manganese-rich slag to be produced along with a high carbon ferromanganese (HCFeMn) alloy (S.E. Olsen *et al*., 2007). This slag is then used as a feed into the SiMn process to recover more manganese (S.E. Olsen *et al*., 2007). A similar process was implemented in Japan using BF technology: the process produced iron with a high phosphorus content and a manganese-rich slag (Zhang, 1992).

Process temperatures can be raised using either electrical energy in a SAF or chemical energy in the BF through the combustion of coke (Tangstad *et al*., 2004). In South Africa, only SAF technology is applied using the waste slag route (Steenkamp & Basson, 2013). Processing route selection is informed by the ore quality: basic ores are preferred for the waste slag route due to better manganese recoveries from basic slags (S.E. Olsen *et al*., 2007). Attractive economic return led to the BF being replaced by the SAF over time (Hooper, 1968; Steenkamp & Basson, 2013). This investigation will primarily focus on the South African context of the FeMn industry. The purpose of the investigation is to understand the financial implications of replacing SAF with BF or alternative technology to challenge the current FeMn alloy production trend.

1.2. Problem Statement

1.2.1. Introduction

The trend of manganese ore export and local sales over 20 years is shown in Figure 1-1. Over the period ranging from 1997 to 2016, the total export sales of manganese ore have increased from just over 50 % of the total sales to over 85 %, as seen in Figure 1-1.

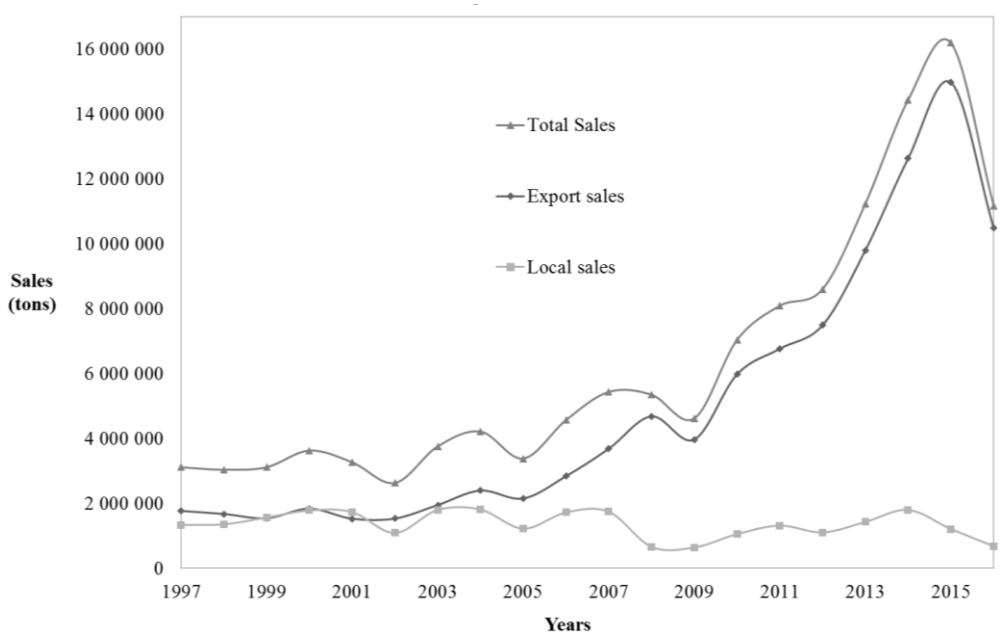

Figure 1-1: Distribution of local and export sales of South African manganese ore (Directorate Mineral Economics, 2017)

In 2004 the gap between local and export sales started increasing, and up until 2016, the gap did not seem to close between export and local sales. Despite the significant increase in the total sales of manganese ore, the ore input into the South African manganese value chain showed stunted growth between 2004 and 2007. Furthermore, slight decreases in ore beneficiation were observed from 2008 which could be attributed to the global economic crisis. It resulted in a decrease in production capacity in response to the drop in commodity prices, which sent the minerals sector into survival mode (Baxter, 2008). Unfortunately, the production capacity was never fully recovered judging by the local ore sales from 2008 up-to 2016.

Van Zyl (2017) investigated the barriers that limit growth in the mineral value chains.

Specifically, the framework developed in the study was used to review key barriers existing in the manganese value chain. One of the barriers identified in the dissertation, among many, is the heavy reliance on electrical energy during production, which was also mentioned by Steenkamp and Basson (2013) (Van Zyl, 2017). SAF technology, currently being used in South Africa, is known for requiring a significant amount of electrical energy (Steenkamp & Basson, 2013).

South Africa has significant ore reserves available locally and is currently supplying ore to the global market. For South Africa to be competitive at beneficiating FeMn products using SAFs, local electricity prices need to be lower when compared to other countries that produce and export the same alloys. The global supply and demand in 2013 reviewed by Van Zyl (2017) indicated that India, South Korea, Australia, France, Spain, Norway, Netherlands, Ukraine, Georgia, and South Africa are the main exporters of FeMn products. In 2015, it was found that South Africa ranked 10th highest when global electricity prices were compared (Van Zyl, 2017). Of the 9 countries that export FeMn products in competition with South Africa, only France exhibited a higher electricity price in 2015 appearing in the 9th position (Van Zyl, 2017). The electricity price increase from 2014 to 2015 in France and South Africa was 4.2% and 8.2%, respectively (Van Zyl, 2017). According to the latest energy statistics, for the period 2013-2018 industrial electricity prices increased by 8.88% on average (Motiang, 2018). If the electricity price increase in South Africa adheres to this trend it will have the most expensive prices when compared to other FeMn exporting countries. The electricity price increase in South Africa reduces the competitive advantage in beneficiating manganese ore locally.

Although institutions and industries are collaboratively investing in the reduction of electrical energy consumption by SAFs, furnaces that use other energy sources could be financially viable alternatives. The first account of HCFeMn production in South Africa in 1937 was carried out in a BF that was designed for pig iron production, then the transition to electric furnaces occurred from 1939 onwards (Basson *et al*., 2007). The transition was due to favourable economic conditions towards electricity prices at the time (Hooper, 1968). Over 25 years ago China (Zhang, 1992) and Japan (Kamei *et al*., 1992) faced a similar electrical energy cost dilemma, among other factors, which resulted in the production of HCFeMn to be carried out in BFs. Significantly larger amounts of coke are required in BF production when compared to SAFs. This is due to catering for chemical energy demands over and above reduction reactions (Çardaklı, 2010). In the FeMn and Ironmaking industries, four types of energy sources are currently used, namely, electricity, crude oil, natural gas, and coal (Hasanbeigi *et al*., 2014; S.E. Olsen *et al*., 2007; Ashpin *et al*., 1975). Unlike the other three sources, electricity is not a primary energy source.

Electricity is derived from fossil fuels, nuclear fuels, and renewable sources like the sun. The energy landscape of South Africa consists of electricity generated predominantly from coal by Eskom (Pollet *et al*., 2015).

However, a smaller fraction of electricity is generated using natural gas, solar, and nuclear energy (Motiang, 2018). South Africa currently does not produce any crude oil supply (Motiang, 2018). Natural gas is derived from oil production and Sasol is the main supplier of natural gas in South Africa using imported resources (Motiang, 2018).

In 2014 South Africa was reported to have the 5th largest coal reserve accounting for 7.5% of the world's coal reserve and the 7th largest producer (Revombo, 2016), which means that coal can be sourced locally. The coal reserves are spread between Mpumalanga, Northern Kwazulu-Natal, and Limpopo provinces (Revombo, 2016). More than 60% of the local coal sales go towards electricity generation based on figures from 2014 (Revombo, 2016). According to Revombo (2016), two types of coal were sold: bituminous coal used for electricity generation and other applications, and anthracite used by the metallurgical industry. Electricity generation can be interpreted as an added cost for the SAF that would not be required if the coal is used directly in the FeMn process. The subsequent rationale of exploring other ironmaking technologies that make use of coal products from the Steel Industry arose.

Climate change caused by global warming is a critical issue that has resulted in governments world-wide implementing new policies in hopes of mitigating the situation. One of the key drivers of climate change is the emission of greenhouse gas (GHG) as a result of human activity (National Treasury Republic of South Africa, 2013). The Carbon Tax Act No 15 of 2019 came into effect in South Africa from 1 June 2019. Countries such as the United Kingdom, Australia, and the United State of America, to mention a few, have implemented similar policies to mitigate GHG emissions into the environment. In South Africa, carbon dioxide (CO_2) accounts for 79% of the total GHG emitted (National Treasury Republic of South Africa, 2013). Predominant sources of these emissions are electricity generation through coal, petroleum refining, transport, agriculture, and industrial sectors (National Treasury Republic of South Africa, 2013). Production of ferroalloys in South Africa will inevitably incur carbon tax either indirectly, through using electricity, or directly through carbon combustion.

1.2.2. Problem Description

The rising electricity prices and progressively unreliable supply in South Africa are causing the manganese beneficiation process to become economically unviable in producing low-cost FeMn. Therefore, feasible process alternatives that do not rely as heavily on electricity as an energy source need to be identified for possible implementation. The Ironmaking industry was identified as a source of a pool of alternative technologies that can be applied in the FeMn industry due to the process similarities and since it has been done using BF technology on HCFeMn.

The application of coal rather than coke in alternative technologies would be advantageous in the South African context. One of the benefits will be due to the local coal supply, unlike the other primary energy sources. A techno-economic feasibility study is required to assess the technologies under review to determine whether the alternative is worth exploring further. The study will consist of two types of models; an underlying material and energy balance will provide the technical basis and an economic model that will provide insight on the financial performance of the solution under investigation.

1.3. Research Objectives

This study aims at conducting a desktop techno-economic feasibility study on selected technologies for the production of HCFeMn. Selected technologies from the FeMn and ironmaking industries will then be compared to the existing SAF technology. The objectives of this study are as follows:

- Review FeMn and ironmaking technologies, to select the most mature and promising flowsheets as alternatives.
- Select an approach that will be applied to model the HCFeMn material and energy balance in selected technologies.
- Define all the variables that will be taken into account when building a financial model for each technology, to conduct a techno-economic comparison of the technologies.
- Conduct a scenario and sensitivity analyses to gain better insight into key economic variables and to assess the robustness of the most attractive flowsheet.

Chapter 2

Literature Study

2.1. Introduction

For South Africa to reap more economic benefits out of the mineral resources produced locally, a significant percentage of the ore produced should be beneficiated in the country. The availability and increasing production of manganese ore in South Africa should, therefore, translate into growth in the manganese value chain. However, judging by the increasing gap between export and local sales observed in Figure 1-1, the growth of the manganese value chain in South Africa has been stunted since 2004. One of the key contributors to the stunted growth was found to be the heavy reliance on electricity, this is a major operational cost in processes that make use of submerged arc furnaces (SAFs). Currently, the South African manganese value chain only applies the SAF for FeMn and SiMn, which is an electrical energy-based technology. The only other well-known commercial scale alternative for producing high carbon ferromanganese (HCFeMn) is the blast furnace (BF), which is a carbon combustion energy based technology that relies heavily on coke. BF technology is prevalent and well established in the ironmaking industry for producing pig iron. Nevertheless, many more technologies are being developed in the Ironmaking industry to replace the BF due to various limitations they experience. Technology limitations arise due to the nature of our evolving world, and the depletion of old or the discovery of new resources. These limitations formed the basis for innovation efforts in the Ironmaking Industry. Extending the exploration of the alternative technologies beyond the Ferromanganese industry and into the Ironmaking industry could introduce possibly new alternatives for processing manganese ores.

This desktop techno-economic feasibility study aims to compare existing and potentially applicable furnace technology. Furthermore, the potentially applicable technology must not rely heavily on electricity and must be applied in the production of HCFeMn. Four literature reviews were conducted, therefore the chapter will comprise of four sections covering the topic of each literature review:

- Techno-economic feasibility study
- Alternative technologies
- High carbon ferromanganese process modelling.
- Economic modelling of process flowsheets and economic performance.

The structured literature search was conducted to source all information that is closely associated with the Ironmaking and the Ferromanganese industry.

2.2. Techno-economic Feasibility Studies

When building a new production facility or renovating an existing facility to increase capacity, a major incentive to continue with the project is the monetary benefit it will potentially yield. This phenomenon is no different when it comes to the ferroalloy production facilities. Commissioning and decommissioning of facilities is based on economic return. Such scenarios give significance to various economic evaluations done before a new plant is erected or process improvement is carried out. The starting point of any economic activity is identifying a product and the market. In the case of existing products, market research is available and it provides information on industry players, the value of the product, and historical and future trends (Mackenzie & Cusworth, 2007). Once it is established that there exists a demand, the raw materials availability and processing methods are explored. The information gathered is organised into a techno-economic evaluation that is used to evaluate the potential economic performance of the project under review. Techno-economic evaluations serve as decision-making tools for stakeholders who invest in new plants or facility expansions.

A techno-economic feasibility study is a system of methods that focus on the technical and economic performance of an investment project. In these assessments information about the particular project is uncovered in stages, which renders techno-economic evaluations continuous by nature (Mackenzie & Cusworth, 2007). Consequently, no evaluation is identical due to the uniqueness of the project and the particular questions that need answers at the time. However, the processes and methods applied to a variety of projects will be the same to be able to establish a basis for comparing different project options. Techno-economic evaluations are categorised by the different phases the study goes through and this will normally be indicated by the adjectives used to describe the type of study it is (Mackenzie & Cusworth, 2007). Mackenzie and Cusworth (2007) presented a framework that describes the various phases in project development; Scoping Study, Prefeasibility Study, Feasibility Study and Funding, Implementation and Start-up, Operation, and Closure and Decommissioning (Mackenzie & Cusworth, 2007). The quality of the estimation methods used to compile the study gives an indication of the phase and completeness of the project under consideration. Therefore, the accuracy range specified for the study is a better indicator of the level of the study as opposed to the attached adjective. As a project approaches construction and ultimately production, the accuracy of estimates improves to within 10 % of the actual project value (Green & Perry, 2008). Due to the qualitative nature of techno-economic feasibility studies, in early stages caution must be exercised when decisions need to be made based on the outcomes.

The focus of techno-economic studies is two-fold, the resolution of the technical challenges and the building of a business plan based on these technical resolutions (Mackenzie & Cusworth, 2007). Major components of techno-economic evaluations are the underlying process flowsheets that detail equipment, capacity,

and other estimates that relay the productivity of the proposed facility. The technical aspect of the feasibility study is a guideline on how the facility must be modified to achieve the economic benefit of the project (Mackenzie & Cusworth, 2007). Both aspects are crucial because without technical soundness the projections made are false. Earlier studies, for example, Identification, are short with inadequate information and seemingly inexpensive when compared to the studies that are done later (project evaluation), however, they play a crucial role. These studies determine whether money and efforts will be wasted by moving to the next phase (Noort & Adams, 2006). For the current study, information available on the alternative technology identified in the ironmaking industry allows for a qualitative pre-feasibility type study to be conducted (Behrens & Hawranek, 1991). According to Behrens and Hawranek (1991), a pre-feasibility study is a Level Two study (out of five) designed for pre-selection or preliminary analysis type decisions. The accuracy of the study is linked to estimation methods used to calculate the capital investment amount. Figure 2-1 shows a list of equipment cost estimation methods and their associated accuracy ranges according to Lemmens (2016).

Class	Type of estimate	Description	Accuracy (%)
5	Order-of-magnitude (also Ratio/Feasibility)	Derived from limited data. Screening concepts	-20 to -50 +30 to +100
4	Study estimate (Major equipment/Factored)	List of major equipment. (Project screening, feasibility assessment, concept evaluation)	-15 to -30 +20 to +50
3	Preliminary design estimates (Scope)	More detailed sizing of equipment. Budget authorization, appropriation, and/or funding.	-10 to -20 +10 to +30
2	Definitive estimate (Project control)	Preliminary specification of all equipment, utilities, Instrumentation, electrical, and off-sites. Bid/Tender.	--5 to -15 +5 to +20
1	Detailed estimate (Firm/Contractor's)	Complete engineering of process and related off-site and utilities required. Check estimate or Bid/Tender	-3 to -10 +3 to +15

Figure 2-1. Classification of capital cost estimates, after Lemmens (2016).

Class 4 estimating techniques and methods are the most suitable for the current study with a maximum deviation between -30% and +50% in the estimation of the fixed capital cost. Investment cost estimating techniques will be detailed in Chapter 2.5.

2.3. Alternative Technologies

Based on the technology transfer of the BF that occurred between the ironmaking and FeMn industries (Hooper, 1968), the current study assumed that all ironmaking technologies used to produce molten pig iron are potentially transferrable to the HCFeMn process. This assumption was made based on the commercial success of the BF technology for HCFeMn production and the alternatives being developed to replace the BF. Furthermore, the liquid state reduction of manganese compounds occurs in a similar environment required by iron compounds. The search for alternative technologies was limited to technologies from the ironmaking industry that produce the same alloy. The first step in identifying alternatives was compiling a list of potential technologies that can meet basic technical requirements for the HCFeMn process. Table 2-1 details the keywords used to search the title, abstract, and keywords in the two abstract and citation databases chosen namely, Scopus and Web of Science.

Table 2-1: Search results for alternative ironmaking technologies.

Databases	**Keywords**	blast AND furnace AND smelting AND reduction AND alternative AND process	corex AND iron AND making AND process	finex AND ironmaking AND process	**Total**
Scopus	**Hits**	61	67	42	170
	Repeats	2	3		
	Read	19	14	4	37
Web of Science	**Hits**	38	31	7	76
	Repeats	1	1		
	Read	8	8	4	20

Search one was aimed at finding publications that focus on alternative technologies that are used to produce alloy quality similar to what BFs produce. The 'repeat' category refers to articles that have already appeared using previous keyword searches. The 'hits' were manually screened by title and abstract to isolate citations that required full texts to be sourced. Once the 27 articles were read one more search was conducted for the technology that was selected, namely, the COREX®. No information was found on the FeMn process in the COREX® using both databases.

The steel-making process constitutes three main stages: ironmaking, crude steel production, and finished steel production (Nill *et al*., 2003). Figure 2-2 elaborates on the three processing stages.

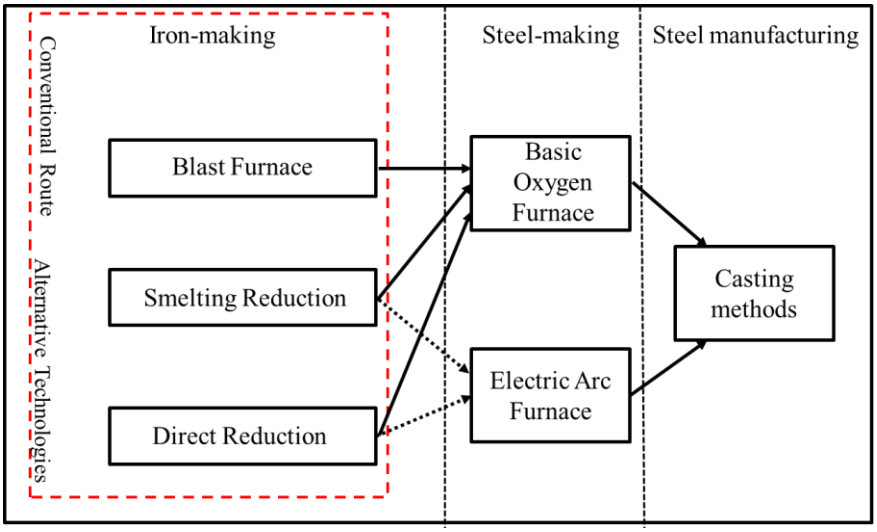

Figure 2-2. Iron and steel process technology options, as after Nill (2003).

These stages can exist on the same site and are then called integrated steel mills, or separately (Hasanbeigi *et al*., 2014; Nill *et al*., 2003). The focus of this section will be based on the rectangle shown in Figure 2-2, which encompasses all the technologies available for ironmaking. The BF is a conventional route that has been used to produce pig iron since 1300. It is still dominant in the ironmaking industry (Dash & Das, 2009). The two alternative processing routes are available, smelting reduction (SR) and direct reduction (DR). The two groups can be distinguished by the type of iron produced. SR technologies produce molten pig iron similar to the BF product, and DR technologies produce solid-state sponge iron (Noldin, 2012).

For the current study, only the SR technologies that produce liquid state iron will be considered as potential alternatives. This due to the technical requirement of liquid state reduction in the manganese process. SR technologies are a direct

alternative to the BF because they produce liquid iron of similar quality (Hasanbeigi *et al*., 2014). Solid-state reduction of manganese ore to manganese alloy is not possible, therefore this necessitates the technical step of liquid alloy formation (Tangstad & Olsen, 1995).

The BF has strict requirements for the feed material for optimal furnace operation. As a reductant and energy source, the BF requires coke produced in coking plants using metallurgical grade coal (Nill *et al*., 2003). Iron sources required by the BF are in the form of large ore particles or agglomerated ore particles in the form of sinter and pellets (Nill *et al*., 2003).

There are three main areas of concern that support the need to develop ironmaking alternatives: technical, economic, and environmental (Noldin, 2012). Some of the technical aspects include the requirement of high-quality raw material that are either in limited supply sometimes due to geographic reasons, or availability (Noldin, 2012). BFs are less flexible when it comes to production scale causing operational challenges at low throughput (Noldin, 2012). Economic aspects include the high capital investment and operational costs associated with the production capacity, the very complex support systems (stoves, coking plant, sinter plants), and raw material quality (Noldin, 2012). The environmental aspects focus on emissions of CO_2, NO_x, volatile organic compounds (VOC), and SO_x (Hasanbeigi *et al*., 2014). These limitations were taken into account during the development of alternative BF technologies.

Under the SR class of alternative ironmaking technologies, several configurations use either coal with electricity or oxygen/air shown in Table 2-2. The technologies listed below are gathered from the lists provided by Dash and Das (2009), Dutta and Rameshwar (2016), and Noldin (2012). The technology rank was adapted from a publication by Noldin (2012). Rank 1– 3 are technologies in the commercial or growth stage. Rank 4 and 5 are still in the pilot or developmental stage.

In the early stages of a techno-economic evaluation, multiple flowsheets are compared. As the study progresses through the different levels, flowsheets are removed from the study as a result of not meeting predetermined criteria. In the final stages, one flowsheet remains, and a study termed a bankable feasibility study is prepared to present to potential project financiers. The current study seeks to explore alternative technologies for the production of HCFeMn. Therefore, at least two flowsheets should be under review: the current flowsheet and the proposed alternatives. The SAF route is the currently applied flowsheet and will be compared with the BF flowsheet and one other alternative technology flowsheets identified in the ironmaking industry. The next section details the steps taken to qualify the chosen technologies to compare to the SAF currently used to produce FeMn. In Chapter 1 it was mentioned that the only other commercially proven technology that can produce HCFeMn is the BF (Hooper, 1968; Kozhemyacheko *et al*., 1987; Madias, 2011).

Table 2-2. Coal-based SR technologies available in the ironmaking industry (Dash & Das, 2009; Dutta & Rameshwar, 2016; Noldin, 2012).

Technology	Reductant	Energy contribution	Iron feed	Maturity Ranking
Redsmelt	Coal	Electricity Air	Pellets	1
Iron dynamics (IDI)	Coal	Electricity	Pellets	1
Fastmelt	Coal	Electricity	Pellets	1
COREX®	Coal	Oxygen	Pellets Lump Ore	1
FINEX	Coal	Oxygen	Fine Ore	2
HIsmelt	Coal	Enriched Air	Fine Ore	3
Ausmelt (AusIron)	Coal	Enriched Air pulverised coal	Lump Ore Fine Ore	4
Romelt	Coal	Oxygen	Fine Ore	4
DIOS	Coal	Oxygen	Fine Ore	5
AISI-DOE	Coal	Oxygen	Pellets	5

Hooper (1968) stated that the choice to use SAF technology was prompted by the cheaper electricity costs when compared to coke in South Africa at the time. This then led to the re-evaluation of the economic feasibility of using the BF due to the rising electricity prices in South Africa. Table 2-3 lists the set of criteria used to assess each technology alternative found in the ironmaking industry.

Table 2-3. Criteria for the selection of alternative technologies for the evaluation.

Criteria	Rationale behind criteria
1: Technical compatibility	Manganese alloys only form as a result of liquid-state reduction (S E Olsen *et al*., 2007). Therefore, technologies that produce liquid pig iron would be technically suitable to reach the required temperatures around 1500℃ to facilitate smelting.
2: Primary problem statement	In the problem statement, electricity was identified as one of the major contributions to the increasing production costs. This investigation aimed to identify and compare options that remove the reliance on electricity for process energy input.
3: Secondary problem	The third criterion addresses the need for solutions that require the least amount of resources to commercialise. TRL is a framework of guidelines used to manage risk and uncertainty that comes with new technologies. Even though putting a new process in proven technology reduces the TRL level. The rationale behind using this measure is a well-researched technology being evaluated on pilot- and demonstration-scale, ultimately fast-tracking commercialisation (Heder, 2017).

Furnace technologies identified in the ironmaking industry were filtered using criteria 1 to 3. However, only criteria 2 and 3 were used for FeMn industry technologies since they have been proven to produce FeMn

Using the constraints given the choice was narrowed down to COREX®, and FINEX®. The COREX® utilises diverse feed and the FINEX® is capable of processing fine ore. It is worth noting that the FINEX® technology is merely a variation of the COREX® technology. It was adapted to process only fine ore (Dutta & Rameshwar, 2016). From the currently available SR class of alternatives, the COREX® was chosen in this study for further investigation using a techno-economic study. Furthermore, a conjecture will be drawn for the FINEX® based on the results of the COREX®.

Any technology that exists has advantages and disadvantages. Certain attributes of the technology can be categorised as either an advantage or disadvantage depending on the context of the application. The COREX® and FINEX® may share a number of their attributes due to how the FINEX® was developed. Table 2-4 lists some of the pros and cons of both the alternative technologies under consideration when compared to the BF from a pig ironmaking perspective. The factors listed in Table 2-4 will need to be considered in the context in which these two technologies will be applied. The advantages and disadvantages need to be captured into the techno-economic analysis for this study where it affects the model output.

Table 2-4: Advantages and disadvantages of the COREX® and FINEX® when compared to the BF (Dutta & Rameshwar, 2016).

	COREX®	**FINEX®**
Advantages	• (Not true for the COREX®) • Direct charging of non-treated coal • Same metal quality as the blast furnace • Lower emissions than the blast furnace • Flexibility in operation • High levels of automation • Lower investment and production costs	• Direct charging of non-agglomerated fine material
Disadvantages	• Low refractory lining life in melter-gasifier affecting the campaign life • Requires sophisticated gas cleaning facilities • Requires more maintenance • Transferring of hot intermediate products poses a safety risk during the maintenance period • The coal quality is important: low ash and medium volatility	

Factors such as South Africa having the 5th largest coal reserves and the 7th largest producer will result in coal transportation costs being lower when compared to coke that is predominantly imported (Revombo, 2016). The accumulation of some of these will need to be incorporated and evaluated using appropriate assumptions in the techno-economic models. The COREX® was chosen for the current study. Furthermore, only qualitative inferences were made about the FINEX® due to the overlaps that exist with the COREX®. The FINEX® was excluded from the models developed in the study.

2.3.1. Overview of technologies

Search two, in Table 2-5, was aimed at delving into technical publications to gather information to compare the SAF, BF, COREX®, and FINEX® on a technical level. This would be achieved by reviewing literature associated with the following topics: i) the HCFeMn process in SAFs; ii) the HCFeMn process in BFs; iii) the ironmaking process in the BFs; iv) the ironmaking process using the COREX® technology and v) the ironmaking process using the FINEX® technology.

Table 2-5: Search results for HCFeMn and ironmaking in the SAF and BF.

Databases	Keywords	high AND carbon AND ferromanganese AND smelting AND process	high AND carbon AND ferromanganese AND process AND technology	high AND carbon AND ferromanganese AND submerged AND arc AND furnace	high AND carbon AND ferromanganese AND process AND model	high AND carbon AND ferromanganese AND blast AND furnace	blast AND furnace AND process AND model AND technology AND ironmaking	Manganese AND ore AND prereduction	Manganese AND ore AND smelting AND reduction	Total
Scopus	**Hits**	22	16	16	14	13	48	5	8	142
	Repeats	-	7	5	7	4	-	0	0	
	Read	9	2	2	2	0	3	4	10	32
Web of Science	**Hits**	11	6	12	13	7	33	1	30	113
	Repeats	-	4	6	5	2	1	1	24	
	Read	6	2	0	0	2	5	0	1	16

Information on the COREX® and FINEX® was collected in search one and search two focused on the SAF and BF. The search extended across two industries: the ferromanganese and ironmaking industry. The keywords that were chosen focused on HCFeMn, ironmaking process, and manganese ore processing in specific furnace technology, namely, SAF and BF. The keywords used and results yielded by each database are shown in Table 2-5. The same 'hits' screening method was used to select articles numbered as 'Read'. Articles were chosen based on a holistic discussion of the processes from input to output in a particular technology. The articles were then used to source relevant references found in the reference list. A search was also conducted in a shared group 'Manganese Ferroalloys' in Zotero and one paper was used from the search.

Some articles were found through referrals through informal peer reviews. The information was used to construct a full picture of both processes in all four technologies from the feed material to the energy input. The information obtained was then summarised to identify the most suitable alternatives and create a process flowsheet to compare the technologies. This section will present a comparison of the four furnace technologies identified in the current study: the SAF produces HCFeMn, the COREX® and FINEX® only process pig iron, but the BF technology produces both products. The comparison of the four technologies and the two processes seeks to draw insights for technical assumptions. Furthermore, the economic characteristics of the technologies will be qualitatively assessed.

Four furnace technologies are shown side by side in Figure 2-3, the FINEX®, COREX®, BF, and SAF. The HCFeMn and ironmaking processes can be outlined using six main areas: raw materials (manganese source, fluxes, and carbon source), solid-state reduction zone, energy source, liquid-state reduction zone, alloy product, and by-products. These six areas have synergistic interactions, therefore they all affect the quality and quantity of the desired product. Two of the furnaces only produce pig iron (FINEX® and COREX®), an adaptable technology to both processes (BF), and HCFeMn (SAF). Most countries that produce FeMn alloys currently use SAF technology. Although the BF is an older technology that was popular before electric furnaces (Hooper, 1968), it is still used in China, Russia, and Ukraine (Çardaklı, 2010). The technical comparison will focus on the raw material and product stream qualities, and process temperatures. Manganese and iron sources are fed as lump/fine ore, pellets, and sinter (Anameric & Kawatra, 2008 and S.E. Olsen *et al*., 2007).

The feed is often blended to suit furnace operational conditions. An example of the chemical species that enter the furnace through manganese and iron sources are listed in Table A-1 in Appendix A (S.E. Olsen *et al*., 2007 and Van der Vyver *et al*., 2009). Manganese and iron ores have similar gangue minerals (SiO_2, Al_2O_3, CaO, and MgO), according to Table A-1, they are approximately 19% in manganese and 3% in iron ore. All these gangue components collect in the slag. An important

quality of manganese ores is the manganese to iron weight ratio (Mn/Fe) which is 5 for the manganese ore in Table A-1.

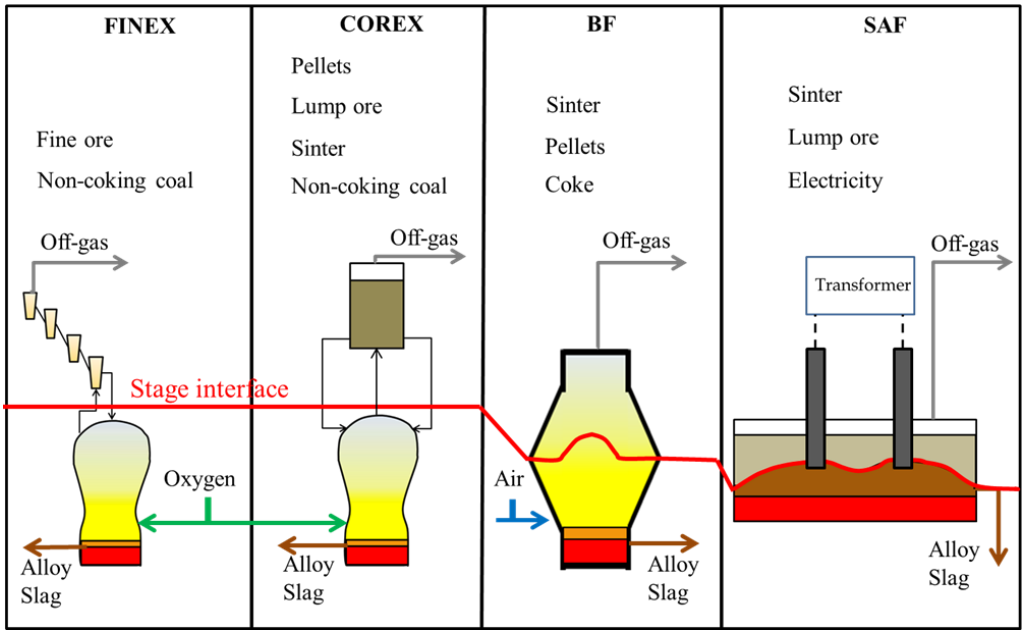

Figure 2-3. FINEX® (after Yi *et al*., 2011), COREX® (after Zhou & Zhongning, 2013), blast furnace (after Vignes, 2013), and submerged arc furnace (after Vanderstaay *et al*., 2004).

Mn/Fe ratio gives an indication of the maximum Mn/Fe that can be obtained in the FeMn alloy (S.E. Olsen *et al*., 2007). The carbon source fulfils two purposes as a reducing agent and as an energy source. Carbon materials used in HCFeMn and ironmaking fall into one of the three categories with their typical compositions listed in Table A-2 in Appendix A. The major chemical difference between the carbon sources, apparent from Table A-2, is the presence of volatile matter. The burden of the SAF uses the coke for its strength to retain shape under pressure, some operations use a mixture of coke and anthracite (Broekman & Ford, 2004), in order to create a coke bed and allow the gases to permeate (Olsen *et al*., 2007). COREX® technology does not require a significant amount of coke for its burden because the raw material is contained in a separate reactor (Zhou & Zhongning, 2013). Table A-3 in Appendix A provides some of the particle sizes required by each furnace technology. The tolerance of fines in the SAF and BF is very low, unlike the COREX® and FINEX® technologies. The COREX® can handle a maximum of 25% of fine ore, sized 0– 12 mm, only in the melter-gasifier (Anameric & Kawatra, 2008 and Sun *et al*., 2010).

Traditional technologies such as the SAF and BF use one unit (also known as a furnace crucible) to process raw materials into the required alloy as seen in Figure 2-3. The proposed alternatives (COREX® and FINEX®) make use of two or more units. The COREX® technology has been in commercial operation since 1989, while the FINEX® technology was commercialised in 2007 after modifications were made to the COREX® (Dutta & Rameshwar, 2016 and Yi *et al*., 2011).

The pre-reduction unit(s) carries out solid-state reduction of the higher oxides. The reducing gases that flow from the smelting reduction unit provide heat energy and carbon in the form of CO for reduction. The partially reduced feed is then fed into the smelting reduction unit along with a solid carbon source and oxygen required for combustion. A similar process occurs in the SAF and BF burden, however, no gas is required in the SAF due to resistive heating. The sintering process heats fine material feeds of ore, flux, and coke to form partially reduced agglomerates (Cores *et al*., 2007). Pelletisation is similar to sintering but uses finer material than sintering, mixed with binders to produce spherical balls (Nomura *et al*., 2015). Briquetting, on the other hand, does not make use of elevated temperatures in its agglomeration process but relies on binders (S.E. Olsen *et al*., 2007). Non-coking coal is turned into agglomerates in a briquetting plant for the COREX®. Coal is taken through the coking process to produce metallurgical grade coke, gaining chemical and physical properties advantageous for the furnace such as lower reactivity, porousness, and strength for the BF (S.E. Olsen *et al*., 2007). Figure A-1 and Figure A-2 in Appendix A show the detailed diagrams of the FINEX® and COREX®. The process flow sheets of the furnaces do not detail major equipment used for raw materials handling, product handling, and off-gas handling. These aspects were addressed later in the study for operational and capital costing.

Basic processing components are mentioned. The Stage interface line that runs across all four flowsheets represents the separation between what occurs in the top unit(s) and the bottom unit. In the case of the SAF and BF, this line is a figurative separation. The first stage above the line is where solid-state reduction occurs and the second stage below the line is where liquid-state reduction occurs:

- Stage 1: heating, evaporating, calcination, and solid-state reduction reactions.
- Stage 2: melting, dissolution, and liquid-state reduction reactions.

Lists of typical reactions to expect in each stage for each process were summarised in Table A-4 in Appendix A. Temperatures at the burden inlet/gas outlet in each furnace are as follows (Madias, 2011; Peacey and Davenport, 1979; Thaler *et al*., 2012; Zhou & Zhongning, 2013):

1. HCFeMn process in the SAF and BF: 400– 600 ºC;
2. Ironmaking in the BF: 150– 200 ºC;
3. Ironmaking in the COREX® reduction shaft: 250– 300 ºC; and

4. Ironmaking in the first FBR of the FINEX®: 400– 750 ºC.

For the HCFeMn process, manganese compounds can be reduced to MnO in the solid-state. Final reduction to manganese only occurs in the liquid-state (Tangstad & Olsen, 1995). On the other hand, iron compounds can be fully reduced to iron in the solid-state (Zhou & Zhongning, 2013). Process temperatures in Stage 1 are assumed to be 1000– to 1200 ºC for HCFeMn production (Tangstad & Olsen, 1995) and 800– 850 ºC for pig-iron production (Zhou & Zhongning, 2013). The main reactions are in the solid-liquid phase where MnO and FeO are reduced by carbon to form an alloy (Madias, 2011). However, for the SAF all the FeO_x is reduced to Fe in the solid phase (Tangstad & Olsen, 1995). The temperature of the HCFeMn metal and slag phase is at around 1400– 1500 ºC (Vanderstaay *et al*., 2004) and for the ironmaking process at 1480 – 1500 ºC (Kumar *et al*., 2008 and Vignes, 2013). Stage 2 yields the slag phase and the desired alloy phase. High temperatures in stage 2 coupled with high pressures increase the vapour pressure of the liquid manganese in the alloy (Kozhemyacheko et al., 1987). As a result, Kozhemyacheko *et al*. (1987) reports the loss of manganese to the off-gas as condensate in the BF technology. This phenomena is a potential technical risk in the COREX® due to the similar temperature and pressures in the furnace. Furthermore, the burden is more fluid and loose without the ability to catch and circulate some of the vapour through raw material particles as in the SAF or BF (Tangstad and Olsen, 1995). However, the dust recycling cyclone could be potentially optimised to return the vapour that leaves the melter-gasifier along with the reducing gases.

The overall energy required by each process is dictated by the reactions. HCFeMn process theoretical energy requirements are calculated to be approximately 7894 MJ/ton metal (2.2 MWh/ton) with reaction 13 in Table A-4 (liquid-state reduction) consuming a significant percentage of the energy required (Ahmed *et al*., 2014). Meanwhile, the ironmaking process requires about 4233 MJ/ton metal (1.2 MWh/ton) based on the BF with the melting, liquid-state heating, and reaction 6 (Boudouard reaction) consuming a significant percentage of the energy (Vignes, 2013). When chemical heat is used in the case of the BF, COREX®, and FINEX® technologies it increases the process gas volume through combustion reaction 29. A stream of hot air (930– 1330 ºC), heated externally, is blasted through the tuyeres at the bottom of the furnace to provide O_2 for the combustion reactions (Peacey and Davenport, 1979). Air contains 78% N_2, by volume, (less when enriched with O_2 to yield up to 25% by volume), which is treated as an inert gas (Peacey and Davenport, 1979). However, NO_x compounds do form in the process. The flame temperature in front of the tuyeres in the BF for HCFeMn is around 2500 ºC (Kamei *et al*., 1992; Kozhemyacheko *et al*., 1987) and for ironmaking, it is around 2200 ºC (Peacey and Davenport, 1979 and Vignes, 2013). The adiabatic flame temperature that results from the char and oxygen in the melter-gasifier can reach up to 4100 ºC (Qu *et al*., 2012). The stream is then fed into the bottom of the reduction shaft at around 850ºC to provide reduction energy and gas reductant (Pal & Lahiri, 2003). The use of coke and coal in the process to generate heat introduces two risks.

Carbon sources normally contain impurities such as phosphorus and sulphur for example which need to be controlled according to the specifications in Table 1-1 for FeMn (ASTM Standards A99-03, 2009). The coal used for the COREX® will need to be selected carefully as most of these impurities go into the alloy phase and circulate in the furnace (Olsen *et al*., 2007; Tangstad and Olsen, 1995). Gas generation is synonymous with emission generation, the more gas produced the higher the emissions which attract carbon taxation. Due to electricity being produced using coal combustion in South Africa, the carbon tax will not be included in the economic model. However, CO_2 emissions will be estimated for informational purposes.

Table A-5 in Appendix A shows the typical properties of both alloys. The HCFeMn alloy contains a significant amount of iron due to its presence in manganese ores. Iron compounds generally exhibit higher recoveries, 99.5% (Vignes, 2013), than the manganese compounds, 80% (S E Olsen *et al*., 2007). The higher mass percentage of gangue material in manganese ores, shown in Table A-1, and the lower recoveries of the HCFeMn process contribute to the higher slag mass. The slag is characterised by a term called *slag basicity* and the formulas are shown below Equation 1 (S E Olsen *et al*., 2007) and Equation 2 (Kumar *et al*., 2008a). In Table A-5 Equation 1 was used to calculate the vales for basicity.

$$Basicity = \frac{(CaO + MgO)}{(SiO_2 + Al_2O_3)} \quad [1]$$

$$Basicity = \frac{CaO}{SiO_2} \quad [2]$$

Slag forms from the gangue minerals found in the ore, the ash components in the carbon source, and fluxes added to adjust the basicity. The slag basicity values for both processes are nearly the same, the values are typically around 1 (Eissa *et al*., 2011 and Peacey and Davenport, 1979). Slag basicity is an imperative control variable as it affects the success in recovering manganese and the resistive heating efficiency in the SAF (S E Olsen *et al*., 2007). The amount of energy contained in the COREX® off-gas stream is over 2.5 times more than that of the BF. This could explain why the energy requirement for the same process in the COREX® is 1.5 times more than the BF. The FINEX® values are assumed to be close to the COREX® off-gas values (Thaler *et al*., 2012).

2.4. High Carbon Ferromanganese Process

Technical evaluations consist of the various steps that lead to fully specified process flow diagrams, with accompanying equipment, instrumentation, and plant design diagrams. The information on these drawings is required to assess the costs and benefits of the proposed investment. Most of the information required for the technical assessment can be obtained from a mass and energy balance over a chosen process boundary. The current chapter will cover three aspects which constitute the technical evaluation for the current study, the mass balance, energy balance, and flowsheet design for a preliminary selection of major equipment.

The HCFeMn process relies on reduction reactions occurring on compounds that contain manganese to extract it in alloy form. In a system containing different compounds, it is impossible to only have the desired reactions occur. Three types of reaction configurations can occur in a system, series, parallel, and independent (Fogler, 2004). In Appendix A, Table A-4 lists reactions that are likely to occur in an HCFeMn smelting furnace. The manganese (Mn) element is isolated through a chain of series reactions that remove all the oxygens (O) bonded to it using carbon (C) compounds. Independent reactions occur due to elevated temperatures in the system, some of these independent reaction release carbon dioxide (CO_2). The CO_2 produced by the series reactions and independent reactions coupled with the increasing temperature profile gives rise to an undesired parallel reaction that occurs, the Boudouard reaction. This reaction not only drives up C consumption, but it also consumes energy. With all these reactions occurring in the same space the concept of yield arises when parallel reactions are considered (Fogler, 2004).

The process is economically viable when the yield of the desired product results in greater economic benefit despite the economic disadvantages caused by the undesired reactions. The ‘Generation’ and ‘Consumption’ terms are calculated using mole balance equations which are synonymous with the material balance equations. Mole balance equations consist of stoichiometric ratios that relate the amount of product produced based on the amount of reactant consumed (Fogler, 2004). The amount of reactant consumed depends on the conditions where the reaction occurs where temperature, pressure, material physical properties, and other materials surrounding it plays a role. A percentage conversion is a simple way to account for all these factors into a single value that states how much of the total reactant will participate in the reaction of interest (Ashrafizadeh & Tan, 2018).

Mathematical equations are used to account for relationships between processes streams. These equations can be derived from two sources of information, fundamental concepts in the fields of chemistry and materials science, or process data collected during pilot tests or commercial production. Models are not restricted to a singular approach, the blending of both approaches is common. A list of publications that detail a version of the HCFeMn process model and operational data in BF technologies is provided in Table 2-6. The use of a particular approach

is highly reliant on the availability of physical data where the behavioural insight of the process can be extrapolated. In circumstances where the operational, pilot plant or experimental data cannot be obtained, fundamental principles of chemical reactions and thermodynamics are useful in modelling process phenomena.

Table 2-6. HCFeMn models collected from literature.

Furnace	Model approach	Description of work done
SAF	First-principles relationships from FactSage software (Steenkamp, 2020)	A model developed for a pilot-scale campaign. The flowsheet consists of material preheating before smelting in a SAF. FactSage thermodynamic software was used.
SAF	Mixture: empirical relationships from commercial data and first-principles energy balance. (Ahmed *et al*., 2014)	Factors that affect energy consumption in an HCFeMn SAF were identified using relationships obtained from plant data and theoretical energy balance equations. The mass balance was an accounting balance from plant data.
SAF	First-principles model. (Jipnang *et al*., 2013)	An optimisation model was developed to predict FeMn/SiMn processes. The model estimates the combination of raw materials to optimise a chosen objective in the process.
Furnace	**Model approach**	**Description of work done**
SAF	Empirical model based on pilot test data. (Eissa *et al*., 2011)	Pilot-scale experiments were conducted while varying properties of the raw materials to find optimum conditions for HCFeMn smelting. From the accounting data, empirical equations were developed.
SAF	Mixture of first-principles and empirical relationships from commercial to-scale operational data. (Broekman & Ford, 2004)	A process and economic model were built to gain insight on the operational performance of the facilities. Empirical enhancements were made to the model to close the gap between theoretical predictions and operational results. The model was used to benchmark the process performance and cost competitiveness with other producers.
SAF	First-principles relationships from HSC software (Vanderstaay *et al*., 2004)	A model of the HCFeMn process was developed using assumptions to select HSC chemistry software inputs. The model predictions were then compared to commercial operation data for verification.

Furnace	Model approach	Description of work done
SAF	First-principles (Swamy *et al*., 2001)	Factors that cause a deviation in the amount of carbon from the stoichiometric requirement are investigated. Process assumptions, that change the theoretical equations, are made to account for the extra carbon consumption observed during operation. A comparison was made with published operational values.
SAF	First-principles (Wasbø *et al*., 1997)	A dynamic predictive model of the process was developed and compared to commercial operational data. The purpose of the simulation model was to increase process understanding and provide operators with a support system.
BF	No model, operational indices of pilot plant (Mishchenko *et al*., 2000)	Fluxed manganese sinter recipes were determined at laboratory scale. The recipes were then tested in commercial scale pilot test work to determine the efficiency of the HCFeMn process when changing sinter basicity.
BF	No model, operational parameters of a commercial scale plant (Mul'ko *et al*., 2000)	The study consisted of producing HCFeMn in a BF designed to produce pig iron and finding ways to improve the technical-economic indices of the process.
Shaft	Mixture: Empirical equations based on experimental data and first principle chemical equations. (Kamei *et al*., 1992)	Experimental tests were done on the production of HCFeMn using a shaft-type furnace (similar to BF) injected with high oxygen and pulverised coal in the coke bed. The furnace was originally used for the verification of a new ironmaking process. The data was used to build and verify the mathematical model. The model was then used to calculate the operational indices of an up-scaled plant.
BF	An accounting type of material balance was performed using commercial operation data. An energy balance was done using fundamental heat equations. The performance indices of the process were provided. (Kozhemyacheko *et al*., 1987)	The work entailed finding an efficient blast temperature for the smelting of HCFeMn. Theoretical flame temperature increases are achieved by either increasing the oxygen content or increasing the temperature of the blast gas.

Based on the literature obtained from the search, HCFeMn models have been developed mainly for the SAF application, furthermore, some operational and pilot

data is available in the BF type furnaces. Unsurprisingly, no model or pilot plant data was found for the HCFeMn in the COREX®. The modelling approach for the HCFeMn process will need to take into account the effects of the different energy sources and reactor configurations. The advantage of empirical models based on data is that they are more accurate in predicting the relation, however, the data limits the scope to the particular operation or very similar setups. First principle models can apply to a wide range of setups because they weren't developed based on particular furnace conditions. The drawback with first principle modelling is the diminished accuracy of the estimates made due to unaccounted interactions. Modelling the HCFeMn in other furnaces will require mass and energy type models that have been developed for the particular technology to inform the assumptions about the different processing conditions that exist in other technologies.

The mass and energy models listed in Table 2-7 have been used as references to gain insight into the important factors which should be taken into consideration when modelling the BF and COREX®. The publications listed in Table 2-7 detail the equations and data used to develop the various models. Two other publications were used to provide qualitative support to the main publications listed in Table 2-7. The articles focused on modelling the effects of different operational characteristics on the dome temperature (Sun *et al.*, 2014; Zhou & Zhongning, 2013).

Table 2-7. Mass and energy balance models for the ironmaking process.

Furnace	**Model approach**	**Description of work**
COREX®	First-principles (Srishilan & Shukula, 2017)	A predictive model benchmarked against industrial data from JSW Steel Plant in India. An elemental accounting type approach was used to obtain a mass balance and an enthalpy distribution was provided.
COREX®	Thermodynamic first-principles (Almpanis-Lekkas *et al.*, 2016)	The model focuses on the melter-gasifier unit which is used by both the COREX® and FINEX® furnaces. The author made use of software such as FACTSage and ChemApp for process thermodynamics. Model validation was approached using literature to validate the reactions selected.
BF	First-principles (Bhattacharya & Muthusamy, 2017)	A comprehensive mass and energy model was conducted on the blast furnace process. Iron ore and sinter were used as feed. The blast air was enriched with 2.39% O_2

2.4.1. Mass and energy balance

Processing systems are assumed to uphold fundamental laws of conservation of mass and energy unless the system has nuclear reactions or operates at extreme conditions (Ashrafizadeh & Tan, 2018). The law of conservation of mass implies that in a system with chemical reactions, all elements that flow into the system boundary must be accounted for in the streams that flow out or the accumulated mass. A similar condition is specified for energy flow in and out of a system supported by the first law of thermodynamics. The conservation law is expressed mathematically using Equation 3, this is generally the starting point for any system to perform a material or energy balance (Fraga, 2014).

Equation 3 General equation that can be applied to each component when performing a material balance.

$$(\text{Input}) - (\text{Output}) + (\text{Generation}) - (\text{Consumption}) = (\text{Accumulation}) \quad [3]$$

Each term in Equation 3 is a place holder for mathematical relationships assumed to exist between the various compounds and energy sources in the system. A model of a system of chemical equations must estimate the desired parameters within reasonable accuracy otherwise it will be deemed useless.

Assumptions are made to guide the selection of correct mathematical relationships to describe the physical phenomena in the furnace. When a model is time-sensitive, meaning the variable is affected when time moves away from zero, it is termed ‘unsteady’ or ‘dynamic’ (Ashrafizadeh & Tan, 2018). Conversely, when a system of chemical reactions is not influenced by the change in time it is termed ‘steady’. Technical evaluations for techno-economic studies are interested in the final product of the furnace. These calculations only take into consideration the accumulated effects of time on each process stream, therefore making the steady-state the final result (Ingham *et al*., 2007). Assuming a steady-state system reduces the term ‘Accumulation’ to zero because over time a steady system is assumed to stay constant (Fraga, 2014). Consequently, the mathematical equation reduces to ‘input’ and ‘generation’ being equal to ‘output’ and ‘consumption’.

The more complex a model is, the more systematic the approach should be to ensure that the process is adequately specified in order to be solvable. A systematic approach to modelling entails drawing a labelled diagram detailing all the streams under consideration, specifying a basis for calculation, and a degrees of freedom analysis is conducted once the equations and assumptions are being specified (Fraga, 2014; Himmelblau & Riggs, 2012; Sinnott, 2005). Once the system is correctly specified, the solving sequence must be determined. The solving sequence is essential when building a new model because it ensures that the calculation will

be executed instead of having the software report an error. Process models are developed around a particular technology, input streams, and output streams (Erwee, 2015; Vanderstaay *et al*., 2004). Despite the various modelling approaches that can be applied, inaccuracies in predicted values are inevitable. The deviations may be due to a lack of information on process variable interactions or process complexities that are hard to model mathematically. These challenges result in assumptions that cannot account for all mass and energy interactions in the system. Validation steps are used to assess the ability of the model to make accurate estimates of the pertinent process variables. Benchmarking data can be obtained from different sources such as industrial-scale plants, pilot test plants, and modelling software (Erwee, 2015; Vanderstaay *et al*., 2004).

There are advantages and disadvantages to the type of data available for validation. The ideal type of data to use when validating a process model is industrial data, however, access and availability of the required measurements poses a challenge. Manganese ferroalloy producers generally do not fully disclose production data due to competitors. Temperature measurements, raw material, and product analyses are data points that incur costs for a plant, therefore, only useful measurements are made frequently. Manganese ferroalloy pilot plant data is also challenging to source. Measurements made during pilot tests are more comprehensive than plant data since pilots are designed to collect data. However, scale-up factors would introduce a degree of error in the reported values. Laboratory scale experimental data normally focuses on a portion of the process, nevertheless, the data can be useful in verifying certain assumptions in the process.

2.4.2. Process flowsheeting

Once the process streams are estimated using mass and energy balance calculations, the plant design process can be initiated by compiling a flow diagram (Parisher & Rhea, 2012). A process flowsheet is a schematic drawing of the sequence of streams, stream details, and the arrangement of equipment, it can be in the form of a block flow diagram (BFD) or a process flow diagram (PFD) (Sinnott, 2005). This flowsheet is then used by different design groups for piping, instrumentation, utility flow diagrams, equipment design, and plant layout (Sinnott, 2005).

Full plant designs require multiple disciplines and specialists in order to produce the various flowsheets to cover all the required information to build a fully functional plant. Process engineers are normally responsible for information on the operating conditions found in a BFD and may to a certain extent be involved in equipment selection and design (Sinnott, 2005). Capital cost estimates are made on the various plant design drawings mentioned, the calculations include all the services and support structures required to build a functional facility. The level of detail provided on a flow diagram has an impact on the accuracy of the capital cost estimate derived from them (Hall, 2012).

Once the basic mass and energy balance is calculated these values are used to construct a basic production schedule based on the desired annual output. Major plant equipment can be sized using the rough estimates on how production will be conducted. Unlike completely novel processes, commercial-scale technologies have information on existing facilities where various inferences can be drawn at lower costs which are suitable for the desired level of accuracy. The current study aims to conduct a techno-economic comparison of existing process flowsheets, some of which produce a different product. Therefore, major equipment selection and production planning will be based on what is currently being implemented commercially. Several publications, listed in Table 2-8, had to be used to compile the process flowsheet with major equipment and processing units according to current industry practice.

Table 2-8. Publications used to specify units and processes.

Furnace	**SAF**	**BF**	**COREX®**
Publication	Steenkamp *et al* (2018) Moolman and Van Niekerk (2018)	(Sen, 1997)	(Kumar *et al*., 2008)

2.5. Economic Modelling

In a free enterprise system, capital projects are chosen based on their ability to yield a return on the investors' money (Sinnott, 2005).

The decision to invest capital in a particular processing plant project is predicated on projections of the economic performance over the life of the project. Most companies or owners only have a limited amount of funds available to invest in a capital project. They possess the option to decline a proposal to build a new processing plant and choose alternative investment vehicles, that may provide more favourable returns (Crundwell, 2008). A project needs to outperform alternative investments to be funded.

An economic feasibility analysis is a tool used to guide the various decisions made concerning capital projects. A checklist of information required to conduct such an analysis was adapted from Perry (2008) and is listed below:

- Total Capital Investment
- Total Operating Expenses
- Marketing Data
- Cash flow analysis
- Project profitability
- Uncertainty analysis
- Risk analysis

These seven items are based on either production figures or mass and energy balance results. Furthermore, items are carried out in phases and each phase provides information for the next analysis. The rest of this section provides details on each item along with the various methods used to execute the analysis.

Total capital investment is the upfront amount required to purchase land, construct buildings, buy and erect manufacturing equipment, and get the processing plant operational until it starts generating revenue (Green & Perry, 2008). The components of the total capital investment are land, fixed capital investment, offsite capital, allocated capital, working capital, start-up expenses, and other capital items (Green & Perry, 2008). The values of the cost components mentioned are only available through quotations or when the plant is constructed. Earlier studies base other estimations on battery-limits fixed capital investment (Green & Perry, 2008). Literature provides a range for these various estimates based on values that are typically obtained. Battery-limits fixed capital investment calculations are more involved than the previous cost. Table 2-10 lists the typical methods provided in literature for conducting fixed capital investment estimates. Process and equipment details guide the accuracy of the estimates generated. Equipment and ultimately the process site consists of many layers to be estimated, from an equipment module, construction material, instrumentation, piping to mention a few items. As a starting point, the plant capacity and the process material need to be established. As more research and more details are uncovered about the process more detailed approaches are required to capture all costs that will be incurred.

Fixed capital cost estimates require the availability of reliable equipment cost data. The data is then used in multiple equations and factors to produce an estimated cost for the processing plant under investigation. When using equipment cost data it is vital to know certain properties about it in order to use it appropriately, as outlined in Table 2-9.

Table 2-9. Equipment cost data properties (Green & Perry, 2008).

Data property	
Cost inclusions	The costs reported may be for equipment at the manufacturer premises, shipped items, unpackaged on the processing site, or fully installed units on site. Equipment costs increase from the cost charged by the manufacturer. Items such as freight, delivery insurance, construction costs, instrumentation, piping, electrical, and insulation to mention a few are accumulated. Knowing what is included in the cost quoted will allow for other costs to be factored into the calculation.
Date	Price changes due to inflation are taken into account through cost indices normally based on the dollar amount of the equipment. Indices are usually quoted for the particular year and disregard the actual date. Cost components such as materials, labour, energy to mention a few incur inflation (deflation)

	at different rates. Publishing of costing data has not been done in recent years, therefore old data is more comprehensive than the most recent data. Therefore, accounting for a +10 year difference is significant.
Capacity	Plant size can be described in terms of product throughput, vessel volume, and power rating. Knowing the size of the plant under consideration will allow for the capacity to be accounted for in the calculation when there is a significant difference.
Applicable range	Certain units have cost capacity curves available for estimation purposes. These diagrams will specify a range that these curves cover. When used out of range caution must be exercised due to the resultant inaccuracies beyond what.
Original currency	Not all data used will be reported in the same currency and therefore it is important to note the currency of the cost data supplied. Other currencies are converted into the base currency according to the average exchange rate for the particular year to facilitate calculations in one currency.

Equipment cost data properties inform the approach in which estimations are made when using the data. In Figure 2-1, Section 2.2, a list of capital cost estimates was provided with the corresponding accuracy range. For study estimates Table 2-10 lists methods provided by Green and Perry (2008). These methods require a preliminary mass and energy balance and knowledge of the major equipment required in the processing plant (Green & Perry, 2008).

Fixed capital cost estimates are based on underlying process models. The models are calculated using process simulation packages or mathematical models designed for the process with complete stream information. CAPEX is a collective word used for the equipment, construction, engineering services, costs incurred by owner/institution, and contingency (Crundwell, 2008). A mixture of the methods can be applied as dictated by available data and the unit process under consideration. Unlike chemical processing plants, metallurgical furnaces are constructed on-site. Building materials such as refractories, furnace shells, and normal construction material such as cement are purchased to be delivered on-site. When calculating capital costs, the actual cost of the unit is unknown since it has not been built and the size is also an estimate. The techniques applied are based on estimating costs using units that have already been built and therefore have a cost attached to the structure (Crundwell, 2008). The estimation methods in Table 2-10 require simple equipment information for the calculation during the early stages. Towards the final stages of the study quotes, tender bids, and invoices are much more reliable for obtaining actual costs.

Table 2-10. CAPEX cost estimation techniques (Green & Perry, 2008; Turton *et al*., 2008).

Method	**Formula**	**Application**
Cost index	$C_2 = C_1 \frac{I_t}{I_0}$	Convert per dollar cost to the current year
Cost-capacity	$C_2 = C_1 (\frac{Q_2}{Q_1})^n$	Different capacities of the same equipment have been built in previous years. Useful for fully installed equipment.
Equipment factors	$C_T = f C_0$	Equipment with several components assembled. Different methods are available such as the Lang factor method, Hang method, Guthrie method, Worth method, Garrett method, and using L+M* factors published by Woods (2007). Normally cost data is available for the components and not a complete processing plant. Furthermore, the components cost data is for free on board (FOB) units which still need various other costs factored in.

Total operational expenditure has many layers to it, but it mainly comprises the general overhead expense and the total product expense (Green & Perry, 2008). General overheads cover expenses that have to do with running the business, activities such as sales, research and development, engineering, and administration. Departments concerned with these activities service all manufacturing plants and the costs are accounted for as a percentage of the annual revenue generated by the product (Green & Perry, 2008). Total product expenses consist of total manufacturing costs, packaging costs, and shipping costs (Green & Perry, 2008). Packaging and shipping depend on how the product is sold. Packaging for a grainy material will be different when compared to large ingots and thus have different packaging needs. Shipping is customer dependent, for multiple customers, several deliveries will need to be made unlike with a single customer. According to Green and Perry (2008) estimating these expenses is challenging, and even more so for earlier studies.

The total manufacturing expenditure has three components raw materials, direct, and indirect costs (Green & Perry, 2008; Ruhmer, 1991). Raw materials are expended in the production process and generally account for a significant fraction of the manufacturing costs (Green & Perry, 2008). Raw material amounts are extracted from the mass balance results. Material costs can be found in appropriate trade journals and government reports on commodity sales. Prices may be quoted higher in a trade journal when compared to quotes generated by suppliers Green and Perry (2008). Supplier quotes are the most reliable. By-products are treated differently from product revenue. If any are produced and there is a market, the income generated is treated like raw material costs (Green & Perry, 2008). Direct and indirect expenses are listed and elaborated in Table 2-11. An estimation of the various manufacturing costs can be made using industry recommended factors for

earlier studies. Accuracy of these costs improve drastically once detailed plant designs and production plans are drafted.

Expenses covered under total capital investment and total operational expenditure are then consolidated into a layout termed a cash flow statement. This is an accounting method that is accompanied by other statements such as a balance sheet and an income statement (Crundwell, 2008). All these data grouping methods do is report on the financial state of a business to the various stakeholders. For the current study, the performance of the proposed flowsheet will be evaluated using only the cash flow statement which includes elements of the other two statements such as the value of capital items, revenue generated and the expenses incurred. The economic performance of a project is measured using economic indicators, these values require cash flow projections over the lifetime of the project (Crundwell, 2008). Cash flow statements capture the movement of money over several years and accounting principles come into effect when interpreting the various movements. Table 2-12 lists the cash flow components that were included in the current study. To make sense of the performance indicators that were used to assess the project, basic accounting principles are covered in Table 2-13.

Accounting principles listed in Table 2-13 factor in charges made by South African Revenue Services (SARS), and the effects of time on the value of the various cash flows. All these factors affect the profitability of the project under evaluation.

Table 2-11. Direct and indirect cost breakdown (Green & Perry, 2008; Ruhmer, 1991).

Direct Costs	
Utilities	Components of the cost element are estimated from the mass and energy balance. It includes steam, electricity, cooling water, fuel, compressed air, and refrigeration.
Operating labour	Labour force costs include wages, pension, housing, bonuses, sick leave, and insurance to mention some items. For processes that run 24/7, it is assumed that one operator requires 4.2 operators per shift. Union contracts quote labour rates.
Indirect Costs	
Supervision	This cost factor depends on the simplicity or complexity of the process. It is estimated as 15% of the labour required.
Maintenance	Items of maintenance are materials and labour, this cost is estimated between 10-15% of the fixed capital cost value. Higher percentages are used for processes that contain multiple moving parts, and high temperature or pressure requirements.
Miscellaneous direct expenses	Items included in this cost factor include laundry, laboratory items, royalties, and environmental control expenses. The other costs are calculated as a fraction of the operating labour between 25-42%. Royalties and patents are 1-5% of the cost of the product.

Indirect Costs	
Depreciation	This is a tax break afforded to companies by the tax authorities for the wear and tear of manufacturing equipment. Details of this cost factor will be more evident in the cash flow assessment.
Plant indirect expenses	Property taxes, insurance, fire protection, maintenance of plant externals such as roads and yards, cafeteria, and plant personnel staff. The sum of these costs are estimated to be 2-4% of the fixed capital investment amount

The various values that make up the components found in Table 2-12 and some of the accounting principles in Table 2-13 were used to compile a cash flow statement. The timing of cash flows relative to time zero is crucial because when a payment is made into the project it starts accumulating borrowing costs the following year. Time zero can be chosen as the time capital investment funds are first made available or the start of production (Green & Perry, 2008). The calculation method differs for both approaches, however, a consistent approach will allow for the projects to be comparable.

Table 2-13 concepts are applied in each year during the life of the project to compile a cash flow forecast for the project under review. Relevant costs are credited (revenue, capital, etc) and others are deducted (manufacturing, taxes, etc). Tax rates and depreciation allowances are provided by the country tax authorities, for the current study the tax authority is the SARS. Money recovered at the end of the project life can either be retained as income or be used to off-set plant decommissioning expenses associated with the environment where the operations took place (Crundwell, 2008). Time zero is another accounting principle that denotes the start of a project and this point is where the point of comparison occurs with other projects (Green & Perry, 2008).

Table 2-12. Cash flow components of a project.

Component	**Description**
Revenue	This amount is from the sales of products/services sold as part of project activities. Forecasts of these amounts can be based on market projections or contracts.
Production costs	These costs are incurred daily as a result of project activities. This component can be further grouped into direct manufacturing and plant overheads. Direct manufacturing costs are closely linked to operational activities that produce sale items. Overhead costs arise from business activities that support operations for instance finance, administration, and sales departments.

Component	Description
Taxes and royalties	These are charges are governed by the country policy where the production facility built. Taxes are charged on income calculated from sales, or capital gains generated from money invested or sales of equipment. Royalties are fees linked to the use of natural resources in the case of mining and oil production.
Capital expenditure	The upfront amount required for land, building the facility, and start-up operations. The money covers tangible equipment and materials for construction. Furthermore, all the services required to prepare the site, install equipment, erect structures, and start-up production processes are included.
Working capital	This is an amount required to hold stock (both raw materials and final products). The amount further includes money owed to suppliers or owed by customers, employees, and taxes.

Table 2-13. Accounting principles applied to a cash flow statement (Crundwell, 2008; Glacier Financial Solutions (Pty) Ltd, 2019; Green & Perry, 2008; Ruhmer, 1991; Turton *et al*., 2008).

Accounting principle	Definition	Mathematical expression
Tax	SARS charges tax on the annual gross earnings. This amount is incorporated into the cash flow statement as an expense.	Corporate tax in South Africa in 2019/2020 is 28% of the profit generated after depreciation allowance is factored in.
Depreciation	SARS allows for wear and tear to be offset from the tax amount that would be payable by the corporation for plant machinery. This is not a real amount, but an accounting term that allows for the payable tax to be recalculated. Depreciation reserves are an accumulation of depreciation allowance that is carried over to the next year to offer a tax break.	New/unused manufacturing assets are depreciated using the fixed capital investment amount at 40% for the first year and 20% for the last three years.
Salvage value	Income generated from the sale of used equipment, normally at the end of the project life. SARS stipulates that 100% of the value of the machinery is depreciated, therefore the salvage value will be a taxable amount similar to income at the end of the project life.	The depreciation method stipulated above assumes a value of zero

Accounting principle	Definition	Mathematical expression
Cash flow equation	Money available to the business to fulfil financial obligations. Financial performance calculations are done on money the remains after several cost items such as operations, tax, and depreciation have been deducted. This is termed the after-tax cash flow.	CF = (R – C – D)(1 – t) + D CF: After-tax cash flow R: Revenue OE: Operating expenses D: Depreciation t: Tax rate
Time value of money	Capital projects thrive on a pool of borrowed funds. The cost associated with borrowing over a period of time translates to this accounting principle. Different methods exist for calculating the cost of borrowing.	
Simple interest	This rate is only concerned with the original unpaid loan amount, and not the full amount. This method is rarely used in business.	$FV = PV(1 + in)$ the future amount (FV) will be interest charged on the principal amount (PV), the interest (i) will be multiplied by the number of periods (n).
Compound interest	This rate takes into account the original capital and the accumulated interest from the previous year. Compounding can happen as often as hourly in certain sectors. For this study, it will occur annually. Essentially the cost of borrowing is more expensive when using this principle and this is what businesses use.	$FV = PV(1 + (\frac{i}{m})^{mn})$ changes to the interest rate are made by the n values being shifted to an exponential value and the number of times the compounding happens annually (m).

Discounting is a method in which the compound interest formula is used to calculate the value of PV, instead of FV as the formula dictates in the table. This is done to account for timing in the value of the cash flow component at a particular year, usually year zero.

The potential revenue generated by the capital project is the most important aspect of motivating for funding because capital needs to be recovered and returns on the investment paid. Some projects may require contracts to secure a market for the product before the investment of capital commences (Crundwell, 2008). Therefore, different arrangements may be negotiated with the customer. These contracts bind the customer to purchase the capacity agreed upon However, the customer can negotiate product costing terms over the contractual period. Economic indicators evaluate the potential of a project to generate satisfactory returns to compel investments to be made. Table 2-14 provides a list of economic indicators accompanied by a short description. Cash flow estimations over the project lifetime form a basis for calculating the various indicators discussed in Table 2-14. Net cash

flows for each year are used to recover the capital expenditure invested in the project. To determine the indicators in Table 2-14 cash flows in and out of a project over the project lifetime are estimated, the lifetime of a project could be well over 10 years.

Table 2-14. Economic performance indicators for capital projects (Crundwell, 2008; Green & Perry, 2008; Sinnott, 2005).

Indicator	**Description**
Discounted Payback period (DPBP)	The payback period is concerned with the number of years it will take to recover the original investment made towards building the production facility. The calculation excludes land and working capital and only focuses on depreciable items. Cash generated after this period is also not taken into consideration. After-tax cash flows are used in payback period calculations. When performing the calculation, there is a choice of factoring the time value of money. An interest rate is used to account for the time value of money. DPBP = Depreciable fixed capital investment - $\sum$(after-tax cash flow)$_n$
Net present value (NPV)	The NPV is concerned with profitability over a certain period at a particular interest rate. This method takes into account the time value effects on the potential profits. Different projects are compared using the NPV value calculated, normally at year zero. Positive NPV values indicate that the project will earn more than the rate used in the calculation and a negative value means the opposite. NPV = $\sum$(Present worth of after-tax cash flow)$_n$ – Present worth of investment amount
Discounted cash flow internal rate of return (IRR)	The IRR is similar to NPV in execution, it is known as the profitability index. The only difference in the calculation is that the interest rate used must yield a zero value for the NPV to estimate the maximum return that an investment project can yield. Those who review investment projects usually have a cut off value for the IRR called the 'hurdle rate. If the calculated IRR is lower than the cut off value, the investment is interpreted as not profitable enough for the investors.
Scenario analysis	Two possibilities are explored, one for the best-case and another for the worst-case estimates. The results are not realistic, however, project extremities are explored.

Indicator	Description
Sensitivity analysis	This group of calculations explores the effects of uncertainty on the profitability of the project. The uncertainty arises from the estimation techniques employed during calculations due to the unavailability of accurate data. Technical or economic variables can be varied to obtain a relationship between the variable and the NPV. Sensitivity analyses are performed on variables that are considered significant enough to affect the return on the investment.

The value of money deteriorates over time due to inflation, risk, and liquidity (Crundwell, 2008). When investment costs are paid into the project sooner, more borrowing costs are incurred due to the length of time the money spends in the project. Conversely, the sooner revenue is generated by the project borrowing costs decrease due to the earlier payments that can be made. Timing is affected by the duration of construction and the time it takes to produce at full capacity. This timing effect of annual cash flows affects the values of all the indicators in Table 2-14.

The probability of events not happening as expected introduces risk to the money invested. The relative ease it takes to convert an asset into cash flow refers to the liquidity of the investment. These concepts are incorporated into cash flow assessments using interest rates. This is simply the cost of using the capital invested, as one would pay rent to use a physical building (Crundwell, 2008). Interest is a recurring cost that could be charged as frequently as daily, however, unless otherwise stated this study assumes an annual basis (Crundwell, 2008).

Modelling has inherent uncertainty and risk that is introduced through the various assumptions and estimations made. Techno-economic models are no different. Process characteristics, equipment specifications, and economic forecasts are some aspects that introduce uncertainty and risk. Sensitivity analyses (SA) are a group of tools used to evaluate the risk and uncertainty in a particular model. The purpose of the SA is to improve the understanding and confidence of the model predictions (Saltelli, 1999). However, SA tools are unable to eliminate the uncertainty and risk associated with the model (Turton *et al*., 2008). Uncertainty focuses on the degree of deviation of the variables under scrutiny, while risk focuses on the probability of a particular outcome (Green & Perry, 2008). Different methods are available to quantify uncertainty and the risk associated with techno-economic models. The next paragraphs present the methods discussed in Turton *et al*. (2008), and Green and Perry (2008).

Forecasting of demand using market conditions explores the uncertainty of the annual sales expected. The other aspect of uncertainty is the selling price of the product which also determines the annual revenue. Economics methods are used to analyse the uncertainty. A convenient method of projecting variability in

commodity prices is fitting regression lines onto historic data and using the resultant equations to estimate future values. Depending on the quality of information available, using economic methods of supply and demand might yield more accurate results as opposed to regression lines. This is because future events that are likely to affect pricing can be incorporated into the forecasting method. However, regression lines capture general trends in historical data (Turton *et al*., 2008). Furthermore, they only take into account what has happened to the commodity price and are therefore blind to different future events.

Scenario analysis considers the accuracy range of multiple variables at the same time and quantifies uncertainty in the estimates made. This analysis explores the extremities of the techno-economic model. Two scenarios are estimated, the best and worst-case, based on the assumed variability in the model inputs. These two cases are compared to the base case where the model outputs are assumed to be at default. Once the variables are changed to their respective best and worst estimations, financial performance indicators such as the NPV and IRR can be calculated for each scenario. The two scenarios are likely unrealistic because the worst-case is too pessimistic and on the other hand the best-case is too optimistic (Turton *et al*., 2008). A decision regarding whether to continue with the project generally relies on positive NPV values for all cases (Turton *et al*., 2008). However, in some situations, a positive NPV value is obtained for the best-case and a negative NPV is obtained for the worst-case. In cases like this probability is introduced into the scenario analysis to further determine the likelihood of a given outcome (Turton *et al*., 2008).

A probability value is assigned to a single change in a variable and that is now termed a scenario. Each scenario has an equal probability of occurring,

therefore the probability of the best and worst-case occurring is a fraction of the number of event scenarios that can be generated using the different variables (Turton *et al*., 2008). A more complex and potentially more accurate way to introduce probability into scenario analysis is through the use of a Monte-Carlo method (Turton *et al*., 2008). In this simulation probability distribution functions are assigned to each variable to incorporate the likelihood of the variable assuming a certain value. Once the probable value of each variable is established, the NPV is then calculated for the particular scenario. The Monte-Carlo method allows for the model to account for probability in individual variables and the combined effects on the NPV are taken into account. One main advantage of this method is the ability to generate multiple scenarios for numerous variables for better probability distributions of the profitability using the NPV or IRR. It is beneficial in projects that straddle the desired outcome or for projects nearing investment because more insight is offered on the probability of the desired outcomes. For projects that produce the desired outcome in all scenarios, the method is unnecessary. Compiling accurate probability distributions and executing multiple scenarios consumes man-hours.

Sensitivity analysis methods take into account incremental changes in the input variables and quantify their effect on the NPV value. An incremental change in an input variable is made and the resultant NPV is obtained, the ratio of the difference in the NPV and the input variable value is the sensitivity coefficient. The riskiness of a change in input values is determined by the extent it affects the profitability of a project (Turton *et al*., 2008). In other words, incremental changes that cause the most significant variation in the NPV value are associated with more risk than those that hardly affect any change. Sensitivity analysis allows for the identification of important variables that require further study to increase model certainty (Green & Perry, 2008).

Another simple sensitivity analysis is a break-even analysis (Green & Perry, 2008). Production costs are first split into fixed and variable costs. Fixed costs are associated with maintenance, insurance, and labour for example. Variable costs consist of raw materials and process-related utilities. This method identifies the minimum capacity required to meet all operational costs termed as the break-even point. Furthermore, the capacity at which the project should shutdown is when only the fixed costs are met. The results can be used to plan profits, price products, equipment changes, and operation level (Green & Perry, 2008).

2.6. Chapter Summary

Chapter 2 aimed to introduce various concepts that are required to compile a techno-economic evaluation. Three furnace flowsheets were evaluated for the production of HCFeMn the SAF, BF, and COREX®. The four sections summarise literature about techno-economic evaluations, alternative technologies to the SAF,

process modelling approaches for the HCFeMn process, and project economic modelling methods.

A techno-economic evaluation is a decision-making framework that takes into account the technical and economic aspects of a capital project. Due to their continuous nature, they are categorised using various levels and are distinguished by the level of accuracy of the estimates made about the fixed capital cost. In the initial stages, different flowsheets are compared using the methods described in the framework. The three other sections of the literature review were then provided to address the requirements of the framework.

Alternative ironmaking technologies that were developed to replace the BF in the Ironmaking industry were reviewed in order to select flowsheets that will be compared to the SAF in the study. Apart from the BF, the FeMn industry has predominantly worked on electricity-based technologies. From the list of alternative ironmaking technologies, two flowsheets were identified using three criteria. However, the two flowsheets were not developed independently. The

COREX® flowsheet was used to develop the FINEX® flowsheet to accommodate fines particles feed. Therefore, the study will use one flowsheet between the two due to the many technical similarities.

Modelling approaches are provided to show what exists in the HCFeMn industry. Furthermore, the chapter highlights the most suitable approaches to modelling the HCFeMn process based on the process information available. Two main approaches exist, empirical and first-principles, the rest of the approaches are a blend. Empirical approaches are well suited for facilities that have production data either from pilot plant or industrial facilities. On the other hand, first-principle approaches make use of fundamental principles of science to approximate process behaviour. When a technology has no published data of the HCFeMn process, as is the case with the Ironmaking technologies, first-principle approaches are more suitable.

Outcomes from the process model are required to compile the economic evaluations. The stream flowrates are also used to calculate equipment, raw material, and utility requirements for CAPEX and OPEX components. Depending on the level of study, other CAPEX and OPEX costs can be obtained from independent sources or estimations can be made using the fixed capital cost value. Economic performance results are evaluated through sensitivity analysis to gain insight into the probability of the desired outcome.

Chapter 3

Model Methodology and Design

The primary motive behind the current investigation was to evaluate the use of alternative furnace technologies in the production of HCFeMn, these alternatives need to be able to reduce the reliance on electricity. To evaluate the feasibility of the alternative technologies that will be compared to the SAF, technical and economic aspects need to be taken into consideration. A conventional way to carry out such an evaluation in the metals and mining sector is through techno-economic evaluation frameworks. These frameworks guide the construction of mathematical models that consolidates all the data and assumptions made about the process required to produce the saleable product. The models are then utilised to inform the evaluator whether the technology under consideration is feasible for the particular application.

Chapter 2 is an amalgamation of literature relevant to the current study obtained from various bodies of literature. Efforts were expended to identify potential solutions, suitable methods available to evaluate these solutions, and the information available that would assist in the evaluation process. The current chapter details the methods chosen to construct the mathematical models and the rationale behind the chosen methods. Chapter 3 is structured into two main sections, the first section (Section 3.1) addresses the aspects related to the technical model. The second section (Section 3.2) deals with the methods relevant to the economic model.

A pre-feasibility study (level 2) (Behrens & Hawranek, 1991) was chosen as a compromise between an opportunity study and detailed feasibility studies. The compromise was made to accommodate the alternative technologies that have not yet been proven to produce FeMn but can commercially produce BF quality pig iron. The opportunity study was condensed into a table (see Table 2-3) of the criteria. Once the flowsheets under consideration are identified, information on the material and energy flow are required. Material and energy flow figures allow for processing equipment costing and running costs estimation (Turton *et al*., 2008). The next two sections detail the methods and tools used to construct the necessary models to perform a pre-feasibility study.

3.1. Mass and Energy Balance Modelling

In Chapter 2.5 a list of the components required to conduct an economic assessment is provided.

The first two components being the total capital expenditure and total operating expenses are obtained after accounting for the material and energy flow through the system and the material phase changes. The chemical engineering field terms this group of calculations mass and energy balancing. Chapter 2.4.1 covers the various methods that can be used to obtain the results of a mass and energy balance. The purpose of the mass and energy balance model is to account for the flow of raw materials and utilities required by the flowsheet and to estimate the capacity of required equipment. The availability of a commercial or pilot plant increases the accuracy of the mass and energy balance estimations. This type of data requires that the furnace is in commercial-scale operation or a substantial amount of research has been conducted on the process. However, in Chapter 2.3 and 2.4, it was shown that there is no literature available in the public domain that details the production or pilot plant data for the HCFeMn process in the COREX® furnace technology. Conversely, the submerged arc furnace (SAF) and blast furnace (BF) have published literature on commercial-scale application of the technologies for the production of HCFeMn. The current chapter will detail the methods chosen, and the model design of the mass and energy balance. Only the SAF, BF, and COREX® will be modelled.

Various process modelling approaches are available in the public domain to model the HCFeMn process in the SAF. The models covered in Chapter 2.4.1 were developed using two main approaches: first-principles and/or empirical relationships. The models were either based on purely first-principles, empirical relationships, or a varying degree of both. The type of approach applied relies on the information available and the purpose of the model being developed. Empirical relationships are only useful when operational or pilot plant data is available to base the process relationships on. Another feature of empirical correlations is that they are unique to the particular furnace and how the furnace is operated. Nevertheless, it is possible to apply empirical correlations to similar furnaces while being aware of the potential errors that will be introduced by the correlation. In contrast, first-principles models are based on scientific relationships that can be explored without relation to any furnace. However, the degree of accuracy for these types of models relies on the assumptions made about the HCFeMn process and how the furnace is operated. Since the current research study aims to conduct a comparison between the four technologies, the first-principles approach was chosen for the HCFeMn process model in all four furnace technologies. The first-principles approach will also address the challenge of insufficient data for the COREX® furnaces. However, the operational data and indices available in the literature for the SAF and BF will be used to guide the assumptions made for all three furnaces.

Figure shows the major steps involved in the development of the mass and energy balance model before any computer programme is used to solve the system of equations.

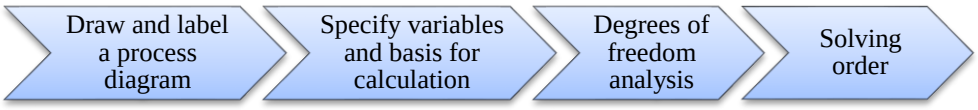

Figure 3-1. The procedure followed to develop the process model (Fraga, 2014).

The system boundary was identified and illustrated in Figure 3-2. The temperature, pressure, composition, and mass flow of the streams crossing the boundary will be used in the calculations. For single-unit furnaces like the SAF and BF, Figure 3-2 suffices as a description of the system boundary. However, double unit flowsheets like the COREX® need an additional system boundary (see Figure 3-3) where the streams between the two units are estimated.

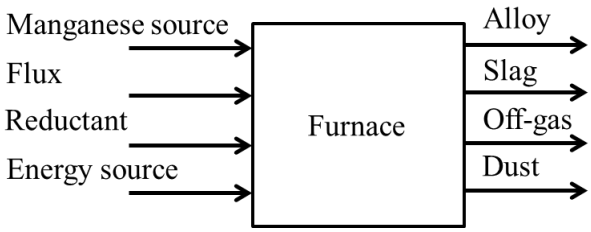

Figure 3-2. General furnace system boundary, and input and output streams used for the material and energy balance.

The first step requires a labelled diagram of the process indicating the information required for a fully specified process. Figure 3-3 details all the stream variables required for a fully specified flowsheet, and it exists within the system boundary defined in Figure 3-2. A two-stage approach was chosen based on the COREX® physical furnace layout discussed in Chapter 2.3, and it was then adapted for both the SAF and BF in the model.

The stream numbering started with the alloy product. The alphabet was used to label the various streams: A alloy, B slag, C reduced solids from stage 1, D carbon source, E electricity or gas stream, F hot reducing gases from stage 2, G manganese source, H fluxing material, I dust, and J off-gases. The symbols in Figure 3-3 are defined as follows: m_T total mass in kilograms (kg), n_T total moles in mole (mol), x_i mass fraction, y_i mole fraction, T is the temperature in Kelvin (K), P is the pressure in atmospheres (atm), and W is the electrical energy (J). All streams enter and leave the process at the same stages for each furnace, except for stream D. In the case of the COREX® stream D is fed into Stage 2, unlike the SAF and BF.

Consequently, some reactions assumed for Stage 1 in the SAF and BF will not occur in the COREX®. The variables described above can be grouped into two types of variables.

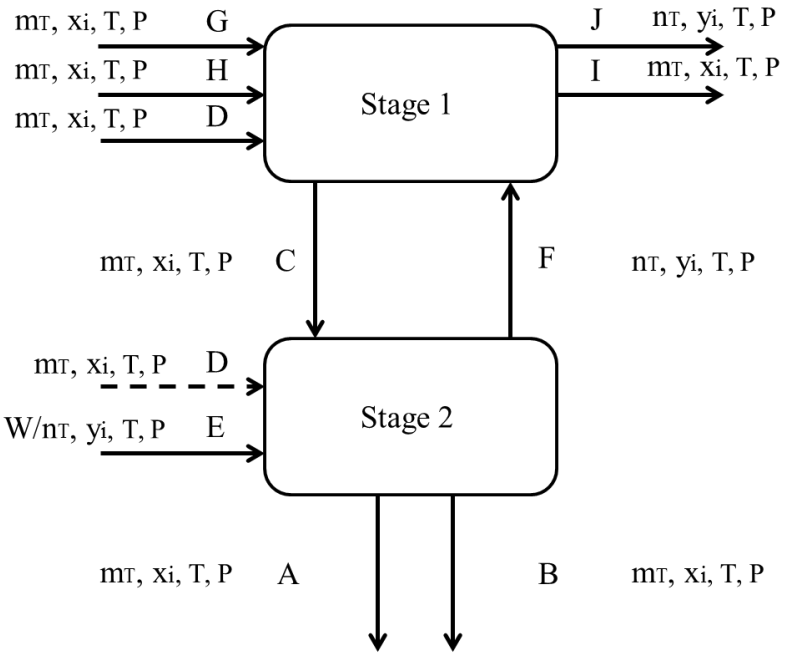

Figure 3-3. Labelled diagram of the process with full specifications of the variables required.

Extensive variables depend on the quantity of material present m_T, n_T, and W, on the other hand, variables like x_i, y_i, T, and P are classified as intensive variables and their values are independent of the quantity of material. The second step consisted of counting the number of variables in the system, the method was adapted from (Himmelblau & Riggs, 2012) in Chapter 12. Himmelblau & Riggs (2012) provided Equation 4 to calculate the number of variables for any mass flow stream in any phase. These variables will then be summed up with any other variable not associated with any mass flow streams.

Equation 4. The number of variables in each stream (Himmelblau & Riggs, 2012).

$$\text{Variable for single stream} = N_{sp} + 2 \qquad [4]$$

For the furnace layout shown in Figure3-3, the number of variables in the system is shown by the final equation obtained in Table 3-1. Stream E can either be a gas stream (BF and COREX®) or an electricity stream (SAF).

The gas stream is associated with mass flow, therefore Equation 5 was applied. From the number of variables identified in Table 3-1,

Equation 5 was used to conduct a DOF analysis on each furnace SAF, BF, and COREX®.

Table 3-1. List of all the furnace variables.

Stream	**Number of variables in each stream**
A	$N_A + 2$
B	$N_B + 2$
C	$N_C + 2$
D	$N_D + 2$
E	$N_E + 2$ OR 1 (SAF)
F	$N_F + 2$
G	$N_G + 2$
H	$N_H + 2$
I	$N_I + 2$
J	$N_J + 2$
Total number of variables	$N_A + N_B + N_C + N_D + N_E$(or 1) $+ N_F + N_G + N_H + N_I + N_J + 20$ (or 18)

Equation 5. Degrees of freedom equation (Himmelblau & Riggs, 2012).

$$N_d = N_v - N_e \qquad [5]$$

N_d is the number of DOF in each furnace system, N_v the number of variables in the system, and N_e the number of independent equations (or assumptions) required to solve for each unknown. N_e can consist of various equations such as component balances, elemental balances, energy balances, chemical reactions with the associated extent of each reaction, relationships between components or streams, and specified components. The only requirement is that each N_e component must be independent of each other (Himmelblau & Riggs, 2012). Table 3-1 listed all the variables to calculate N_v and Table 3-2 lists all the sources uses to obtain N_e. The general approach described was then used to calculate the value of N_d. for each furnace system to know the degrees of freedom before solving. Details of the equations and assumptions used to populate the DOF analysis are available in Appendix B, Table B-1 to Table B-6. The various compositions of the stream A were chosen in such a manner that they adhered with grade B ASTM FeMn alloy standards.

Table 3-2. List of specifications, equations, and relations used in the DOF analysis.

Stream	Origin of equation
	Specified compositions
N_A	Mass fractions, the total mass
N_B	Two mass fractions
N_G	Mass fractions
N_H	Mass fractions
N_D	Mass fractions
N_E	Mass fractions
	Material balances
N_G	2 elemental balances
N_H	Basicity relationship
N_C	Reaction and extent of the reaction for each component in N_C from N_G and N_H, component balance for non-reacting components
N_B	Component balance for non-reacting components
N_D	Reaction with the extent of reaction and component balance for each component in N_C to form N_A.
N_F	Same reactions used by N_D and component balance for non-reacting species
N_E	Reaction with the extent of reaction equation used for N_D for combustion
N_I	Thermal decomposition reactions with the extent of reaction and component balances
N_J	Reaction and extent of the reaction for relevant components in N_G, N_H, and N_D. Component balance for non-reacting species from N_F
Stream	**Origin of equation**
	Energy balance
N_A	Temperature specified based on literature
N_B	$T_B = T_A$ thermal equilibrium
N_C	Temperature specified
N_D	Ambient temperature
N_E	Ambient temperature (COREX®), Temperature specified based on literature (BF)
N_G	Ambient temperature
N_H	Ambient temperature
N_I	$T_I = T_J$ thermal equilibrium
N_J	Temperature specified based on literature
	Relations
N_B	Slag to metal ratio
N_G	Dilution of the manganese iron ratio by reductant ash
N_I	Assume a fraction of solid feed goes to dust

The composition (data available in the Appendix) of all the input streams were specified based on published literature.

Appendix B lists the different manganese ores used to create various feed blends changing the Mn/Fe ratio between 4 and 8. The manganese compositions listed in

Table B-1 are representative versions of the complex mineralogical compositions of the ore material (Chetty & Gutzmer, 2018). Mineralogical compounds are simplified to make mass and energy balance calculations possible (Erwee, 2015). The complex compounds that exist in manganese ores have not been studied extensively enough. Therefore, no enthalpy and reaction data exists to describe the reduction process and the associated energy consumptions (Chetty & Gutzmer, 2018). However, the simplification method introduces errors in enthalpy calculations, because the complexity is not captured in the calculations (Chetty & Gutzmer, 2018). Table B-1 and Table B-3 in Appendix B lists the composition of the carbon and flux sources used in the different furnace models, respectively.

Stream A, the alloy stream, was chosen as the basis in order to closely match the quality of the alloy produced by all furnace systems. Furthermore, the operational items will be specified per unit alloy. Even though production by-products could generate a fraction of revenue, the alloy stream was chosen because it is the principal revenue-generating product in the HCFeMn process. The alloy price is dependent on the Mn composition and the quality of the alloy product which is measured by the composition of various impurities. All the other stream variables were calculated with the aim of producing the same quality and mass alloy from each furnace. Based on the literature by Steenkamp (2020) (assumed equilibrium) and Lagendijk *et al*. (2010) (pilot plant test) the alloy and slag were not assumed to be in equilibrium, because the HCFeMn process does not reach equilibrium. The calculations relied on assumptions from the HCFeMn SAF process to guide the choice of recovery, the deportment of manganese to the off-gas stream, and the slag basicity. The recovery was chosen as 82% for the SAF (Lagendijk et al., 2010) and 83% for the BF and COREX® (Madias, 2011; Kamei et al., 1992). Manganese losses to the slag were based on a 0.8 slag to metal ratio with a 25% MnO slag (Lagendijk et al., 2010). These values were then used to calculate the manganese losses to the off-gas stream as condensate and dust. The assumption of dust losses was used to estimate the vapour loss. This value was adjusted for the COREX®, two thirds of the manganese vapour was assumed to get recycled by the cyclone. The iron was initially assumed to report to the alloy and a Mn/Fe ratio could then be estimated and used to choose the manganese feed mix and the mass. The basicity of the mixture was then calculated and the difference in basicity assumed for the slag was used to estimate the fluxing requirement. The addition of reductant, combustion carbon, and flux was varied to meet the energy requirements and the basicity value. The model requires an iterative process in accounting for the iron that comes in with the ash because it alters the Mn/Fe ratio required.

The following three figures below illustrate the sequence described above to provide more clarity. In solving the furnace systems, slightly different approaches had to be applied due to the link between the mass and energy balance for combustion technologies and how the furnace is physically operated. For the SAF, the energy input calculation is not linked to the mass species inside the furnace which made the calculation less complex. Conversely, combustion energy involves

species reacting and forming other species, therefore, linking the energy balance to the mass balance. The BF stream D, which consists of a carbon source, affects six other streams because it is fed into stage one of the furnace. On the other hand, stream D in the COREX® only affect four other streams, because stream D is fed into stage two. To solve the BF and COREX® systems, iterations were performed using an algorithm that forces the solutions towards convergence to avoid indefinite iterations that lead to no solution (Chapra & Canale, 2010). The energy balance equations across both stages for the BF and stage two for the COREX® were used as the function in the algorithm. The energy balance equation incorporates complex enthalpy equations that will pose a challenge if the function were to be derived.

The diagrams of each sequence are shown in Figure 3-4 to Figure 3-6. Variables need to be obtained in sequence due to how the system was variables and equations were specified. The approach sought to link the key input material stream (manganese source) with the key output stream (alloy).

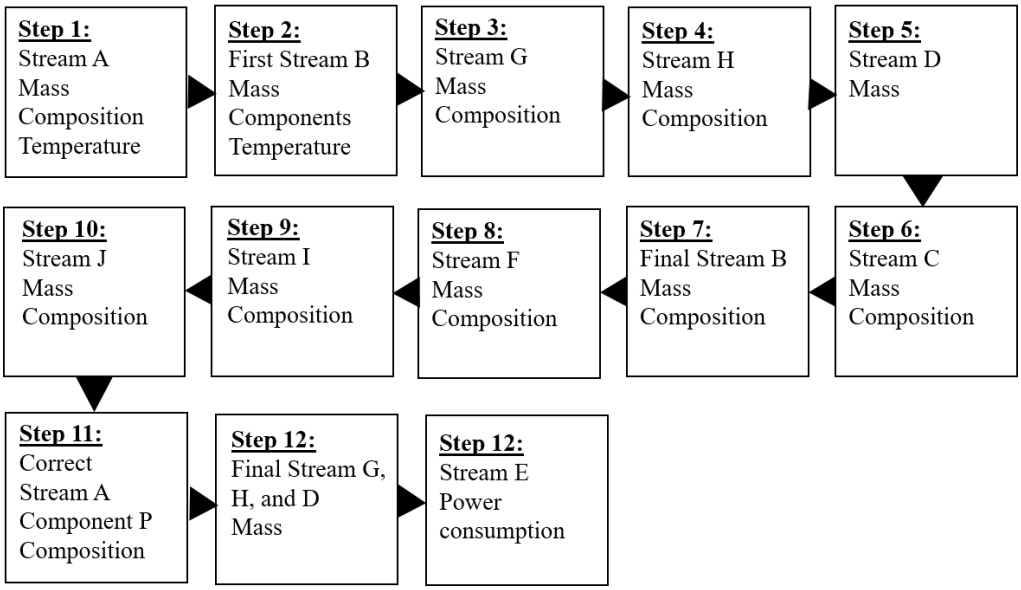

Figure 3-4. Solving sequence flow diagram for the submerged arc furnace.

All the other material streams and the resultant energy consumption are closely related to the mass and quality of the manganese source feed stream G. The manganese source feed was directly estimated from the alloy product using mass balances and assumptions about the process. The SAF solving sequence, Figure 3-4, was the simplest out of the three furnaces due to the nature of the energy source. The first three steps of the sequence were initiated the same way, by estimating and fully specifying the basis and assuming the two slag compositions (stream B) to calculate the manganese ore required by the alloy product. The challenging aspect of the calculation was estimating the iron that comes in with the manganese source

since the coke-anthracite mix contains iron and the electrode casing adds more iron to the process. Once the manganese feed (stream G) requirement was known the flux blend (stream H) was estimated based on an imaginary basicity value.

The value accounted for fluxing compounds that come in with the carbon source and report to the slag. Carbon requirements were mainly based on reaction equations in the furnace. Stream E (electricity) only contributes electrical energy into the system and therefore doesn't affect the mass balance of the exit streams. This property of the energy source made the calculation sequencing less complex when compared to the combustion-based furnaces. The mass flows of the streams were calculated directly before the last step where an energy balance equation was used to estimate stream E.

In Figure 3-5 andFigure 3-6, a slightly different approach was taken due to combustion being the primary source of energy for the process.

An iteration loop towards the end of the sequence was implemented to address the relationship between the streams.

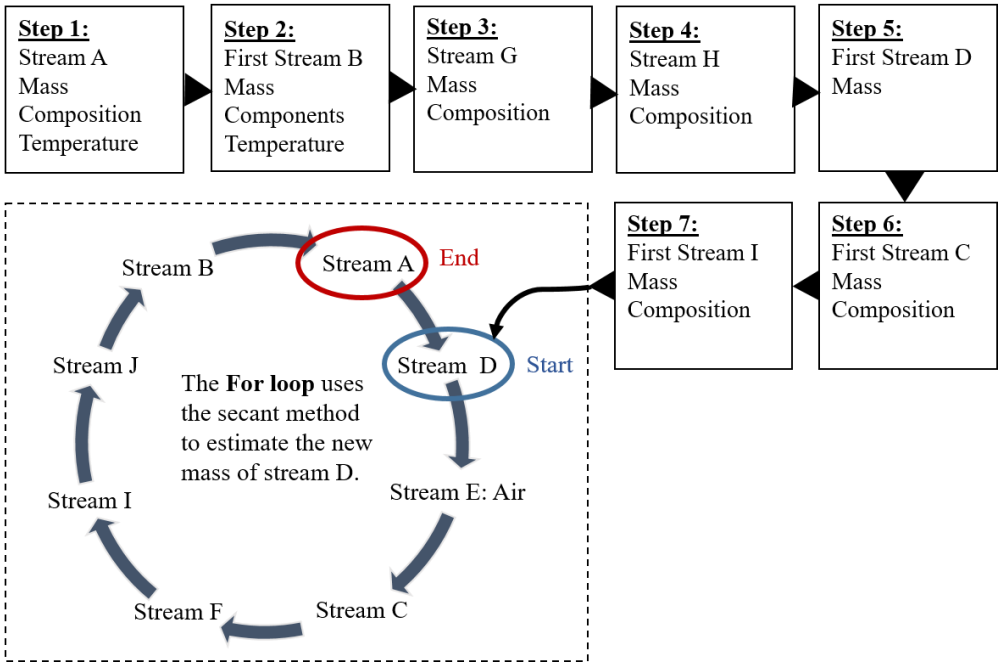

Figure 3-5. Solving sequence flow diagram for the blast furnace.

The iteration loop uses a numerical method, illustrated in Equation 6 below called secant to closely approximate the mass flow rate of the carbon (stream D) and

air/oxygen (stream E). The method involves updating stream information and recalculating stream D and E to yield a better approximation with each iteration. The first three steps were kept the same, without accounting for any electrode iron. In the BF more slag is generated as a by-product of combustion, as a result, more flux will be required to significantly change the basicity value of the slag. The initial estimation of carbon source (stream D) mass was made using the amount of carbon required to achieve reduction in the furnace. Once an estimation of the stream D was available, other streams (C and I) were estimated. The loop was terminated when the last three values of stream D were nearly identical. The secant method was chosen for its ability to utilise only the function in the iterative equation (Chapra & Canale, 2010).

Equation 6. The secant method iterative equation

$$z_{i+1} = x_i - \frac{\delta z_i f(z_i)}{f(z_i + \delta z_i) - f(z_i)} \quad [6]$$

With each numerical method, there are advantages and drawbacks. The secant method doesn't require complex derivatives, it converges quickly, and uses a simple algorithm. However, it can be inefficient and possibly divergent if the value of δ is too large (Chapra & Canale, 2010).

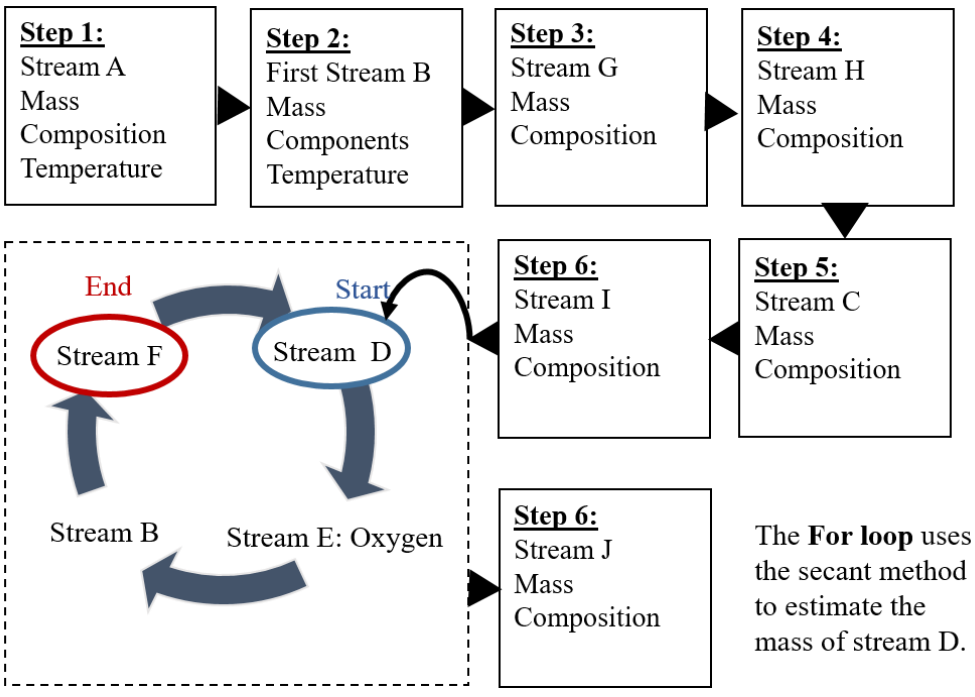

Figure 3-6. Solving sequence flow diagram for the COREX®.

The difference between the BF and COREX® solving sequence in Figure 3-6 is where the stream D crosses the furnace boundary and the physical boundary that exists between the solid-state reactions zone and the liquid-state reactions zone. The differences in the physical setups of the furnaces reduced the number of streams required in the iteration loop from 8 to 4. The estimation of stream D only includes the liquid-state reduction carbon requirement. The same process is done at the start of the sequence and the last step (6) calculates the off-gas (stream J) mass and composition once the reducing gases (stream F) are known. Once the DOF analysis was achieved and the solving sequence was determined the next step was to develop the models on the Python programming language and Excel as an interface. Building process calculations using Python code rather than Excel worksheets is different. Unlike the list of values found in Excel spreadsheets, Python code allows for more flexibility in the structuring of data and methods of calculation. The model was based on many basic code building blocks available in Python 3.3 some of which are covered in the current section. Appendix B shows the different parts of the Python code and the Excel spreadsheets used when modelling.

Energy recovery was assumed for all three furnaces making use of off-gas components such as CO and H_2. For the SAF, no other units require recovered energy all electricity generated is directed back into the process. The BF has various processing units that require recycled energy. The energy was distributed to sintering, blast air heating to 1050 ℃, and some of the electricity went towards operating the BF. COREX® recycled energy is all converted into electricity first since the oxygen is fed at room temperature and no other units are required. Once converted, a portion of it is used for oxygen production and operating the COREX® unit. The model assumed that the efficiency of the electricity generation unit is 0.4 (Kemp, 2007). Furnace CO_2 emissions were estimated by accounting for all the known carbon that comes into the process (Lindstad *et al*., 2007). This was done by accounting for CO and CO_2 in the off-gas, carbon emitted through coking (BF), and the carbon content of the electrodes (SAF). Furthermore, SAF electricity indirect emissions from the energy provider were accounted for in the final calculation (Cairncross, 2017).

3.2. Economic Modelling

Three main financial statements report a company's performance the balance sheet, income statement, and cash flow statement (Crundwell, 2008). However, the balance sheet reports accumulated information over the life-time, while the last two reports address annual performance. Capital project appraisal methods are based on the cash flows statement approach for each year over the lifetime of the project (Crundwell, 2008). Cash flow statements consist of values based on two aspects of the process model and accounting principles. Chapter 3.2 deals with the approaches chosen to develop the various elements of the economic model applied to all three flowsheets. The model provides estimates of the fixed capital expenditure (CAPEX) through equipment sizing and costing, operating expenditure (OPEX) from the raw

material stream and energy balance, revenue forecast based on the quantity of product, and working capital estimations from the production schedule (Crundwell, 2008).

Metallurgical plants utilise various equipment to execute the processing steps required to achieve the product specification. The HCFeMn process model focuses on the changes that occur in the furnace to estimate different stream specifications such as temperature, composition, and mass flow rate. Some of these streams that flow in and out of the furnace still require pre-processing before feeding into the furnace and post-processing before sale or waste disposal. These changes are achieved using unit processes that alter the temperature, composition, particle size distribution, phase, and many more stream characteristics. Unit processes usually consist of various equipment dedicated to producing the specified stream specifications. Unlike in chemical plants where streams can be continuous and consist of fluid material such as gas or liquid, metallurgical plants process and sell solid material. However, fluids such as gases are produced or fed into the process, and liquids are mostly used in cooling or cleaning. All these smaller unit processes, apart from the furnace, contribute to the capital required to build the plant. Moreover, unit processes may have individual fuel and utility demands which contribute towards production costs. For the current study, a hypothetical boundary around the process was defined so that battery limit capital estimates can be executed.

Financial modelling methods are addressed in the next two sections (3.2.1 and 3.2.2). The first section (3.2.1) focuses on methods used to estimate the various cash flow components as a result of capital investment and production activities. In the second section (3.2.2), methods used to consolidate all the cash flow patterns and the analysis of the financial performance over the project life are provided.

3.2.1. Cash flow statement components

Section 2.4.2 mentions the various types of process diagrams that convey certain process information for different applications.

Equipment information required by this study can be adequately described by a block flow diagram (BFD). Figure 3-7 to Figure 3-9 are BFDs for the three furnaces under evaluation. Major unit processes were taken into account and these unit processes could either consist of a group of smaller equipment or a single item. Capital cost estimations associated with these unit processes require operating variables calculated from the mass and energy balance model. The operating variables are obtained from the mass and energy balance and are expressed in unit material per unit alloy product. Major raw material flows and utilities were taken into consideration in the calculations. Extras such as minor fuels and motor lubricants, for example, were not explicitly included in the calculations.

The SAF BFD in Figure 3-7 shows the major processing areas required when producing HCFeMn using a SAF. Each processing area, demarcated with a block, groups an array of activities and equipment applied to produce a stream into the next block. Major equipment that was used to estimate the capital cost component are listed in Table 3-3. The raw materials handling area has a briquetting plant that recycles the furnace dust captured from the off-gas system and alloy handling plant fines. A closed furnace accompanied by a power plant to recover energy in the form of electricity was chosen for the SAF flowsheet. Gas handling involves the processes required to separate the dust recycle stream and the gas generated in the process. The by-product gas is then used to recover energy in the form of electricity. Alloy reclamation requires crushing, screening, and magnetic separation equipment to facilitate separation of the slag and alloy that got entrained. Similarly, the alloy plant facilitates material size reduction to meet ASTM particle size specifications.

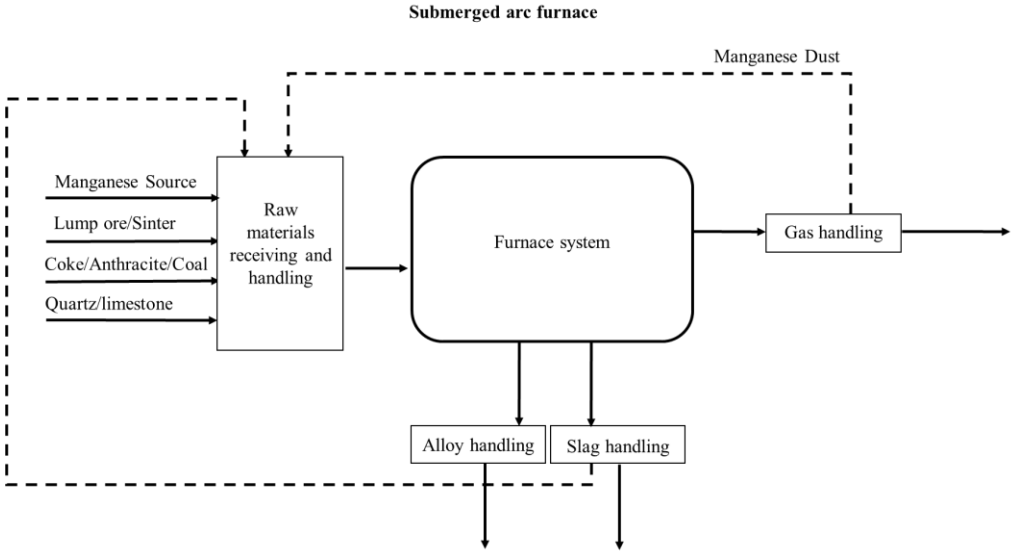

Figure 3-7. Submerged arc furnace block flow diagram showing major unit processes (Moolman & Van Niekerk, 2018; Steenkamp *et al*., 2018).

Table 3-3. Major equipment identified in the Submerged arc furnace block flow diagram (Moolman & Van Niekerk, 2018; Steenkamp *et al*., 2018; Wellbeloved & Kemink, 1995).

Raw Materials	**Furnace System**	**Gas Handling**	**Alloy Handling**	**Alloy Recovery**
Briquetting plant	Transformers Furnace system (closed)	Venturi scrubber: two-stage Wet electrostatic precipitator (ESP)	Grizzly screen Multi-deck screen 1 (x3)	Grizzly screen Jaw crusher

		Power plant	Jaw crusher Multi-deck screen 1 (x3) Multi-deck screen 1 (x3) Multi-deck screen 1 (x3)	Screens x 4 Jig x 2 Cone crusher Electromagnet

The BF, BFD in Figure 3-8 and the equipment list in Table 3-3, has extra processing units in the raw materials handling area. The manganese ore is sintered before it is fed into the furnace along with the coal coked in ovens. Blast air is preheated in a gas-to-gas type heat exchanger that uses recycled off-gas combustion as a heat source.

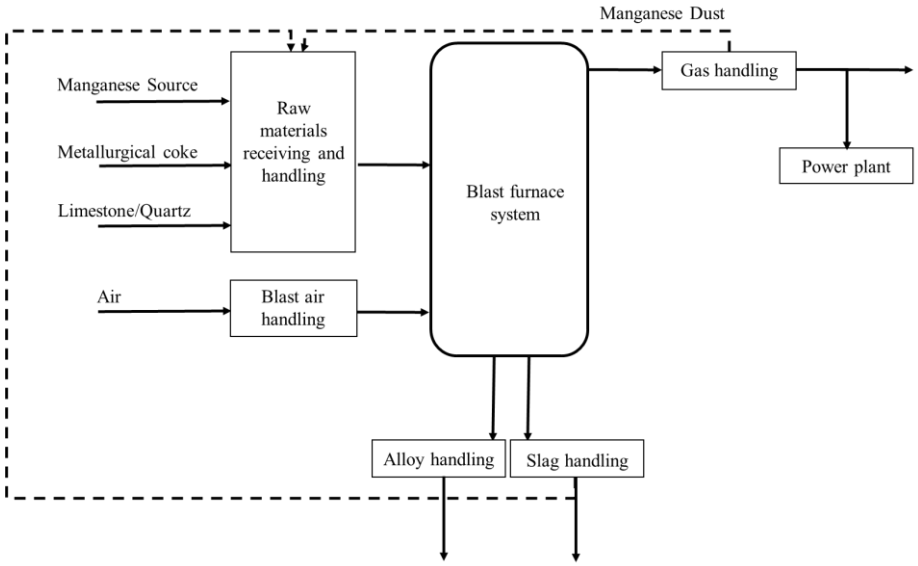

Figure 3-8. Blast furnace block flow diagram showing major unit processes (Sen, 1997).

The surplus of the gas is fed into a power generation unit to recover energy in the form of electricity. Alloy resizing and reclamation unit processes remained the same from what was described in the SAF process flowsheet. The furnace system mentioned in Table 3-3 includes the bell top feeding system. Gas handling facilitates gas clean-up of the off-gas for use during combustion and electricity generation.

Table 3-3. Major equipment identified in the blast furnace block flow diagram (Pfeifer, 2009; Sen, 1997).

Raw Materials	**Furnace System**	**Gas Handling**	**Alloy Handling**	**Alloy Recovery**
Sinter plant	Furnace system	Dust cyclone	Multi-deck screen 1 (x3)	Jaw crusher
Coking plant		Venturi scrubber	Jaw crusher	Screens x 4
		Wet electrostatic precipitator (ESP)	Multi-deck screen 1 (x3)	Jig x 2
		Power plant	Multi-deck screen 1 (x3)	Cone crusher
			Multi-deck screen 1 (x3)	Electromagnet

The COREX® process BFD and equipment list are shown in Figure 3-8 and Table 3-4. The equipment layout in the COREX® process flowsheet is slightly different from the previous two flowsheets. Recycling of the dust and off-gas occurs online, unlike with the previous flowsheets where the dust is collected and mixed with fresh material for recycling. Once the particles are removed using a cyclone, the reducing gas stream is produced. The stream is then split between the reduction shaft and a scrubber that recycles some of the cooled gas back into the furnace system. The second scrubber cleans the export gas and it is sent to the power plant for electricity generation. The COREX® furnace system is more complex than the BF and SAF. This is due to the gas and dust recycling units being classified as part of the furnace system. Therefore, the COREX® unit boundary will consist of all the gas handling units listed in Table 3-4. A hot gas cyclone is used to recycle particulate matter back into the melter-gasifier, and the scrubbers are used to remove CO_2 before the gas is returned into the reduction shaft. Other unit processes include coal agglomeration, oxygen production, and power generation. FINEX® has a very similar layout. However, the reduction shaft is replaced with 3 or 4 fluidised bed reactors (FBR) to carry out reduction. Furthermore, a hot compacting unit is required to agglomerate the particles from the reactors in series. Depending on the capital cost of one FBR and the hot compacter, the FINEX® could potentially have slightly higher capital costs when compared to the COREX®.

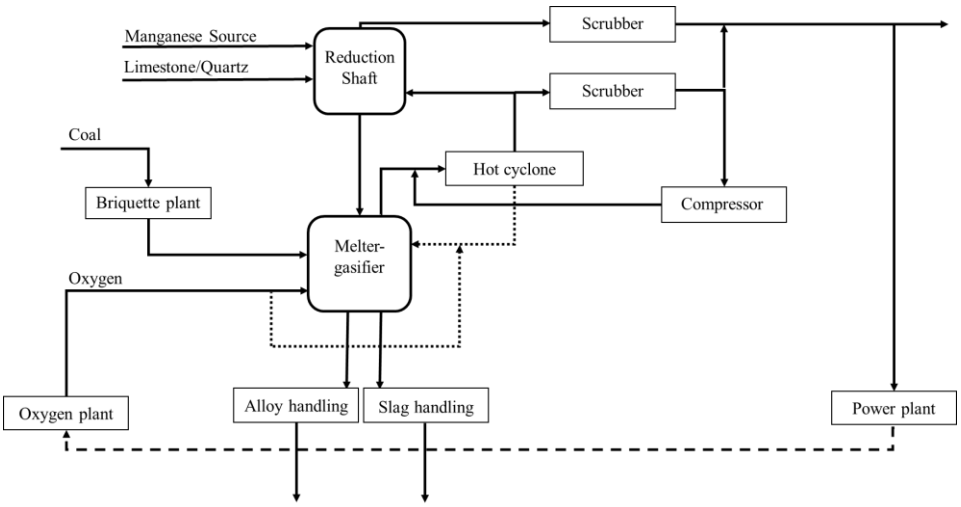

Figure 3-9. COREX block flow diagram showing major unit processes (Kumar *et al.*, 2008).

The equipment list derived for the various plant configurations were used to guide data gathering required for the economic model along with the stream information from the furnace model. Apart from raw materials and energy directly required for the product, all auxiliary equipment requires additional energy and materials to function.

Table 3-4. Major equipment identified in the COREX® block flow diagram (Kumar *et al.*, 2008).

Raw Materials	**Furnace System**	**Gas Handling**	**Alloy Handling**	**Alloy recovery**
Briquetting plant	Reduction shaft	Power plant	Multi-deck screen 1 (x3)	Jaw crusher
Oxygen plant	Melter-gasifier		Jaw crusher	Screens x 4
	Burden distribution system		Multi-deck screen 1 (x3)	Jig x 2
	Hot cyclone		Multi-deck screen 1 (x3)	Cone crusher
	Venturi scrubber		Multi-deck screen 1 (x3)	Electromagnet
	Venturi scrubber			
	Compressor			

However, this study only considers the production costs to consist of the raw materials and electricity directly required for the HCFeMn product, electricity generated by the power plant, and the required process water to cool the furnace crucibles.

The mass and energy balance developed for the HCFeMn process only estimates raw materials and the off-gas by-product. Cooling water requirements were estimated using values found in published literature. In the auxiliary units, only the raw material streams required as feed into the furnace crucible were taken into account. Fuel and utility requirements for other processing units such as raw materials handling, gas handling, alloy handling, and alloy recovery were not considered. However, estimates were made where significant amounts of recycled fuel such as off-gas or electricity were required by the unit process. Detailed specifications of auxiliary units that allow for estimating fuel and utility requirements are beyond the scope of the calculations executed in the current study.

Table 3-5 identifies the main raw materials, utilities, and consumables required by each furnace type. These flow rates are based on production at full capacity and these figures were used to calculate direct manufacturing costs. The values obtained from the mass and energy balance for the components listed in Table 3-5 were then used in conjunction with the formulas found in Table 3-6. Equipment cost calculations involved estimating the cost of equipment using flowrates estimated from the mass and energy balance model.

Table 3-5. List of raw materials and utilities required by different furnace flowsheets.

Production item	**Units**	**SAF**	**BF**	**COREX®**
Manganese ore	t/t	✓	✓	✓
Anthracite	t/t	✓		
Coke	t/t	✓		
Coking coal	t/t		✓	
Coal	t/t			✓
Quartzite	t/t	✓		
Limestone	t/t		✓	✓
Oxygen	Nm^3/t			✓
Electricity	kWhr/t	✓		
Electrode paste	kg/t	✓		
Water	m^3/t	✓	✓	✓

Equipment costing methods were guided by the cost data available in literature in the public domain. Some authors provide costs for erected equipment which

normally includes extra items such as instrumentation and construction costs, for example.

Cost data for other equipment was found in capital cost estimation textbooks where a free on board (FOB) cost is provided. Various factors are provided to account for extras such as instruments, buildings, freight, taxes, and other extras. The cost index formula was used to account for the effects of inflation over the years.

Table 3-6. Equipment costing equations, extracted from Table 2-8 in Chapter 2.5.

Method	**Formula**	**Application**
Cost index	$C_t = C_0 \frac{I_t}{I_0}$	Same capacity was built years ago, only the facility cost needs to be adjusted.
Cost-capacity	$C_2 = C_1(\frac{Q_2}{Q_1})^n$	Different capacities of the same equipment have been built.
Method	**Formula**	**Application**
Bare module method (Woods, 2007)	$TM = fC_2$	Total module costs comprise various factors being accounted for such as; concrete, piping, insulation, electrical, paint, support, labour, material type, instruments, taxes, freight, and duties.

Cost-capacity estimates were used on all equipment, however, some need the extra step of adding factors to account for various extra costs. More details of the data and various assumptions that were used to calculate equipment costs are available in Appendix C. Table 3-7 lists the cost factors that were taken into account when estimating the OPEX.

Table 3-7. OPEX components calculation methods.

Component	**Application**
Raw materials	Material balance with a predicted production schedule and transportation costs.
Labour	$L_2 = L_1(\frac{Q_2}{Q_1})^n$ account for capacity differences in labour costs for equipment.
Utilities	Material balance: water, air, fuels, water, waste disposal Energy balance: Electricity Municipality specific

Maintenance	A fraction of the CAPEX 4%– 12%
Insurance	1% of fixed capital costs
Rentals	Average fees per area in plant location
Administrative, Sales and distribution	Estimated as a percentage of the annual production

OPEX classifies costs associated with direct production, plant overheads, administrative, and sales and distribution (Crundwell, 2008). At the current phase of the study, only the direct manufacturing costs such as the raw materials and utilities could be estimated from the material and energy balance. Costs that are not directly linked to the material and energy balance were estimated as a fraction of an OPEX component or the CAPEX itself. Some costs were either lumped together or neglected for the current level of study due to information being insufficient to make a reasonable estimation.

Working capital is a term used for funds required by the project to sustain operations which includes accounts payable, inventories, and accounts receivable (Crundwell, 2008). For the current study, the working capital was estimated at 15% of the fixed capital costs (Crundwell, 2008).

Price forecasting is an important aspect of estimating the amount of money that will be generated by the product termed revenue. Furthermore, raw material and utility costs fluctuate over time and this affects the cost of production. The price is derived from analysing the market requirements of the commodity industry. Service agreements assist in determining production targets to meet demand. A take-if-offered service agreement was assumed where-by all product manufactured will be purchased (Crundwell, 2008). This agreement allows for the throughput to be fixed over the analysis period. Furthermore, this type of agreement reduces the risk of debt financing (Crundwell, 2008). Commodity price inflations were estimated using historical data found in the public domain. Regression lines were fitted onto the data and the various equations were used to project commodity price inflations.

3.2.2. Discounted cash flow analysis

Cash flow statements consolidate all economic activities that cause money to flow in and out of the project. All economic activities should adhere to the laws that govern a particular country. All companies are legally required to adhere to the tax laws stipulated by the current government. Discounted cash flow (DCF) calculations are conducted on the after-tax amount, therefore taxation is an important cost to factor in (Crundwell, 2008). Taxes are costs charged by the government on the profit a company has generated from economic activities in a particular country. The tax position of a company/project can be influenced by many factors. Projects are normally treated as stand-alone projects where-by the losses incurred by the project are carried over to the next tax year and no other projects can off-set the losses (Crundwell, 2008). Depreciation or capital allowances are tax deductions made on the cost of tax due to equipment that was

purchased for the production facilities (Crundwell, 2008). The South African government has tax guides for capital incentive allowances for plant and machinery. The guide states that new or unused assets acquired after 1 March 2002 are subject to allowances over 4 years (PKF South Africa Inc., 2017). For the first year 40% and 20% for each year thereafter (PKF South Africa Inc., 2017). For used machinery, the depreciation is at 20% each year (PKF South Africa Inc., 2017).

Cash flow models are designed to calculate the value that can be derived from capital projects by investors (Crundwell, 2008). When choosing a project to invest in, there is an opportunity cost attached to it. An opportunity cost is a loss an investor incurs after investing in a less lucrative project with a similar magnitude of risk as another one that offers greater returns (Crundwell, 2008). Analytical techniques are applied to facilitate decision-making between projects. The aim is to select a project(s) that creates value at a greater rate with a similar magnitude of risk (Crundwell, 2008). Chapter 2.5 covered methods applied to a cash flow statement when assessing capital projects. Methods that were applied to determine value in the current study were discounted payback period, net present value, profitability index, and internal rate of return (IRR). These discounted cash flow methods take into account the time value of money. In conjunction, the criteria summarise the value of the capital project.

The methods chosen are the most widely applied when assessing capital projects and they were chosen to meet the criteria required for decision-making.

Table 2-13 and Table 2-14 lists the various equations used to conduct the financial analysis using the cash flow statement generated. Details of the cash flow statement and the various outcomes are available in Appendix C and Chapter 4.

Uncertainty and risk were explored using two approaches: a scenario and sensitivity analyses. The scenario analysis involved exploring variables from two perspectives, the best-case and the worst-case. Raw material and electricity prices were varied using the average difference between the actual historical data and values estimated using the regression line fitted onto the same data. Other estimated production costs were varied using the extreme limits of the range suggested by literature for the particular variable, where applicable. For the CAPEX amount, the estimation accuracy of the chosen level of study was used to vary the capital cost estimation during the scenario analysis. A sensitivity analysis was then performed using Equation 7 on the base case scenario (Turton *et al*., 2008). Three cost elements were explored, namely, energy source price, manganese feed price, and the alloy selling price.

Equation 7. Sensitivity analysis equation.

$$\Delta NPV_i = \sum S_j(\Delta w_i) \qquad [7]$$

$$S_j = \frac{\Delta NPV}{\Delta q}$$

Equation 7 makes use of the two points to estimate the coefficient S_j for each variable in the system. All the S_j coefficients are used to create the ΔNPV equation. For the current study, the variable S_j was estimated for the product FeMn, energy source, and manganese feed.

The FeMn product was chosen because it is directly linked to the revenue generated by the project. The manganese feed and energy source were chosen due to the significant contributions towards production costs. Each variable was varied between -20% +20%, the NPV was determined for each change, and a sensitivity plot was constructed.

A break-even analysis was conducted on the three furnace technology to get insight into how sensitive the project is to product demand. Production cost items were divided into two groups, fixed and variable costs. Fixed costs are incurred regardless of production capacity and variable costs are directly linked to the production capacity. Two equations, Equation 8 andEquation 9, were applied to calculate the break-even and shutdown point capacity requirements.

Equation 8. Break-even capacity

Break-even capacity = (Fixed costs + Variable costs)/Revenue [8]

Equation 9. Shutdown capacity

Shutdown capacity = Fixed costs/Revenue [9]

Break-even indicates the production capacity required for the project to meet its production costs and not make a profit. The shutdown capacity indicates a point where the plant only meets the fixed cost obligation and makes a loss on any costs incurred to produce the required capacity, which indicates that operations need to be discontinued at this point.

The best performing technology was subject to a sensitivity analysis of the NPV to process details. In HCFeMn production, the recovery of manganese to the alloy

phase is the most important variable to control. This variable determines the amount of value extracted from the primary raw material which is the manganese source. However, direct control of this variable is not physically possible. Therefore, changes in this variable will affect more than just the amount of ore fed into the furnace. This analysis assumed that the same quality alloy gets produced at differing recovery conditions. In the model, changes were made to the percentage of MnO in the slag while the alloy Mn percentage was kept constant. The recalculated NPV value was then captured in a separate sheet. Accumulated effects of the changes in reductant fed, energy demand, and ore mass flow changes were equated to an NPV value. The sensitivity of the NPV value to operational aspects was quantified to assess the risk associated with not operating at the optimal recovery specified in the base case.

3.3. Chapter Summary

Chapter 3.1 details the criteria used to select the flowsheets under investigation and the various methods used to build the necessary two-part models. This chapter details the criteria used to select the ironmaking technologies.

They were selected using three main categories. Each category addresses an aspect of the problem statement. The first category requires the technology to be able to produce the desired product when compared to the BF ironmaking process. Category number two is focused on the main problem statement, which is removing the heavy reliance on electrical energy in the process. The third category is concerned with the maturity of alternative technology and how far it has been implemented in the Ironmaking industry. Two technologies matched the criteria, however, they were developed in succession. Therefore, the COREX®, which was developed before the FINEX® formed part of the study. However, inferences for the FINEX® were drawn from the COREX® flowsheet outcomes.

Due to the lack of data of the HCFeMn process in the COREX® the mass and energy balance model approach was predominantly first-principles-based. However, the HCFeMn process is well document for the SAF and somewhat documented for the BF. The data obtained for the process in the other two furnace flowsheets were used to inform the choice of assumptions for the COREX® to create a more realistic model. Details of the data, equations, assumptions, and approaches are provided in Chapter 3.1 and Appendix B.

Chapter 3.2 details the methods used to collect the necessary economic data and consolidate it into one model. BFDs based on published literature were constructed and the mass and energy balance model outcomes were used to size the equipment. Cost components that were directly linked to the technical model were the fixed capital estimates, raw material usage, and electricity usage. Other cost components were estimated using the recommended industry averages. Raw material and electricity costs inflations over the life-time of the project were modelling using

regression lines fitted on historical data. Methods used for the scenario analyses and sensitivity analyses were also provided. The data used, for example calculations, equations, and images of the user interface are provided in Appendix C.

Chapter 4

Results

In earlier chapters, furnaces from ironmaking were reviewed and one was selected to compare to the existing furnace technologies that can produce HCFeMn. Techno-economic analyses were conducted on the SAF, BF, and COREX® furnace technologies. Technical and economic models were developed to assist in the evaluation. In the current Chapter, the results of the modelling efforts discussed in Chapter 3 are presented. Chapter 4 consists of two sections, the first section discusses the outcomes of the process modelling, and the second section presents the outcomes of the techno-economic evaluation. Process model results are presented as quantities required to produce a ton of HCFeMn alloy. Economic modelling results are provided as economic indicators for a base case and a sensitivity analysis.

4.1. Mass and Energy Balance Outcomes

In Chapter 3.1 the design of the mass and energy balance model was presented and the following section details the outcomes yielded shown in Table 4-1 to Table 4-3. The mass and energy balance outcomes of the SAF are compared and discussed using literature values as guidelines. However, due to the gaps that exist in operational data found in the public domain for the BF and the COREX®, only qualitative comparisons were conducted on the outcomes. Table 4-1 to Table 4-3 only list important input variables, however, Appendix B provides all the inputs and outputs of the models. Mass and energy balance outcomes for the COREX® were compared to BF and SAF published literature values.

All three models produced an HCFeMn alloy with 75% manganese and a maximum of 6% carbon. The alloy components were kept constant. A target recovery value was obtained from literature along with a typical basic process slag manganese content. Assuming that all the iron in the process goes into the alloy the Mn/Fe ratio was estimated and used to choose an ore blend. The target recovery and the typical losses to the slag were used to fix the amount of manganese lost to the off-gas stream. The target basicity value chosen was also informed by literature and used to estimate the flux requirements based on the ore mixture. Once the ore Mn/Fe ratio and mass were estimated, forward calculations using various assumptions obtained from literature were conducted. The values of the recovery and basicity were recalculated as adjustments were made to the amount of flux and reductant. Once the alloy and off-gas deportment was calculated, the excess manganese reported to the slag.

In Table 4-1, the SAF base case outcomes are provided and two different sets of literature data. Lagendijk *et al*. (2010) reported data obtained from SAF pilot plant tests. The tests made use of South African ores, Gloria and Nchwaning, which are known to have basic properties (Steenkamp & Basson, 2013). South African ores produce higher slag basicity values and require fluxing with quartzite (S E Olsen *et al*., 2007). Ahmed *et al*. (2014) provided data produced through modelling the HCFeMn process. The model made use of unnamed ores with a higher percentage of acidic components, SiO_2 and Al_2O_3. As a result, a mixture of limestone and dolomite was used to flux the slag (Ahmed *et al*., 2014). The SAF recovery target was 82% (Lagendijk *et al*., 2010). Slag basicity was monitored around 1.1– 1.4 (initial estimate 1.3) based on the equation supplied in Table 4-1.

Table 4-1. Values of the mass and energy balances in the SAF compared to two sources of literature.

Stream ratios (per ton alloy)	**SAF model**	**(Lagendijk *et al*., 2010)**	**(Ahmed *et al*., 2014)**
Inputs and assumptions			
Manganese in alloy (%)	75.0	77.1	75.2
Carbon in alloy (%)	6	6.5	7
Manganese recovery (%)	82.8	82.1 ± 0.5	75.7
Basicity ($CaO+MgO/SiO_2$)	1.2	1.3	1.4
Outputs calculated			
Manganese feed (t/t)	2.15	2.73	2.02
Mn/Fe ratio - feed	6	5.4	5.9
Reductant (t/t)	0.304	0.735	0.458
Flux (t/t)	0.141	0.11	0.385
Slag/metal	0.69	0.82	0.69
MnO in slag (%)	31	26 - 27	19
Electricity (kWh/t)	3224	3150	2500– 3906
Outputs - Off-gas components			
CO/CO_2 off-gas	0.7	No data	4.1
Emissions (indirect included) (t CO_2/t alloy)	4.2	No data	1.4 (process only)

Manganese feed estimates were within ranges for the SAF (Ahmed *et al*., 2014; Broekman & Ford, 2004). Higher masses of manganese feeds will be required for higher manganese content alloys (Lagendijk *et al*., 2010). However, the manganese feed has a higher Mn/Fe ratio when compared to literature. This is due to the model assuming the higher value of manganese losses to the slag with higher MnO mass fractions than observed in literature. Furthermore, more iron was assumed to come in with the ore. Manganese recovery calculated are in line with basic ore recovery values in the 82– 83% range (Lagendijk *et al*., 2010). Reductant estimations made, using the model, were 33– 58% lower. The simplifications in the model did not account for the circulation of alkalis between the solid and liquid-state (Tangstad

and Olsen, 1995). Flux additions in the model were 28% higher than the basic ore process. However, the slag mass calculated by the model was lower by 19% with lower basicity. This observation could be attributed to the lower manganese content in the ore and higher manganese content in the alloy in the data from literature. All these variables impact the operational costs estimated using the model. Higher estimated manganese losses and flux additions increase energy consumption, as a result, operational costs increase. Underestimated reductant additions reduce the operational costs when considering raw material consumption. The mass and quality of the manganese feed also impact the costs associated with raw material purchasing.

BF base case model inputs and outcomes plus two literature sources are listed in Table 4-2. BF literature data was more challenging to find, select, and consolidate into a coherent list. This is due to the data being outdated, therefore, the data collection and reporting style is not of a similar standard (Featherstone, 1974 and Kozhemyacheko *et al*., 1987). Furthermore, some sources publish data with different feeds such as low-quality ores, oxygen enriched blast air, pulverised coal fed in with the blast air, and steam (Kamei *et al*., 1992 and Madias, 2011). All variables affect the coke energy requirement, slag, and alloy properties which inevitably alter the production costs. Only qualitative comparisons can be conducted on the BF.

Featherstone (1974) reported South African production data based on very high-quality ores using a mixture of basic South African ores and various foreign acidic ores. Furthermore, only hot air and coke were fed into the furnace. Kamei *et* al. (1992) reported pilot test data feeding acidic ores, pulverised coal, oxygen enriched blast air, and steam into the furnace. The manganese recovery target was 83% in the middle of the range 80– 85% (Madias, 2011; Kamei et al., 1992). Furthermore, the basicity was kept around 1.3– 1.5 (initial estimate was 1.4) (Featherstone, 1974; Kamei *et al*., 1992, and Madias, 2011).

The off-gas ratio of CO to CO_2 for the SAF model reports much lower CO in the off-gas when compared to the calculations by Ahmed *et al*. (2014). However, Swamy *et al*. (2001) report the value 0.7 similar to what the model estimated. The lower CO justifies the lower reductant requirements estimated by the model. SAF emissions for the process are 1 t CO_2/t alloy and the 3.2 accounts for indirect emissions from electricity production. Ahmed *et al*. (2014) report 28% higher emissions than what the SAF reports and this is a direct result of lower reductant feeds.

Table 4-2. Values of the mass and energy balances in the BF compared to two sources of literature

Stream ratios (per ton alloy)	**BF model**	**(Featherstone, 1974)**	**(Kamei *et al*., 1992)**
Inputs and assumptions			
Manganese in alloy (%)	75.0	78.4	75.1
Carbon in alloy (%)	6	No data	6.7
Manganese Recovery %	82.5	No data	79.3– 85.6
Basicity (CaO/SiO_2)	1.4	1.5	1.3– 1.4
Outputs calculated			
Manganese feed (t/t)	2.00	2.20	2.57– 2.68
Mn/Fe ratio - feed	5.5	>7.4 (not specified)	10 – 13
Coke (coking coal) (t/t)	1.428 (1.651)	1.800	N/A (mixed fuel types)
Flux (t/t)	0.136	No data	No data
Slag/metal	0.58	0.85	No data
MnO in slag (%)	22	14	30– 32
Outputs - Off-gas components			
CO/CO_2 off-gas	8.4	No data	No data
Emissions (t CO_2/t alloy)	4.3	No data	No data

The BF feed was under-estimated by 9% according to Featherstone (1974) and over 22% according to Kamei *et al*., (1992), however still within range. Differences in manganese feed requirements are due to the quality of ore, and the quality of alloy produced by the ore blend. Mn/Fe ratios more than 25% higher are reported in the literature when compared to the assumed model input values (Featherstone, 1974 and Kamei *et al*., 1992). The estimated Mn/Fe ratio is higher in literature due to the higher recovery and the surplus iron that comes in with the coke ash which is 21% lower than what was published by Featherstone (1974). Less coke per mass alloy translates to less surplus iron fed in the system. Significantly lower flux is added in the model, however, the basicity of the slag is within a suitable range for operation. Lower flux requirements are related to lower alloy quality, which translates to lower coke requirements and less slag production.

MnO content in the model slag is 37% higher than the value quoted by Featherstone (1974). Unfortunately, the data supplied does not provide the manganese recovery and the amount of manganese fed in through the ore. Overall, the BF model underestimates the coke and flux requirements which will result in a reduction in production cost estimates made based on the model outcomes. The simplification of the model leads to underestimations of the carbon required for reduction due to the circulation of alkalis and vapours between the solid and liquid-state similar to the SAF.

Most BF operational literature did not report CO and CO_2 produced by the off-gas. However, Madias (2011) reports the range 7-8 CO/CO_2 for FeMn production in a

shaft furnace. The model estimates a value in the mid-upper range of what is normally observed. Emissions from the BF model are likely to be also underestimated due to the assumption that the reductant is also underestimated to the same degree as the SAF due to simplifications in the model.

The COREX® furnace model made use of assumptions derived from the SAF and BF operational and pilot plant data, where applicable. No data was found in the public domain for the HCFeMn process in the COREX®. Therefore, Table 4-3 compares the model inputs and outcomes for the COREX® with the BF model inputs and outputs. Furthermore, basic ore production data published by Featherstone (1974) was included for qualitative comparison. The manganese recovery target was 84% based on BF literature (Madias, 2011; Kamei *et al.*, 1992).

Table 4-3. Values of the mass and energy balances in the COREX® compared to three sources of literature.

Stream ratios (per ton alloy)	**COREX® model**	**BF model**	**(Featherstone, 1974)**
Inputs and assumptions			
Manganese in alloy (%)	75.0	75.0	78.4
Carbon in alloy (%)	6	6	No data
Manganese Recovery %	84.1	82.5	No data
Basicity (CaO/SiO_2)	1.5	1.4	1.5
Outputs calculated			
Manganese feed (t/t)	1.86	2.00	2.20
Mn/Fe ratio - feed	4.3	5.5	>7.4 (not specified)
Coal (t/t)	1.495	1.428	1.800
Flux (t/t)	0.364	0.136	No data
Slag/metal	0.58	0.58	0.85
MnO in slag (%)	23	22	14
Outputs - Off-gas components			
CO/CO_2 off-gas	1.3	8.4	No data
Emissions (t CO_2/t alloy)	3.1	4.3	No data

The manganese feed Mn/Fe ratio and quantity estimated by the COREX® model are 21.81% and 6.86% lower than the BF model values, respectively. Furthermore, COREX® feed properties were slightly underestimated when compared to the BF operational indices (Featherstone, 1974). This observation could be explained by the iron content in coal used in the model. Furthermore, the assumption that less vapour is lost to condensation due to recycling cyclone in the COREX® furnace. Table B-2 in Appendix B lists the carbon source compositions. Anthracite and coke contain iron compounds meanwhile the coal used in the model has no iron. Less excess iron translates to lower Mn/Fe estimations in the feed in the case of the COREX®.

The model ore mixture at 4.3 Mn/Fe ratio has 48.5% manganese and at 5.5 Mn/Fe ratio the manganese content is 45.6%. Higher manganese mass fractions in the ore mixture translate to lower feed mass estimated by the model.

The recovery for the COREX® model was estimated as 1.94% higher than the BF model recovery, however within range of what the BF process can yield at production capacity. The presence of the recycling cyclone resulted in the assumption of partial losses (33% of the losses assumed for the BF) of manganese to condensate. Lower recoveries due to manganese vapour formation are a concern in the BF due to the method used for the energy input (Kozhemyacheko *et al*., 1987). These losses are related to the theoretical combustion temperature in contact with the alloy and the pressure of the furnace gases (Kozhemyacheko *et al*., 1987). In the case of the COREX®, combustion is also used to generate heat for reduction reactions. Therefore, a similar phenomenon is expected to occur in the COREX®, however, the dust recycling cyclone captures solid particles and returns them back into the furnace. The extent of manganese vapour loss and recycling is unknown due to the non-existent process data.

Based on the COREX® model, coal requirements are estimated to be 4.69% higher than coke required for the BF model. From the outcomes of the SAF and BF, the COREX® carbon requirement is likely to be underestimated to a similar degree to both furnaces due to model simplifications. The slag generated in the COREX® model is 1% lower than the BF model slag estimated. This is due to smaller percentages of slag components in the ore and coal which are supported by the flux requirement that is 2.68 times higher than the BF model. Slag basicity estimations were within range when compared to the BF model and operational index. The MnO content is 4.5% higher in the COREX® than the BF model. This could be due to the lower slag mass and the higher manganese content in the ore fed into the model.

COREX® model CO/CO_2 ratios are more in line with the SAF value provided by Ahmed *et al*. (2014). Overall emissions were also lowest for the COREX® model if electricity generation emissions are accounted for in the SAF. Lower reductant estimation due to model simplifications could result in a slight increase in emissions. For the SAF, the emissions generated from the electricity production (3.2 t CO_2/t alloy) were factored into the calculation. The COREX® had 25% fewer emissions when compared to the other two projects.

Table 4-1 to Table 4-3 values were used as the base case scenario when evaluating the economic performance and conducting the sensitivity analysis presented in the next chapter.

4.2. Techno-economic Evaluation Outcomes

In Chapter 4.1 details of the technical outcomes of the base case for the techno-economic evaluation were presented. These outcomes were then used to estimate production and investment costs for each capital project. The base case assumed 300 000 tons per annum capacity of ASTM grade C HCFeMn. This capacity was chosen based on the largest installed HCFeMn capacity at Metalloys (Basson *et al*., 2007). In the current chapter, the economic model and the results are presented.

Chapter 4.2 is delivered in two portions. The first portion will cover the assessment made on all three capital projects to facilitate a comparison of the economic performance. The second section is concerned with further evaluating the sensitivity of the NPV to technical variables of the best performing capital project. Furthermore, a breakeven analysis will be conducted.

4.2.1. General project performance evaluation

Annual production rates listed in Table 4-1 were used to estimate the raw material requirement per annum. Production costs associated with extra utilities, such as steam and fuel, were not factored into the model, only water and electricity were accounted for. All other production components such as labour, direct costs, and indirect costs were estimated using cost estimating literature guides and factors. Capital cost estimates were based on the capacity requirements for the various unit processes. Major capital items associated with significant unit processes were taken into account. Where data was available, costs associated with fully installed units which include extras such as construction were used.

Some unit processes did not have costs quoted for fully installed units, for example, gas handling and water treatment. Therefore, capital costing guidelines compiled by Woods (2007) using capacity estimations and various factors to account for the expenses beyond the module cost was applied. Extra capital items required for materials movement, feeding, alloy movement, and slag movement, which may consist of various trucks and tractors, were not explicitly factored into the calculation.

Project-specific assumptions were made for each evaluation, these assumptions influence the results obtained for the evaluation. The SAF project consists of two furnace crucibles that will collectively produce the desired capacity. Construction of these two crucibles was inferred from the construction schedule reported in the Timnor Smelter Study (Anderson *et al*., 2015). The furnace crucibles were completed in series, where start-up and production commenced in other units while others were being completed. The current study assumed that construction for the SAF facility is concluded at the end of year 3, however, production commences during year 2. Full-scale production is only reported from year 4 onwards. Construction and production for the BF and COREX® were assumed to be similar because each project requires one unit to produce the desired capacity.

Construction of the BF and COREX® unit was assumed to be concluded towards the end of year 2, similarly to the SAF. However, production only commences in year 3 and full scale is reached by the end of the same year.

All 3 capital projects included an electricity generation unit using the off-gas generated. The SAF project directs all the off-gas produced by the closed furnaces towards electricity production to offset the electricity requirement. The BF project rations the off-gas energy between the sinter plant fuel requirement, blast air heating, and electricity production. Electricity produced in the BF power plant supplies the demand from the furnace system and the rest is credited towards the production costs at the same rate charged for electricity during the same year. In the COREX® project, all the exported gas is used to generate electricity. The produced electricity satisfies the estimated demand from the oxygen generation unit and the COREX® furnace setup.

Thereafter, the surplus is credited towards the production costs at the same rate charged for electricity during the same year. Energy distributions were rough estimations made for unit processes to account for the reuse of the energy before crediting the amount in the production costs.

Water required for processing was not calculated from the mass and energy balance. Published literature with rough estimates based on the capacity of the furnace was used. Consequently, the water treatment unit capital cost estimate accuracies are subject to the estimated accuracy of the water requirement.

Gas cleaning and furnace shell cooling were assumed to be the major contributors to water consumption. Treated water is recycled back into the process and it was assumed that a 15% replenishment will be required as a result of water loss due to evaporation.

All the assumptions listed above were consolidated into a cash flow statement and various economic indicators were calculated. In Table 4-4, the various economic indicators and base case cash flow variables estimated using the model, are listed. The South African corporate tax rate for the year 2018/2019 was set at 28% (Glacier Financial Solutions (Pty) Ltd, 2019). According to Glacier Financial Solutions (Pty) Ltd (2019) depreciation allowances for new plant machinery spans over 4 years, 40% in the first year, and 20% for the subsequent years. Revenue, raw materials, and electricity were varied according to distributions based on historical data. Other costs such as maintenance, labour, supplies, and insurance were fixed over the 20 years.

Table 4-4. Inputs and outputs of the techno-economic evaluation of the SAF, BF, and COREX®.

Economic indicator	**SAF**	**BF**	**COREX®**
NPV (15% rate, 20 years, R mil)	7 706.36	7 267.29	11 430.46
Discounted payback period DPBP (15%)	8 years	9 years	7 years
IRR (NPV ≈ 0)	28.07%	26.89%	33.11%
Average annual OPEX (R/ton)	16 134.49	16 202.63	11 405.25
Fixed CAPEX per unit alloy (R/ton)	18 515.23	25 294.05	25 002.04

An arbitrary interest rate 2 times higher (15%) than the South African repo rate in 2019 was chosen to calculate the NPV and the DPBP over a 20-year project lifetime. The lowest NPV and IRR values obtained were for the BF. Despite the lowest CAPEX per unit product, the high production costs reduce profit margins which are reflected in the smaller NPV and IRR for the SAF. The BF project financial indicators are marginally lower than the SAF, the combination of high CAPEX and OPEX per unit further the diminished profit margins. COREX® capital project performance indicators are the highest out of all three furnaces. Even though the CAPEX per unit product is the highest, the OPEX per unit product compensates by being significantly lower. Invested capital is returned within 8 years for both the SAF and BF, however, the COREX® project returns it a year earlier.

Key cost drivers in FeMn production are the manganese source, electricity, and the reductant source (Steenkamp & Basson, 2013). High production costs reduce profit margins and result in poor financial performance for any project. Figure 4-1 charts the estimated percentage contribution of the energy source towards the production costs. In the case of the BF and COREX®, a distinction was made in the carbon source required for combustion and direct reduction reactions. Production of electricity was assumed to be done using a unit with a 0.4 efficiency. Off-gas reuse for other unit processes such as blast heating, sinter fuel, electricity for the furnace, and oxygen production was accounted for. The surplus electricity was then accounted for as money coming in from the by-product. In the case of the COREX®, the electricity by-product generated is worth more than the coal used to generate it. This distinction allowed for the reductant portion to be excluded from the calculations in Figure 4-1.

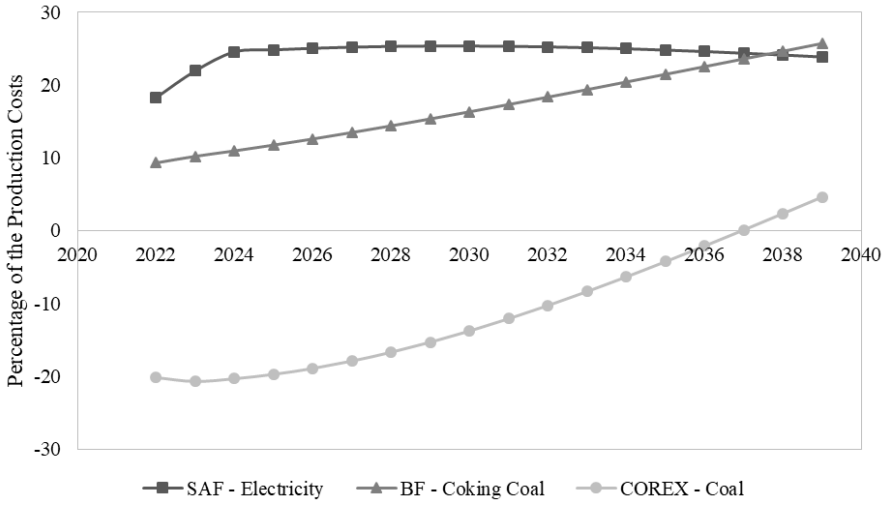

Figure 4-1. Percentage of energy contribution towards production.

Electricity contributions towards production costs in the SAF increased to over 25% in the first three years of production and stayed between 24-25% over the project life-time. BF energy costs from coking coal gradually increased from 10% to 26% over the lifetime of the project. COREX® energy cost trends are significantly different. Due to the quantity and price of coal when compared to electricity, the electricity surplus completely offsets the cost of combustion coal for 16 years of production. Furthermore, the electricity credit further reduces the production costs beyond the coal requirement as it is seen with the negative percentage in Figure 4-1. The average contribution of the manganese source over the project life-time is 49% COREX®, 38% for the SAF, and 37% for the BF.

A scenario analysis was then conducted using the base case model that yielded the results in Table 4-4. Worst-case estimates were used for the capital cost and production cost components. Historic data was used to estimate the potential variance in projected values. This was achieved by estimating historical values using the distribution obtained. The data was then used to calculate the percentage difference between the actual and estimated values. An average of the positive (actual value is higher) and negative (actual value is lower) were then estimated. These two values were then used as the worst- and best-case percentage change in the raw material and product prices in the analysis. Table 4-5 lists the outcomes of each scenario analysed.

Table 4-5. Scenario analysis of the furnace technologies.

	SAF		BF		COREX®	
R'000 000	**NPV**	**IRR**	**NPV**	**IRR**	**NPV**	**IRR**
Best-case	20 412.48	57.13%	19 334.52	50.56%	23 508.92	58.35%
Base case	7 706.36	28.07%	7 267.2.84	26.89%	11 430.46	33.11%
Worst-case	-1 295.26	13.09%	-2 564.50	11.08%	2 582.36	18.59%

In all scenarios, the COREX® had a positive NPV value, unlike the BF and SAF with a negative NPV in the worst-case scenario. In part, the BF experienced a sharp price increase observed in the original data in 2008 and 2011 where the coking coal price was 94% and 26% higher than what was estimated by the distribution. These sharp price changes resulted in the worst-case having expensive coking coal prices. The BF is outperformed by both the SAF and COREX® in the extreme scenarios. However, a marginal performance is observed over the SAF in the base case. The COREX® outperforms the SAF in all cases according to the NPV and IRR values. The difference in the IRR of the SAF and the COREX® is highest in the worst-case scenario at 5.80%.

The last group of analyses that was conducted for all projects was a sensitivity analysis of the NPV to the major operational items. During each analysis, all other variables were kept at their respective base case values while one variable was varied between -20% and 20% in increments of 2%. The behaviour of the NPV was plotted against all the percentage changes made to the three variables. The three variables that were chosen are the energy source, manganese source, and the ferromanganese product. Figure 4-2 shows plots of the NPV value over the range of percentage changes and Table 4-6 lists the sensitivity coefficients calculated. The sensitivity coefficients apply over the range of percentages shown in Figure 4-2.

Table 4-6. Sensitivity coefficient values are derived from the economic model and used to construct Figure 4-2.

Coefficient	**SAF**	**BF**	**COREX®**
Energy source (ΔS_{ENE})	-3 755.49	-3 045.24	716.37
Manganese Source (ΔS_{MN})	-5 537.54	-4800.86	-4 436.03
Alloy (ΔS_{FEM})	28012.95	26 076.46	26 076.46

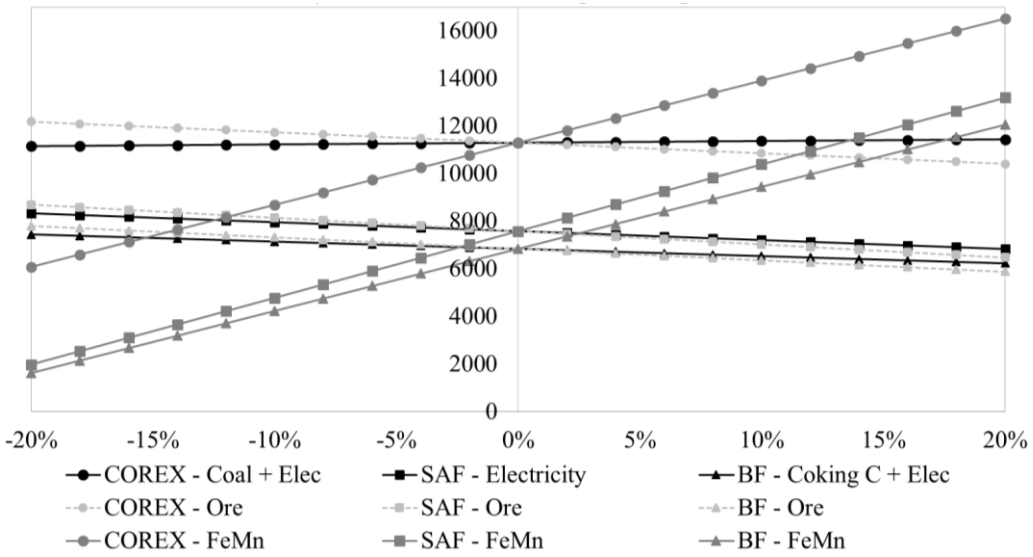

Figure 4-2. Sensitivity of the NPV to key variables.

Higher NPV values are observed for the COREX® model when compared to the BF and SAF. Similar responses to changes are observed for the SAF and BF, evident from the overlapping lines. A 20% decrease in the price of the alloy product doesn't result in a negative NPV for any of the capital projects. From Figure 4-2 and Table 4-6, it is evident that the price of the alloy product causes the most significant changes to the NPV value for each project. In the SAF and BF model, changes in the ore and energy source affect a similar change to the NPV. Conversely, in the COREX® model, the sensitivity of the NPV to changes in energy and manganese source prices differs. From the sensitivity coefficients calculated, it is evident the effect of the energy source has an opposite effect when compared to the other furnace models. The effect of the manganese source is within range with the other furnace models, however, it influences the NPV to a lesser extent.

Break-even analysis and a shutdown analysis were performed. Both the results are shown in Figure 4-3. Some of the fixed costs were not varied over the lifetime of the project, only the variable costs changed, and the costs were based on variable cost items such as patents.

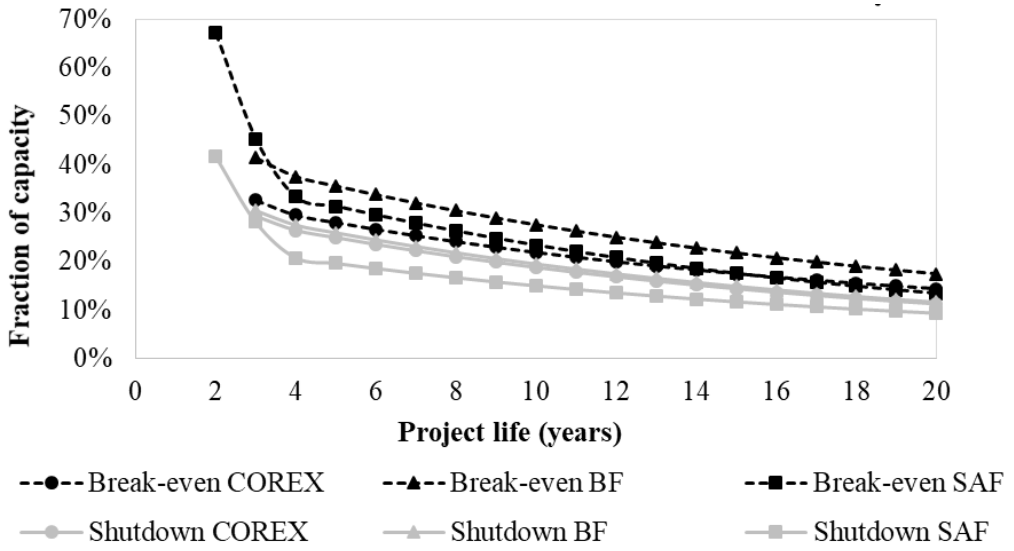

Figure 4-3. Analysis of the break-even and shut down points for the SAF, BF, and COREX® project.

SAF production starts in year 2 with a break-even capacity of 67.14% which translates to 201 420 tons of alloy that need to be produced. Production in the BF and COREX® commenced a year later in year 3, 33%, and 41.39% of the revenue was required to break-even which translates to approximately 98 000 and 124 170 tons of alloy, respectively.

Based on the estimations made to generate Figure 4-3, a shutdown will require severe production capacity drops for the BF and COREX®, lower than 29% (87 000 tons) at the beginning of the project. The SAF has a higher shutdown capacity of 41.72% which means if the alloy demand is lower than 125 160 tons the project should not be initiated. As the project matures lower capacities are required to break-even or to prompt a shutdown in operations. The SAF experiences a sharp drop in the capacities required to meet break-even and shutdown production costs.

4.2.2. Outperforming project evaluation

Based on the NPV and IRR values yielded by the COREX® techno-economic model for all scenarios, a further investigation into the model was done. The unavailability of technical data for the process created a challenge when it came to verifying the model estimations. The current section will present the evaluation of the sensitivity of the NPV value to operational changes in the COREX® furnace. The operational variable of interest for the technical sensitivity analysis was the recovery of manganese to the alloy. Figure 4-4 charts the changes in the NPV as the recovery of manganese decreases by changing the percentage MnO in the slag.

Furthermore, the alloy quality was kept constant. The results display the combined operational effects of a change in the assumed recovery.

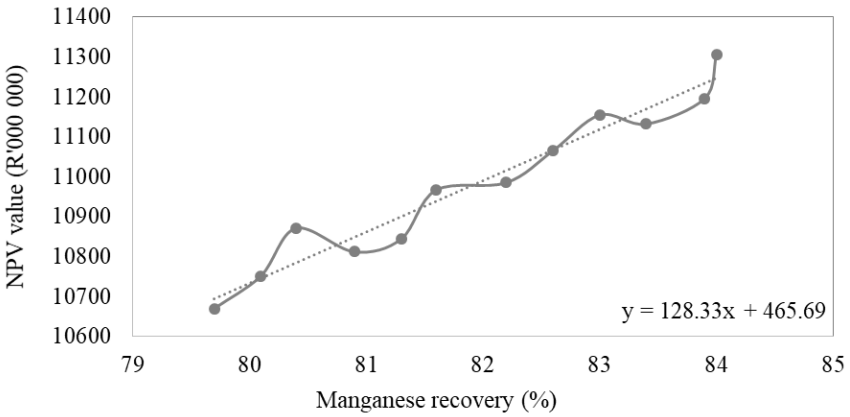

Figure 4-4. NPV value response to lower recoveries for the COREX® furnace.

Direct control of manganese recovery is impossible because it relies on numerous other variables in the process. This current analysis investigates the combined effects that result in lower recoveries than expected. Based on the trend line gradient in Figure 4-4, the NPV will decrease by approximately 1.14% for a percentage drop in the recovery. Recoveries as low as 79.7% caused the NPV value to decrease by 5.62%.

Chapter 5
Discussion

In previous chapters, models were constructed to conduct a techno-economic evaluation for three furnaces the SAF, BF, and COREX® furnaces for the production of HCFeMn. The work entailed mass and energy balance models of the HCFeMn process in all three technologies. Process modelling results were subsequently used to approximate fixed capital expenditure items, Production expenditure costs, and cash flow analyses that are used to perform economic analyses. The results of the modelling were detailed in Chapter 4. In the current chapter, the implications of the outcomes produced by the various models and analyses are to be discussed. Lastly, inferences to the FINEX furnace technology are made based on the outcomes observed in the models.

5.1. Blast Furnace versus Submerged-arc Furnace

The first comparison was done between two technologies that have been proven to produce HCFeMn on a commercial scale the SAF and BF. The comparison was conducted to investigate whether continuing using the SAF for the production of HCFeMn will be financially feasible going forward.

Outcomes of the mass and energy balance models show that ore mass flow requirements for the SAF and BF are within a similar range (Eissa *et al*., 2011; Madias, 2011). However, the BF model predicted lower Mn/Fe ratio requirement than the SAF. The ratio indicates the maximum possible Mn/Fe of the alloy since iron recoveries to the alloy are much higher than manganese (S.E. Olsen *et al*., 2007). Higher Mn/Fe in the feed ratios counter dilution as a result of iron that is fed in with electrode casings, anthracite, and coke. BFs have been proven to be more operationally lenient when it comes to feedstocks with lower manganese content in them (Madias, 2011). Lower Mn/Fe ratios in the feedstock attract lower purchase prices (S E Olsen *et al*., 2007). Both furnaces prefer larger particles during operation based on Table A-3 in Appendix A, with the BF sticking to a narrower size range of 10– 50 mm for ore. Feed requirements are important for efficient gas permeation through the burden to facilitate solid-state reduction, heat transfer, and to avoid ruptures due to gas build-up (Sithole *et al*., 2018).

In the SAF model, manganese recovery is 82.8% only 0.3 % higher when compared to the BF recovery, however, a median value of 83% was selected for the BF recovery which can potentially get to 85% (Madias, 2011). Manganese recovery is a combination of multiple process influences, however, manganese researchers have related this variable to the slag basicity value (S E Olsen *et al*., 2007). Slag basicity is controlled using flux additions as raw materials to alter the composition. The addition of flux comes at a cost through the energy consumption and raw material cost, therefore close control of the amount added is required.

Recoveries are also affected by losses of manganese through vapour formation (Kozhemyacheko *et al*., 1987; S E Olsen *et al*., 2007). Manganese vapour formation is caused by high electrode temperatures in the SAF and the combustion temperatures in BF. For shallow burdens in the SAF and high flow rates in BF stacks, a fraction of the manganese is lost to the dust. Energy consumption increases as it is invested in manganese that is ultimately not recovered into the alloy.

The Boudouard reaction is unavoidable especially in the presence of high CO_2 levels and a carbon source. Though not explicitly quantified in the model, the BF gas system experiences significantly more carbon and energy losses from this side reaction. This can be deduced from the higher CO percentage in the off-gas. However, the recovery of some of the energy lost is possible. In the SAF electricity is generated and returned to the process. In the BF a portion heats the blast air, another portion is used for sintering, and the rest generates electricity that offsets some of the production costs. Electricity recovery has lesser efficiencies than direct heating of raw materials using the gas, therefore energy value is lost.

The three main cost drivers in the HCFeMn process are the manganese source, energy source, and reductant. In Figure 4-1, the cost of energy required to produce the same quality alloy per unit in the SAF is higher than what is required by the BF for the first 16 years. In the final year, coking coal contributions increase past the electricity cost in the SAF. From an operational perspective, the SAF attracts slightly higher costs when it comes to raw materials and energy consumption per unit alloy for the furnace only. Due to the cost of electricity in South Africa, the recovered energy in the form of electricity allows for a significant production cost offset. Annual average production costs per unit alloy for the SAF and BF over the life-time of the project are approximately the same. On the other hand, the BF has auxiliary units for coking and sintering. Auxiliary plants require extras such as fuel or electricity to function beyond raw material. Once quantified, these costs will diminish the offset estimated by the model. The use of coal in both furnace setups is a viable option to reduce raw material costs associated with coking coal, coke, and anthracite. A change in raw material usage would significantly impact the BF operational costs due to the volume of coke that can be displaced by using pulverised coal, unlike the SAF (Kamei *et al*., 1992).

The SAF CAPEX included a briquetting plant, gas cleaning equipment, two furnace crucibles and accompanying transformers, an alloy handling plant, an alloy recovery plant, a power plant, and a water treatment facility. Meanwhile, the BF CAPEX included a sinter plant, coking plant, one furnace crucible and gas heat exchangers for the blast gas, gas cleaning system, alloy handling plant, alloy recovery plant, power plant, and a water treatment facility. Due to the BF size and operational requirements, auxiliary units such as coking and sinter plants are built on-site, therefore increasing the CAPEX cost per unit alloy (Featherstone, 1974). The extra units resulted in a 39.26% higher CAPEX cost per unit alloy when compared to the SAF.

Financial performance results in Table 4-4 show that overall the SAF performs only slightly better than the BF. The payback period is 1 year earlier and the NPV value is 6.04% higher than the BF NPV. Scenario analyses results, in Table 4-5, show that in each scenario the SAF outperforms the BF. In the best-case scenario, the NPV is 5.58%, and the IRR value 5.81 percentage points higher than the results of the BF. In the worst-case, both NPV values become negative meaning that the investors lose money at a 15% discounted rate. This is further confirmed by the low IRR values calculated. However, the discrepancy between the best and worst-case is narrow for South African electricity prices based on historical data. The worst-case saw the projected price increase by 2%, unlike coking coal increasing by 26%. This implies that an electricity increase over 3% in the worst-case could result in poorer performance of the SAF economic outcomes. The break-even analysis conducted on the two projects shows that the BF project can operate with 39% lower demands when compared to the SAF project. A sharp drop in break-even and shutdown capacities in the SAF are observed which remain lower than the BF over the lifetime of the projects. BF's were designed for large scale and continuous operations which require more stability, unlike the SAF (Madias, 2011). SAFs are known to be robust in terms of changes in capacity and changes in alloy quality (Madias, 2011).

Even with the significantly lower capital cost and slightly lower operational expenditure when compared to BF, the SAF only marginally performs better than the BF financially. The operational benefits of using a SAF that were observed by Hooper (1968) are gradually diminishing due to the cost of electricity. Improvements that result in a decrease in electricity usage for the SAF, and coking coal consumption for the BF, could improve the operational economics enough for better profit margins over the project life.

5.2. COREX® versus Blast Furnace

The second comparison was done on two technologies that produce pig iron on a commercial scale, the BF and COREX®.

Development and commercialisation of the COREX® furnace and other alternatives were to remove the dependency on metallurgical coal among other important reasons such as reduction of emissions (Dutta & Rameshwar, 2016). Mass and energy balance outcomes for the COREX® were modelled using BF operational indices for the HCFeMn process as guidelines. Manganese feed requirements for the COREX® are lower when compared to the BF. The slightly lower feed requirements are due to the quality of manganese ore blend used with a higher manganese percentage, but more iron which brings down the Mn/Fe ratio. Lower Mn/Fe ratio is required by the COREX® process due to the coal ash having no iron compounds to further dilute the alloy. Lower quality feedstock can be used in the COREX® to yield similar Mn/Fe ratio alloys due to less dilution from other raw

materials. When the price of lower Mn/Fe ratio manganese feeds is taken into account,

it could result in the actual feedstock prices being lower for the COREX® when compared to the BF. Based on Table A-3 in Appendix A, COREX® units allow for smaller particles to be fed into the process and tolerates a wider range when compared to the BF. However, COREX® primarily uses lumps in the operation and a smaller percentage of the particles are recycled dust. Tolerance for dust is attributed to the semi-fixed bed in the melter-gasifier when bed permeability is easier due to the semi-fluidised upper section (Pal & Lahiri, 2003).

Alloy recovery values for the COREX® were estimated to be 1.5 percentage points more than the BF recoveries. This estimation was a result of the manganese losses in the form of sublimates mentioned in BF literature, furthermore, the losses are dependent on the flame temperature and pressure in the hearth of both furnaces (Kozhemyacheko *et al*., 1987). Manganese vapour generation is likely in the COREX® melter-gasifier unit since the temperatures are approximately 3200°C and operating pressures around 330-350 kPa (Kumar *et al*., 2008; Pal & Lahiri, 2003; Qu *et al*., 2012). However, the dust from the melter-gasifier is recycled back into the unit using a dust cyclone (Zhou & Zhongning, 2013). Therefore, manganese losses from vapour would reach equilibrium through the constant dust recycling implemented in the process.

Coal feed mass for the HCFeMn in the COREX is estimated to be 1.46 times more than for ironmaking and this is due to higher process energy demands (Zhou & Zhongning, 2013). Operationally, the BF coking coal costs over 2.4 times more than the COREX® coal at the beginning of the project, which is in agreement with the reason why the COREX® was developed (Dutta & Rameshwar, 2016). Both furnaces experience high proportions of the Boudouard reaction due to the high volumes of CO_2, however, the volatile matter from the coal further increases the energy value of the gas generated.

The separation of the pre-reduction unit in the COREX® allows for minimizing the extent to which the Boudouard reaction occurs in the burden in the BF. Energy recovered in the form of electricity is higher in the COREX®, however, some of the energy is reused to generate high purity oxygen for the process. The rest is credited to operational costs at the cost of South African electricity. The COREX® has one unit process that was not taken into account beyond raw material consumption. The BF has two units which are the sinter plant and coking plant. One of the main cost drivers is the energy source. Based on Table 4-4 and Figure 4-1, production expenditure in the COREX® project is significantly affected by electricity recovery. COREX® techno-economics are maximised through energy recovery from the off-gas generated by the process (Hasanbeigi *et al*., 2014). For the first 16 years, the

electricity offsets coal expenditure and there is still more money to offset other production costs.

Fixed CAPEX costs of the COREX® used one value to account for the reduction shaft, melter-gasifier, hot gas cyclone, heat exchanger, two scrubbers, and any other hidden unit that allows for the process to produce an off-gas, alloy, and slag similar to the BF process. Gas cleaning equipment is an integral part of the COREX® due to the recycling that occurs. Extra units that were included as a part of the fixed CAPEX estimate were the power plant, oxygen plant, coal briquetting plant, alloy handling, and alloy recovery. In terms of capital expenditure per unit alloy, the BF requires 1.04 times more capital when compared to its counterpart the COREX®. However, the COREX® is known for being more capital intensive than the BF due to the multiple units required mainly for gas handling (Bhattacharya & Vishwakaram, 1998; Gordon *et al*., 2018). This discrepancy could be due to the other units such as the coking plant or sinter plant because the HCFeMn requires higher flow rates of material to meet process outputs. The extra units are predominantly used for recycling dust and process gas, which doesn't impact the operational expenses as much as the BF.

Financially, the COREX® outperforms the BF with 36.42% and 6.22 percentage points higher NPV and IRR, respectively. Furthermore, capital is recovered 2 years earlier in the base case. Significantly lower operational costs of the COREX® allow for better performance over the BF. In all scenarios the COREX® outperforms the BF, surprisingly the NPV value of the COREX® is never negative. Even in the worst-case scenario, a return of 15% for the COREX® project is expected. A major variable that affects the profitability of the COREX® is the fixed CAPEX component and other related costs such as maintenance. The COREX® route financial performance could improve even more if preowned facilities could be purchased at a lower cost than a new facility, as is the case with the BF in HCFeMn production (Featherstone, 1974). This could reduce the payback period and more earnings could be observed through a higher NPV and IRR.

Break-even capacity requirements for the COREX® are lower than the BF due to lower production costs. However, shutdown capacity requirements are almost identical. This is likely due to the fact that both technologies were designed for the ironmaking process which requires high production capacities and steady operations.

5.3. Submerged-arc Furnace versus COREX®

In the previous sections, comparisons were conducted between the SAF and BF, and BF with the COREX® that concur with published literature values and observations. Based on these successful comparisons, the model outcomes were

used to compare the performance of the SAF and COREX® in the current subchapter.

When the mass and energy balance outcomes in Table 4-3 are assessed, the COREX® uses 16.36% less manganese feed with a 1.7% lower Mn/Fe ratio requirement when compared to the SAF. The manganese source accounts for a significant percentage of production expenditure, lower feed mass, or quality per mass alloy reduces the costs associated with the manganese source (Van Zyl, 2017). Recoveries observed in the COREX® process are slightly higher at 84.1% when compared to the 82.8% of the SAF, the little to no dilution from the coal is advantageous for the COREX®. Furthermore, manganese losses are assumed to be minimised through dust recycling in the COREX® which aids in curbing vapour losses experienced in the SAF furnace. Other process aspects such as the slag generation and basicity are within specified ranges with published literature for the SAF and BF. COREX® slag outputs were slightly lower than the SAF even though the COREX® feeds 3.3 times higher flux masses. Lower manganese recoveries are associated with an increased slag mass. Feed particle size allowances in the COREX® are favourable over the SAF when feeding finer material in the melter-gasifier.

The energy contribution towards production cannot be directly compared from the mass and energy balance results. Better insight is drawn from Figure 4-1, where the price of energy is factored in. The SAF process pays more for energy when compared to the COREX®, even though some of the energy is recovered through power generation. Large volumes of gas in the COREX® are advantageous for producing more electricity. Furthermore, if the cost of electricity is much higher then it completely displaces the cost of coal utilised in the process. The extent of energy off-set observed in the COREX® makes the project superior when it comes to minimising operational costs. In Figure 4-2, it is shown that the COREX® project NPV is the most sensitive to changes in the manganese source price when compared to energy. However, the SAF with high production costs is almost equally sensitive to the cost of both the energy and the manganese source. The operational cost element of the HCFeMn process mainly consists of the manganese and energy source (Van Zyl, 2017).

When CAPEX items are assessed, the SAF requires 34.28% less fixed capital when compared to the COREX®. The main processing unit of a COREX® comprises multiple gas and dust recycling units, which contributes to higher fixed capital cost estimates. Furthermore, the various raw material and energy recovery auxiliary units that reduce production costs, increase the fixed capital cost component of the model. The COREX® electricity generation unit is 4.79 times larger than what is required for the SAF project resulting in increased CAPEX requirements. Furthermore, other costs estimated using the fixed capital investment amount such as land, start-up, and maintenance will be estimated higher for the COREX® project.

However, the COREX® utilises more units when compared to the SAF and this would increase maintenance-related costs.

When observing the economic model outcomes of the SAF and COREX®, a trade-off between the production costs and fixed capital costs is identified. The financial performance indicators were then used to assess the effect of the trade-off. Capital invested in a new COREX® facility will be paid back 1 year sooner than an investment made in a new SAF facility with two furnaces at a 15% discounted rate. Furthermore, a COREX® project of this nature would generate more money for investors judging by the NPV value that is 1.48 times more than the SAF at a 15% discounted rate. Furthermore, the IRR of 33.11% for the COREX® is 5.04% more than what the SAF project can offer at base-case assumptions. Despite the high capital investment required for the COREX®, the energy offsetting in the production cost is advantageous. COREX® economics are sensitive to the cost of capital and the cost of the manganese source. On the other hand, the SAF economic model is sensitive towards more production variables due to the narrow profit margins. In the scenario analyses conducted, the best-case shows how much better the COREX® can perform when the capital component is reduced. In the worst-case where the capital charge is 30% more than what was estimated, the COREX® project makes enough profit to see a 15% return on investment. In all scenarios, the COREX® meets the cost of debt, unlike the SAF that loses money in the worst-case scenario.

The SAF is outperformed by the COREX® purely due to better production expenditures that increase cash flow towards profit margins. The COREX® requires lower capacities to break-even when compared to the SAF due to the lower production cost as a result of the electricity off-set. On the other hand, lower shutdown capacities are required in the SAF from year 3. This could be a result of the COREX® being designed for larger capacities and the higher CAPEX requirements.

5.4. Best Performing Project

The technical and economic aspects of the SAF, BF, and COREX® furnace technologies were discussed in Chapter 5.1 to 5.3. In the current section, the discussion points are summarised and the best performing technology project is identified out of the three possibilities. Further analyses were conducted on the best performing technology to explore NPV sensitivity to lower manganese recoveries. Furthermore, less optimal processing conditions were also investigated.

Based on the mass and energy balance outcomes, the COREX® outperforms both the SAF and BF operationally. This was seen from higher manganese recoveries and lower Mn/Fe ratio requirements for the ore. Higher energy recovery levels in the form of electricity further increased the operational performance of the

COREX® against the other two projects. As a result, COREX® performed the best operationally due to the lowest operational costs. The SAF had the second-lowest operational cost which was slightly higher than for the BF project.

When plant equipment requirements were taken into consideration through capital cost estimates, the SAF required the least amount of capital when compared to the other furnaces. The BF had the highest costs as a result of extra auxiliary units required for raw materials processing. The COREX® was not far behind due to the complex two-part furnace and the largest power plant. Techno-economic results indicated that the COREX® outperforms the other two technologies by far. The IRR value of the project is at least 5% higher and the NPV 48% higher than the SAF and BF projects. The best- and worst-case scenario showed the COREX® will always yield a 15% return on investment. From this analysis, it can be assumed that the probability of successful profitability of the COREX® project is 1. Both the SAF and BF projects cannot guarantee a 15% return in the worst-case scenario which reduces the probability of the projects being successfully profitable. The scenario analysis suggests that the COREX® project should be pursued further.

Based on Figure 4-3, low capacities between 14– 33% will ensure that the project breaks even over the lifetime, which makes the COREX® project more attractive. In reality, projects aim to perform better than merely breaking-even (Green & Perry, 2008). A project will only be implemented on the account that capacity close to full production is met to maximise profits. A conjecture that can be drawn from the break-even analysis is that the COREX® can handle tougher economic climates when product demand declines during the life-time of the project.

A sensitivity analysis of the NPV based on operational changes that cause the process to recover lower levels of manganese was conducted. Based on a linear relationship fitted onto the data in Figure 4-4, a 1% decrease in the recovery of manganese will result in a 1.14% decrease in the NPV value. Recoveries that were as low as 79.7% yield an NPV of R 10 670.06 million, which is still more than 40% higher than the SAF NPV at the base case. This analysis gives insight into the operational robustness exhibited by the COREX® model. A break-even analysis was conducted to assess critical production capacities for the project.

In Section 2.3 two technologies were identified from the BF alternative pool of ironmaking technologies, the COREX® and the FINEX. However, only the COREX® was chosen for the techno-economic evaluation. The FINEX® furnace was developed using the COREX® as a template and the technology aimed to replace lump feed with dust feed for solid-state reduction. Reduction is carried out using fluidised-bed reactors in series and compacting of the material is required before feeding into the melter-gasifier unit similar to the COREX®. This discussion assumes that the mass and energy balance for the FINEX® resembles that of the COREX® and only differences in CAPEX and OPEX components exist.

Concerning capital investment requirements, the FINEX® requires 1-2 more units than the COREX® depending on the number of fluidised-bed reactors. Furthermore, a compacting unit for the reduced material is required for compacting before smelting. These extra units could result in a 10-20% increase in capital requirements estimated for the COREX® at the base case.

Operationally, similar quality manganese feed will be required by the FINEX®. The cost reduction might result from a preference for fine particles instead of lump ore (Gordon *et al*., 2018). Techno-economics of the FINEX® is likely to be better than that of the SAF or be in close competition. An important aspect that needs to be evaluated for the FINEX® is the possible reduction in production costs from what is currently estimated for the COREX®. The financial performance of the FINEX® is not perceived as better than the COREX® due to higher capital costs associated with it and production costs that are likely to remain the same. Lower production costs are paramount for the financial attractiveness of the FINEX®.

For the context of the Northern Cape in South Africa, the COREX® is economically attractive. The proximity of the main and most costly raw material will reduce transportation costs associated with moving heavy masses. There will be no need to erect infrastructure to deliver electricity to the project site as it will generate sufficient capacity to sustain demands and possibly supply neighbouring operations at a fee. Availability of rail transportation between the Kalahari manganese field area and the Port of Saldanha will avail the alloy product to international customers. Implementation of untested technologies introduces risk from the process, business, and operation perspective (Gordon *et al*., 2018).

In the early phases of a project, process risk is first mitigated through various process simulations, laboratory-scale testing, and pilot plant testing to obtain sufficient data for successful operation and scale-up. Technical aspects that could potentially introduce risk are the presence of impurities that could report to the alloy in the coal. Other risks involved loss of manganese as vapour and the re-oxidation of manganese in the presence of the pure oxygen blast gas. These risks could diminish product quality and/or increase production costs. Business risk is mitigated through using various economic projections to determine future commodity prices and demand for the product of interest. Operational risk has to do with the human-technology relationship (Gordon *et al*., 2018). The risk of the operational team not executing the process as expected needs to be incorporated into the modelling outcomes. COREX® emission levels could potentially be problematic in a case where South Africa moves towards cleaner energy that retails at lower costs than the values assumed in the SAF model.

Chapter 6
Conclusions and Recommendations

This study was initiated due to the decline in local manganese ore beneficiation in South Africa. One of the main contributing factors, identified by Van Zyl (2017), was sought to be addressed by the current study, namely the rising cost of electricity in South Africa. Electricity accounts for a significant proportion of the production costs. As a result, increasing costs will eventually render manganese beneficiation using the SAF economically unfeasible. The current study sought to identify and assess techno-economically feasible technology options that do not heavily rely on electricity for manganese processing.

In the study, a structured literature review was utilised to identify technologies that have been proven to produce FeMn. The SAF, BF, DC-arc furnace, BHPR-NL process, and AlloyStream processes have been proven to produce FeMn. However, all technologies rely on electricity in the process except for the BF. Alternative technologies that were developed to replace the BF in the ironmaking industry were identified as a potential pool of technologies to choose from. It was assumed that technologies that produce the same quality alloy as the BF would be technically suitable to produce the same quality HCFeMn as the BF.

Mass and energy balance models and economic models for the SAF, BF, and COREX® were developed to compare the techno-economics of each furnace. The COREX® mass and energy balance model was inferred from SAF and BF operational indices. Lastly, sensitivity analyses were conducted on the techno-economic models.

6.1. Conclusion

The commercially proven ironmaking alternative COREX® that utilises coal as an energy source was chosen for the current study as a potentially viable replacement for the SAF. From the mass and energy balance model outcomes, the COREX® showed higher recoveries of manganese into the alloy with lower Mn/Fe ratio feed, which was better than the SAF and BF. This was attributed to the minimal iron that comes in with the coal and the continuous dust recycling hot cyclone. The SAF and BF lose manganese due to vaporisation around the hottest zones in the furnace burden. From the economic model results, the operational cost expenditure items for the COREX® were significantly less for when compared to the SAF and BF.

Capital expenditure was the lowest for the SAF and highest for the BF. A collective effect of these variables resulted in the financial performance of the COREX® being superior to both the SAF and the BF.

Furthermore, the SAF marginally outperformed the BF. The COREX® had significantly higher NPV and IRR values in all scenarios that were explored. No scenario resulted in a negative NPV or a return lower than 15% for capital borrowed. The superior performance of the COREX® was attributed to the operational costs being credited with costs associated with recovering and selling electrical energy and low prices for coal. The conclusion was to pursue the COREX® project in the South African context due to the lower energy costs and the high energy offset from electricity.

The COREX® model still has the highest NPV values even when manganese recoveries are reduced. Production costs for the COREX® are met at low capacities which makes the project robust enough to handle risks associated with demand constraints. Implementing the project in the Kalahari manganese field has the potential to reduce costs associated with delivering key raw materials and access to international customers through the port of Saldanha. Furthermore, the electrical transmission infrastructure that will connect the facility to the municipal supply will only be required if the municipality purchases the excess energy. In April 2020 it was reported that a COREX® facility owned by ArcelorMittal was shut down due to financial strain (Nkondlo, 2020). The facility located in Saldanha Bay is a potential site for the production of HCFeMn. However, more research is required to improve confidence in the estimates to support the decision to commence production of HCFeMn using new or existing plant facilities.

6.2. Contributions to Industry

The research that was carried out in the study developed models to compare the techno-economic feasibility of the SAF, BF, and COREX®. Conclusions derived from the results of the modelling process gave insight on a possible new and potentially feasible alternative to the SAF and BF, the COREX®. This research could provide the confidence required to conduct further research that requires physical test work at a laboratory-scale or pilot-plant scale.

6.3. Limitations of the study

Models require accurate and updated data to make informed assumptions and yield reliable results. Limitations of models, therefore, arise from the type of data that is available to make accurate predictions of the future. Based on the literature available in the public domain provided in Chapter 2, HCFeMn production data is only available for the SAF and BF.

Furthermore, SAF has the most updated operational process data, unlike the BF. The COREX® has no operational or pilot plant data available in the public domain. The process modelling methods had to rely on first-principles and assumptions made based on experience with the SAF and BF at commercial scale.

The limitation in using assumptions from other furnace systems is that process phenomena unique to the COREX® cannot be accounted for.

Capital cost estimations were either derived from similar plants with different capacity or estimation techniques. These costs were based on generic unit process equipment requirements that are applied in existing processes. Some raw material and product prices obtained were averages over different material qualities. The price could potentially be over-or understated by the average price quoted. Price forecasting was obtained using regression models which possibly yield different figures from price forecasting conducted by industry experts. These various limitations add uncertainty to the model outcomes. Subsequent studies that pursue to refine the model constructed in the current study will need to address the limitations identified.

6.4. Recommendations and Future Work

Conclusions were on the techno-economic evaluation of the SAF, BF, and COREX® were drawn and provided in section 6.1. The limitations of the study were then addressed in section 6.3. Section 6.4 consolidates these observations to propose recommendations on how to address the limitations encountered and possible activities that can be carried out in the future.

6.4.1. Recommendations

To further develop the models and increase the accuracy of the estimate generated further work is suggested:

1. Generate more reliable process data for the COREX®, for better accuracy of consumption rates and alloy recovery. This can be done through the use of thermochemical software to account for process phenomena, and pilot plant facilities that simulate the reduction shaft and melter-gasifier.
2. Obtain more accurate cost data from equipment manufactures and reliable commodity market reports.

6.4.2. Future Work

- Thermochemical modelling of the reduction shaft and melter-gasifier units of the COREX® using FactSage or similar software to get better estimates of the operational data using a variety of manganese sources.
- Laboratory scale or miniature pilot plant testing of the COREX® plant to obtain physical data.
- Obtain more accurate capital cost estimates from relevant equipment suppliers that build COREX® units.
- Obtain more accurate commodity price data and market projections.

References

Ahmed, A., Haifa, H., El-Fawakhry, M.K., El-Faramawy, H. & Eissa, M. 2014. Parameters affecting energy consumption for producing high carbon ferromanganese in a closed submerged arc furnace. *Journal of Iron Steel Research Int*ernational, 21(7):666–672.

Almpanis-Lekkas, O., Weiss, B. & Wukovits, W. 2016. Modelling of an ironmaking melter gasifier unit operation with multicomponent/multiphase equilibrium calculations. *Journal of Cleaner Production* 111(2016):161–171.

Anameric, B. & Kawatra, S.K. 2008. Direct iron smelting reduction processes. *Mineral Processing and Extractive Metallurgy Review International Journal*. 30(1):1–51.

Anderson, G. & North, R & Gulf Manganese Corporation Limited. 2015. *Timor smelter study report* [electronic]. Available: https://www.gulfmanganese.com/wp-content/uploads/2016/07/25-May-2015-GMC-Timor-Smelter-Study-Combined.pdf [2016, July 25]

Ashpin, B.I., Sleptsov, Zh.E., Gusarov, A.K., Dunaev, N.E., Peshkov, V.R., Foigt, V.A. & Admakin, F.K., 1975. Injection of crude oil into the hearths of high-capacity blast furnaces. *Metallurgist*, 19:564–569.

Ashrafizadeh, S.A. & Tan, Z. 2018. *Mass and energy balances: Basic principles for calculation, design, and optimization of macro/nanosystems*. Switzerland: Springer International Publishing.

ASTM Standards A99-03. 2009. Standard Specification for Ferromanganese.

ASTM Standards A483 / A483M – 10. 2010. Standard Specification for Silicomanganese.

Auchterlonie, A. 2019. Commodity Prices, E-mail to A. Sithole [Online], 29 Aug. Available E-mail: apheleles@mintek.co.za.

Basson, J., Curr, T.R. & Gericke, W.A. 2007. South Africa's ferroalloys industry - Present status and future outlook, in *INFACON XI conference proceedings*. 18-21 February, New Delhi, India, pp. 3–24. Available: https://www.pyrometallurgy.co.za/InfaconXI/003-Basson.pdf [2015, September 2].

Baxter, R. 2008. The global economic crisis and its impact on South Africa and the country's mining industry, in *South African Reserve Bank Conference Series: Challenges for monetary policy-makers in emerging markets*. pp. 105–116. Available:

https://www.researchgate.net/publication/242540468_Financial_innovation_and_a_new_economics_of_banking_Lessons_from_the_financial_crisis

Behrens, W. & Hawranek, P.M. 1991. *Manual for the Preparation of Industrial Feasibility Studies*. Vienna: United Nations Industrial Development Organization.

Bhattacharya, A. & Muthusamy, S. 2017. Static heat energy balance mathematical model for an iron blast furnace. *International Journal of Mineral Processing and Extractive Metallurgy*. 2(5):57–67.

Bhattacharya, S. & Vishwakaram, U.K. 1998. A comparison of blast furnace and corex routes for ironmaking on the basis of costs. *Operational Research Society of India.* 35(2)

Bjorkvall, J., Sichen, D. & Seetharaman, S. 2016. Thermodynamic model calculations in multicomponent liquid silicate systems. *Ironmaking & Steelmaking*. 28(3):250-257.

Broekman, B.R. & Ford, K.J.R. 2004. The development and application of a HCFeMn furnace simulation model for Assmang Limited, in *Tenth International Ferroalloys Congress conference proceedings*. 1-4 February, Cape Town, South Africa, pp. 194–205.

Cairncross, E., 2017. Assessment of Eskom Coal Fired Power Stations for compliance with their 1 April 2015 AELs over the period 1 April 2015 to 31 March 2016; and ranking of their pollutant and CO_2 emission intensities.

Çardaklı, İ., Seçkin, 2010. Production of high carbon ferromanganese from a manganese ore located in Erzincan. Unpublished masters thesis. Middle East: Middle East Technical University.

Chapra, S.C. & Canale, R.P. 2010. *Numerical Methods for Engineers*, 6th. edition. New York: McGraw-Hill.

Chetty, D. & Gutzmer, J. 2018. Quantitative mineralogy to address energy consumption in smelting of ores from the Kalahari Manganese Field, South Africa, in *INFACON XV conference proceedings*. 25-28 February 2018. Cape Town, South Africa.

Cores, A., Babich, A., Muniz, M., Isidro, A., Ferreira, S. & Martin, R. 2007. Iron ores, fluxes, and tuyere injected coals used in the Blast Furnace. *Ironmaking and Steelmaking*, 34(3):231–240.

Crundwell, F.K. 2008. *Finance for Engineers: Evaluation and Funding of Capital Projects*. London: Springer.

Dash, R.N. & Das, C. 2009. Recent developments in Iron and steel making industry. *Journal of Engineering Innovation and Research*, 1(1):23–33.

Directorate Mineral Economics, 2017. Mineral Production and Sales Statistics: Provisional.

Dutta, S.K. & Rameshwar, S. 2016. Smelting reduction process. *Encyclopedia of Iron, Steel, and Their Alloys*, New York: Taylor and Francis, 3208–3236. Available: http://dx.doi.org/10.1081/E-EISA-120050892.

Eissa, M., Ghali, S., Ahmed, A. & El-Faramawy, H. 2011. Optimum condition for smelting high carbon ferromanganese. *Ironmaking and Steelmaking*. Available: https://www.researchgate.net/publication/263258130.

Erwee, M.W. 2015. A simplified mass/energy balance model for high carbon ferromanganese production. Mintek internal report 42122, Johannesburg: Mintek.

FactSage 7.2. 2018. *FACT Databases. Software and databases.*

Featherstone, R.A. 1974. Applications of Mamatwan manganese ore, in: *INFACON I conference proceedings*. 22-26 April 1974. Johannesburg, South Africa, pp. 263–271.

Fogler, S.H. 2004. Chapter 6: Multiple reactions, in *Elements of Chemical Reaction Engineering*. New Delhi: Prentice-hall.

Fraga, E.S. 2014. Chapter 1: The importance of mass and energy balances, in: *Process Analysis*.

Gallaher, M. & Depro, B. 2002. *Economic impact analysis of final coke ovens NESHAP: Final report.* [Virginia]: U.S. Environmental Protection Agency.

Gasik, M.I. 2013. *Handbook of Ferroalloys: Theory and Technology*. United Kingdom: Butterworth-Heinemann.

George, M., Corathers, L.A., Kuck, P.H., Papp, J.F., Polyak, D.E., Schnebele, E.K., Shedd, K.B. & Tuck, C.A. 2015. *U.S. Geological Survey Minerals Yearbook 2013: Ferroalloys.*

Glacier Financial Solutions (Pty) Ltd and Sanlam Life Insurance Ltd. 2019. *Tax Guide 2019 - 2020.*

Gordon, Y., Yaroshenko, Y. & Spirin, N. 2018. Chapter 22: Principles of selection of new technology and risk assessment: A case study for the selection of ironmaking process technology, in *Advanced Methods and Technologies in Metallurgy in Russia*. Canada: Springer International Publishing. pp. 185–192.

Green, W.G. (ed.). & Perry, R.H. (ed.). 2008. Section 9: Process economics, in *Perry's Chemical Engineers' Handbook*. New York: McGraw-Hill.

Hall, S. 2012. Chapter 17: Process Evaluation, in *Branan's Rules of Thumb for Chemical Engineers*. Oxford: Butterworth-Heinemann.

Hasanbeigi, A., Arens, M. & Lynn, P. 2014. Alternative emerging ironmaking technologies for energy-efficiency and carbon dioxide emissions reduction: A technical review. *Renewable and Sustainable Energy Reviews*. 33(2014), 645–658. Available: http://dx.doi.org/10.1016/j.rser.2014.02.031.

Heder, M. 2017. From NASA to EU: The evolution of the TRL scale in Public Sector Innovation. *The Innovation Journal: The Public Sector Innovation Journal*. 22(2):1-23.

Himmelblau, D.M. & Riggs, J.E. 2012. *Basic principles and calculations in chemical engineering*. 8th edition. Michigan: Prentice-Hall.

Hooper, R.T. 1968. The production of ferromanganese. *Journal of Metals*. 20:88–92.

Index Mundi: Coal: South African export price [Online]. 2020.. Available: https://www.indexmundi.com/commodities/?commodity=coal-south-african&months=12&currency=zar.

Ingham, J., Dunn, I., Heinzle, E., Prenosil, J. & Snape, J. 2007. *Chemical engineering dynamics: An introduction to modelling and computer simulation*, 3rd edition. Weinheim: WILEY-VCH Verlag GmbH & Co. KGaA.

Investing.com: Metallurgical coke futures [Online]. [n.d.]. Available: https://www.investing.com/commodities/metallurgical-coke-futures [2020, March 2].

Jipnang, E., Monheim, P. & Oterdoom, H. 2013. Process optimisation model for FeMn and SiMn production, in *INFACON XIII: Efficient Technologies in Ferroalloy Industry conference proceedings*. 9-12 June 2013. Almaty, Kazakhstan.

Kamei, Y., Miyazaki, T. & Yamaoka, H. 1992. Production test of high-carbon ferromanganese using a shaft furnace with coke packed bed injected with highly oxygen enriched air and a large quantity of pulverized coal. *Iron and Steel Institute of Japan International*. 33:529–266.

Kemp, I.C., 2007. Chapter 5: Utilities, heat and power systems, in *Pinch Analysis and Process Integration*. Elsevier Butterworth-Heinemann.

Kozhemyacheko, Yu.N., Pervushin, S.I., Varava, V.I., Strelets, A.I., Vasyura, G.G., Osadchii, V.P., Nikolaev, K.A., Anishchenko, Yu.V. & Shubravyi, N.S. 1987. Efficient Blast Regime in the Production of Blast-furnace Ferromanganese. *Metallurgist.* 12:9–11.

Kumar, P.P., Gupta, P.K. & Ranjan, M. 2008. Operating Experiences with Corex and Blast Furnace at JSW Steel Ltd. *Ironmaking and Steelmaking*. 35(4):260–263.

Lagendijk, H., Xakalashe, B., Ligege, T., Ntikang, P. & Bisaka, K. 2010. Comparing manganese ferroalloy smelting in pilot-scale AC and DC submerged-arc furnaces, in *INFACON XII: Sustainable Future*. 6-9 June 2010. Helsinki, Finland, pp. 497–508.

Lemmens, S. 2016. Cost engineering techniques and their applicability for cost estimation of organic rankine cycle systems. *Energies 9*. 9:485-502

Lindstad, T., Olsen, S.E., Tranell, G., Faerden, T., Lubetsky, J., 2007. Greenhouse Gas Emissions from Ferroalloy Production, in *Innovations in Ferro Alloy Industry*. 18-21 February 2007. Presented at the International Ferroalloys Congress XI, Southern African Institute of Mining and Metallurgy, New Dehli, India.

Mackenzie, W. & Cusworth, N. 2007. The use and abuse of feasibility studies, in *Project Evaluation conference proceedings*. 19-20 June 2007. Melbourne, Australia.

Madias, J. 2011. A Review of the production of ferromanganese in blast furnace, in *AISTech 2011 conference proceedings*. 4-7 May 2009. Missouri, USA, pp. 401–412.

Mishchenko, I.M., Varava, V.I., Bondarenko, N.M., Malkin, V.I., Krizhevskii, A.Z. & Osadchii, V.P. 2000. Making blast-furnace ferromanganese with the use of fluxed manganese-bearing sinter. *Metallurgist.* 44:38–40.

Moolman, M.D. & Van Niekerk, A.A. 2018. Constructing and commissioning Malaysia's most advanced ferromanganese smelter complex, in *INFACON XV conference proceedings*. 25-28 February 2018. Capetown, South Africa. pp. 169–182.

Motiang, M. 2018. *2018 South African Energy price statistics*. [Pretoria]: South African Department of Energy.

Mul'ko, G.N., Bondar', A.A., Zaitsev, V.A., Nitskii, E.A. & Cherkasov, E.G. 2000. Making ferromanganese in blast furnaces. *Metallurgist*. 44:1-2.

National Treasury Republic of South Africa, 2013. *Carbon Tax Policy Paper* [Online]. Available: http://www.treasury.gov.za/public%20comments/Carbon%20Tax%20Policy%20Paper%202013.pdf [2020, January 5].

Nill, J., Dehnhardt, A. & Lorenz, A. 2003. *Technological competition, time, and windows of opportunity: The case of iron and steel production technologies*. [Berlin]: Institute for Ecological Economy Research.

Nkondlo, N. 2020. *Daily Maverick: Covid-19 and Retrenchment Double Whammy for Workers at ArcelorMittal in Saldanha* [Online]. Available: https://www.dailymaverick.co.za/opinionista/2020-04-01-covid-19-and-retrenchment-double-whammy-for-workers-at-arcelormittal-in-saldanha/#gsc.tab=0 [2020, May 25].

Noldin, J. 2012. An overview of the new and emergent ironmaking technologies, in *IAS 18th Steelmaking and 8th Ironmaking conference proceedings*. Rosario, Argentina, pp. 19-25

Nomura, T., Yamamota, N., Fujii, T. & Takiguchi, Y. 2015. Beneficiation plants and pelletizing plants for utilizing low grade iron ore. *Kobelco Technology Review*. (33):8–15.

Noort, D.J. & Adams, C. 2006. Effective mining project management systems, in *International Mine Management conference proceedings*. 16-18 October 2006. Melbourne, Australia, pp. 87–96.

Olsen, S.E., Tangstad, M. & Lindstad, T. 2007. *Production of manganese ferroalloys*. Trondheim, Norway: Tapir Academic Press.

Pal, S. & Lahiri, A.K. 2003. Mathematical Model of COREX melter gasifier: Part I steady-state model. *Metallurgical and Materials Transactions B.* 34B:103–114.

Parisher, R.A. & Rhea, R.A. 2012. Chapter 7: Flow diagrams and instrumentation, in *Pipe Drafting and Design*. Elsevier, pp. 134–153.

Peacey, J.G. & Davenport, W.G., 1979. *The Iron Blast Furnace*. Oxford: Pergamon Press.

Pfeifer, H.C. 2009. *Mini Blast Furnace – MBF* [Online]. Available: http://www.minitec.eng.br/ingles/mbf-ingles_16-07-09.pdf [2018, December 2].

PKF South Africa Inc. 2017. *Tax Guide 2017/2018* [Online]. Available: https://www.pkf.co.za/media/10030933/pkf-tax-guide-2017-2018-web.pdf [2019, April 11]

Pollet, B.G., Staffell, I., Adamson, K., 2015. Current energy landscape in the Republic of South Africa. *International Journal of Hydrogen Energy*. 40:16685–16701.

Qu, Y., Zou, Z. & Xiao, Y. 2012. A Comprehensive Static Model for COREX Process. *Iron and Steel Institute of Japan International*. 52:2186–2193.

Revombo, K.L. 2016. Energy minerals: Coal. *South African Minerals Industry 2014/2015* [Online].

Ruhmer, W.T. 1991. *Handbook on the Estimation of Metallurgical Process Costs*, 2nd edition. Johannesburg: Mintek special publication.

Saltelli, A. 1999. *Evaluation of sensitivity and uncertainty analysis methods in a quality assessment framework with application to environmental and business statistics: Final report*. [Italy]: Institute for Systems, Informatics and Safety.

Sen, R. 1997. Production of ferro manganese through blast furnace route. *Ferro Alloy Industries in the Liberalised Economy*. 83–91.

Sinnott, R.K. 2005. *Chemical Engineering Design*. 4th edition. Oxford: Elsevier Butterworth-Heinemann.

Sithole, N.A., Rambuda, N., Steenkamp, J.D., Hayman, D.A. & Hockaday, C.J. 2018. Silicomanganese production at Mogale Alloys. *Journal of the Southern African Institute of Mining and Metallurgy*. 118:1205–1216.

Srishilan, C. & Shukula, A.K. 2017. Static thermochemical model of COREX melter gasifier. *Metallurgical and Materials Transactions B*.

Steenkamp, J.D. 2020. FactSage-Based Design calculations for the production of high-carbon ferromanganese on pilot-scale, in *11th International Symposium on High-Temperature Metallurgical Processing. 23-27 February 2020.* San Diego, California, USA.

Steenkamp, J.D. & Basson, J. 2013. The manganese ferroalloys industry in Southern Africa. *Journal of the Southern African Institute of Mining and Metallurgy*. 113:667–676.

Steenkamp, J.D., Maphutha, M.P., Makwarela, O., Banda, W., Thobadi, I., Sitefane, M., Gous, J.P. & Sutherland, J.J. 2018. Silicomanganese production at Transalloys in the twenty-tens. *Journal of the Southern African Institute of Mining and Metallurgy*. 118.

Sun, H., Lone, M.Y., Ganguly, S. & Ostrovski, O. 2010. Wettability and reduction of MnO in slag by carbonaceous materials. *Iron and Steel Institute of Japan International*. 50:639–646.

Sun, J., Wu, S., Kou, M., Shen, W. & Du, K. 2014. Influence of operation parameters on dome temperature of COREX melter gasifier. *Iron and Steel Institute of Japan International*. 54:43–48.

Swamy, K.N., Robertson, D.G.C., Calvert, P., Kozak, D. 2001. Factors affecting carbon consumption in the production of high carbon ferromanganese, in *INFACON IX conference proceedings*. 3-6 June 2001. Quebec City, Canada, pp. 293–301.

Tangstad, M., Calvert, P., Brun, H. & Lindseth, A.G. 2004. Use of Comilog ore in ferromanganese production, in *INFACON X conference proceedings*. 1-4 February 2004, Cape Town, South Africa, pp. 213–222.

Tangstad, M. & Olsen, S., E. 1995. The ferromanganese Process - Material and Energy balance, in *INFACON VII conference proceedings*. 11-14 June 1995. Trondheim, Norway.

Thaler, C., Tappeiner, T., Schenk, J., Kepplinger, W., Plaul, J.F. & Schuster, S. 2012. Integration of the blast furnace route and the FINEX: Process for low CO_2 hot metal production. Steel Research International. 83(2):181–188.

Turton, R., Bailie, R.C., Whiting, W.B. & Shaeiwitz, J.A. 2008. *Analysis and Synthesis, and Design of Chemical Processes*. 3rd edition. Massachusetts, United States: Prentice Hall.

Van Zyl, H.J. 2017. Identifying barriers to growth in mineral value chains: An analytical framework approach. Unpublished masters thesis. Stellenbosch: Stellenbosch University [Online]. Available: http://hdl.handle.net/10019.1/100813 [2017, March]

Vanderstaay, E.C., Swinbourne, D.R. & Monteiro, M. 2004. A computational thermodynamics model of submerged arc electric furnace ferromanganese smelting. *Transactions of the Institution of Mining and Metallurgy*. 113:38-44.

Vignes, A. 2013. Chapter 4: Blast furnaces. *Extractive metallurgy 3: Processing operations and routes.* Wiley Online Library.

Van der Vyver, W.F., Pistorius, P.C., Brand, S.A. & Reid, M. 2009. Disintegration of Northern Cape iron ores under reducing conditions. *Ironmaking and Steelmaking*. 36(5):354–362.

Wafiq, A., Soliman, A., Moustafa, T.M. & Nassar, A.F. 2012. Optimum process conditions for the production of pig iron by COREX process, in *SCANMET IV: 4th International Conference on Process Development in Iron and Steelmaking*. 10-13 June 2012. Lulea, Sweden.

Wasbø, S.O., Foss, B.A. & Tronstad, R., 1997. Object-oriented ferromanganese furnace model. *Modeling,. Identifaction and Control.* 18(4):249–259.

Wellbeloved, D.B. & Kemink, M. 1995. The economic and technical implications of the use of coal rather than coke as a reductant at Metalloys, in *INFACON VI conference proceedings*. 11-14 June 1995. Trondheim, Norway, pp. 191–199.

Woods, D.R. 2007. *Rules of Thumb in Engineering Practice*. Weinheim, Germany: WILEY-VCH Verlag GmbH & Co. KGaA.

Yi, S.H., Joo, S., Lee, H.C., Kang, T.I., Cho, I.H. & Lee, H.G. 2011. Operating experience of the first commercial FINEX ironmaking plant. *Steel Times International*. 35:32–34.

Zhang, T. 1992. The Two-stage production of high-carbon ferromanganese in a blast furnace: A method for the treatment of a lean manganese ore, in *INFACON 6 conference proceedings*. 8-11 March 1992. Cape Town, South Africa, pp. 155–159.

Zhou, X. & Zhongning, D. 2013. The introduction of COREX process development. *Advanced Materials Research*. 774–776(2013):1430–1433.

Appendix A: Flowsheets

In Chapter 2.3 four technologies were compared side by side the SAF, BF, COREX®, and FINEX®. Due to the various recycle streams in the alternative ironmaking technologies, the COREX® and FINEX®, Figure A-1, and Figure A-2 were provided to further elaborate on the various units used in each that form an integral part of the furnace system. Due to similarities in the processes, a detailed explanation will be provided for the FINEX® and only the differences in the COREX® diagram will be discussed.

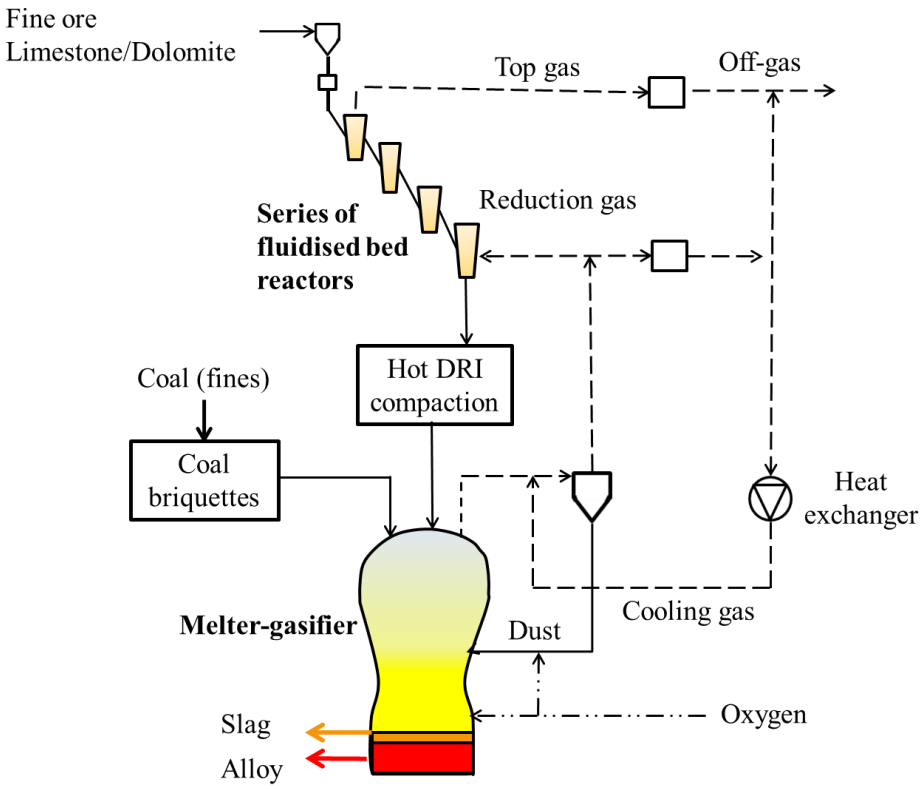

Figure A-1: Process flow diagram of the FINEX® furnace for pig iron production (Yi *et al.*, 2011).

FINEX® predominantly used fine material in the process. Fluidised bed reactors in series facilitate the heat exchange between the fine feed material and the recycled reduction gas. The melter-gasifier requires a particle size range between 5– 40 mm, therefore the product from the fluidised bed reactors is sent to a hot compactor for agglomeration.

Coal fines are agglomerated separately in a briquetting unit before smelting. In the melter-gasifier, some of the particles disintegrate and generate dust particles that get carried out with the gas. The gas is then sent through to a hot cyclone to recover the dust and recycle them back into the melter-gasifier. Solid free gas is then sent into two processing sets, a portion of the gas is sent to the fluidised-bed rectors while it still contains the heat energy generated in the melter-gasifier. Another portion is sent to CO_2 removal steps, this is achieved using scrubbers.

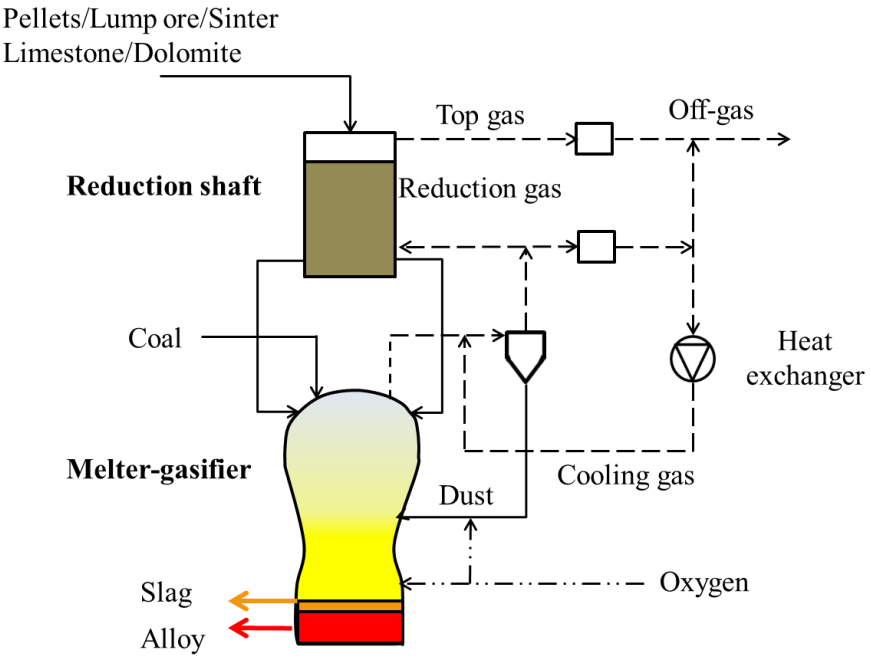

Figure A-2: COREX® Process flow diagram for pig iron production (Zhou & Zhongning, 2013)

The COREX® system replaces the 3-4 units with one reduction shaft that processes particles between 5– 30 mm, therefore there is no need for agglomeration of the reduced material before feeding into the melter-gasifier.

The quality of manganese ore typically fed into SAF furnaces and iron ore typically fed into BF and COREX® are shown in Table A-1. Manganese deposits always contain iron as a result the quality of the ore is measured in Mn/Fe ratio. The presence of gangue materials that report to the slag also has an influence on the amount of manganese in the ore. These two quality measures affect the alloy quality and process energy consumption.

Table A-1: Manganese/iron source - ore composition (S E Olsen *et al.*, 2007; Van der Vyver *et al*., 2009).

Constituent (wt%)	Manganese Ore	Constituent (wt%)	Iron Ore
MnO_2	35	-	-
MnO	36	**FeO**	0.47
Fe_2O_3	15	**Fe_2O_3**	95
SiO_2	3.6	**SiO_2**	1.6
Al_2O_3	0.4	**Al_2O_3**	1.3
CaO	5.6	**CaO**	0.17
MgO	1.0	**MgO**	0.02

Different carbon and flux sources are utilised when smelting ferrous alloys, Table A-2 lists typical compositions.

Table A-2: Carbon and flux sources species and composition (Kumar *et al*., 2008).

Carbon sources (wt%)				Flux sources (wt%)			
	Coal	**Coke**	***Anthracite**		**Limestone**	**Quartzite**	**Dolomite**
Fixed carbon	58	80	83	**CaO**	44	0.36	27
Volatiles	27	1	4	**MgO**	5	0.25	18
Moisture	5	6	1	**SiO_2**	9	96	7
Ash	10	13	12	**Al_2O_3**	2	0.43	1

The use of a carbon source is dictated first by process requirements and cost per unit of raw material considered. Coke has superior processing qualities, however, it is known to be expensive raw material. Anthracite and coal can be used as a replacement in shallow burden operations like the SAF. However, the price of anthracite in South Africa is in the range of coking coal. In the BF the use of anthracite has not been mention. The use of coal in the BF is well published, the coal is fed as a pulverised substance along with the blast air for combustion purposes. The main burden in the BF still consists of coke. The choice of flux is determined by the ore basicity and the reductant ash composition. The carbonates

Different furnaces operate optimally using certain particle size ranges. Table A-3 lists typical size ranges fed into each furnace. SAF and BF have a preference for larger particle size ranges than the COREX® and FINEX®. Particle sizes affect the burden porosity which determines the gas permeability. The ability for the gas to flow evenly through the burden affects heat transfer and gas reduction of the burden materials.

Table A-3: Particle sizes of furnace feed materials (Kumar *et al*., 2008).

Feed size (mm)	SAF*	BF	COREX®	FINEX®
Lump ore	6.35– 75	10– 50 [#]	10– 30 [§]	n/a
Sinter	0.15– 6.35	10– 30 [#]	5– 30 [§]	n/a
Pellets	n/a	10– 20 [#]	8– 16 [§]	n/a
Fine ore	< 6	n/a	0– 12 [§]	0.05– 8 [¥]
Coke	n/a	~ 50[8]	52 [§]	n/a
Coal	n/a	n/a	5– 40 [€]	5– 40 [€]

The smaller particle size range of the COREX® and FINEX® indicates that fine materials are more tolerable during operation. Furthermore, the melter-gasifier burden is not tightly packed similar to the SAF and BF is rather semi-fluidised towards the top (Pal & Lahiri, 2003).

Reactions in the FeMn and ironmaking process are listed side by side in Table A-4. Equation numbers in bold italics are shared by both processes. These two processes have 9 similar reduction equations. The other equations are mostly due to the manganese and iron ore mineralogical composition. For the SAF process equation 29 does not exist due to the energy source using electricity.

Table A-4: Reactions expected to occur in HCFeMnn and ironmaking smelting processes (Swamy *et al*., 2001; Tangstad & Olsen, 1995; Wafiq *et al*., 2012; Wasbo & Foss, 1995; Zhou & Zhongning, 2013).

HCFeMn			Ironmaking		
Stage 1					
#	$H_2O_{(l)} \leftrightarrow H_2O_{(g)}$	***1***		$H_2O_{(l)} \leftrightarrow H_2O_{(g)}$	
#	$H_2O_{(g)} + CO_{(g)} \leftrightarrow H_{2(g)} + CO_{2(g)}$	***2***		$H_2O_{(g)} + CO_{(g)} \leftrightarrow H_{2(g)} + CO_{2(g)}$	
#	$MgCO_3 \rightarrow MgO + CO_{2(g)}$	3	¥	$3Fe_2O_3 + CO_{(g)} \rightarrow 2Fe_3O_4 + CO_{2(g)}$	17
§	$MnCO_3 \rightarrow MnO + CO_{2(g)}$	4	¥	$Fe_3O_4 + CO_{(g)} \rightarrow 3FeO + CO_{2(g)}$	18
#	$CaCO_3 \rightarrow CaO + CO_{2(g)}$	***5***	¥	$CaCO_3 \rightarrow CaO + CO_{2(g)}$	
#	$C_{(s)} + CO_{2(g)} \rightarrow 2CO_{(g)}$	***6***	¥	$C_{(s)} + CO_{2(g)} \rightarrow 2CO_{(g)}$	
#	$MnO_2 + \frac{1}{2}CO \rightarrow \frac{1}{2}Mn_2O_3 + \frac{1}{2}CO_{2(g)}$	7	¥	$FeO + 3CO_{(g)} \rightarrow 2Fe + 2CO_{(g)} + CO_{2(g)}$	19
#	$\frac{1}{2}Mn_2O_3 + \frac{1}{6}CO \rightarrow \frac{1}{3}Mn_3O_4 + \frac{1}{6}CO_2$	8	¥	$3Fe_2O_3 + H_2 \rightarrow 2Fe_3O_4 + H_2O_{(g)}$	20
#	$\frac{1}{3}Mn_3O_4 + \frac{1}{3}CO \rightarrow MnO + \frac{1}{3}CO_2$	9	¥	$Fe_3O_4 + H_{2(g)} \rightarrow 3FeO + H_2O$	21
#	$\frac{1}{3}Fe_3O_4 + \frac{4}{3}CO \rightarrow Fe + \frac{4}{3}CO_2$	10	¥	$FeO + 3H_2 \rightarrow Fe + 2H_2 + H_2O$	22
			¥	$CaMg(CO_3)_2 \rightarrow CaO$□$MgO + 2CO_{2(g)}$	23
			¥	$H_2 + CO_{(g)} \leftrightarrow 2H_2O_{(g)} + C$	24
			¥	$3Fe + 2CO \rightarrow Fe_3C + CO_2$	25
§	$Mn_3O_{4(l)} + C \rightarrow 3MnO + CO$	11			
§	$FeO_{(l)} + C \rightarrow 2Fe_{(l)} + CO_{(g)}$	***12***	¥	$FeO_{(l)} + C \rightarrow Fe_{(l)} + CO_{(g)}$	

HCFeMn			Ironmaking		
Stage 2					
§	$MnO_{(l)} + C \rightarrow Mn_{(l)} + CO_{(g)}$	***13***	¥	$MnO_{(l)} + C \rightarrow Mn_{(l)} + CO_{(g)}$	
§	$SiO_{2(l)} + 2C \rightarrow Si_{(l)} + 2CO_{(g)}$	***14***	Σ	$SiO_{2(l)} + 2C \rightarrow Si_{(l)} + 2CO_{(g)}$	
§	$C \rightarrow C_{sol}$	15	¥	$2FeO_{(l)} + Si \rightarrow 2Fe_{(l)} + SiO_2$	26
			¥	$FeO_{(l)} + Mn \rightarrow Fe_{(l)} + MnO$	27
			¥	$3Fe + C \rightarrow Fe_3C$	28
8	$2(MnO) + Si \leftrightarrow 2Mn + (SiO_2)$	***16***	Σ	$2(MnO) + Si \leftrightarrow 2Mn + (SiO_2)$	
Combustion					
	$C + O_{2(g)} \rightarrow CO_{2(g)}$	***29***		$C + O_{2(g)} \rightarrow CO_{2(g)}$	

Mineralogy plays a major role in energy consumptions due to the reactions that need to occur. The reactions listed in Table A-4 use a simplified version of the manganese and iron compounds that are found in ore.

The take-home from these equations is that in both processes manganese alloy in equation number 13 is produced, even though to a much lesser extent in the ironmaking process due to low concentrations. It is wise to note that manganese compounds may be present in their higher oxide state in iron ores, however, the low concentrations allow for an oversimplification of assuming it is in MnO form. Not all equations will be incorporated into the model due to the likelihood of occurrence based on literature recommendations and the availability of data for necessary energy balance equations.

Carbon combustion in the furnace made use of the ultimate and proximate analysis to estimate the mass of carbon in the volatile matter. The difference between the two carbon values (ultimate analysis C – proximate analysis C) was then converted into moles and it was assumed to be the total moles of methane (CH_4). The mass of hydrogen required in the methane compound was deducted and the remaining portion was assumed to be hydrogen (H_2). The rest of the compounds N and S were left as is. For coke combustion in the BF, CH_4 was assumed to combust to 2CO and $2H_2$. Assuming that the products of combustion consume carbon in the boudouard reaction and the water-gas shift produces H_2. The solid carbon was assumed to fully combust, however, the boudouard reaction converts most of the CO_2 into CO. In the COREX® the coal comes in at the top of the dome where the volatile matter first undergoes gasification into CH_4, H_2, S, and N_2. The solid carbon then proceeds to the burden to be fully combusted and the boudouard reaction is accounted for. The model assumes that reducing gas components consist of CO, CO_2, H_2O, CH_4, H_2, S, and N_2 (Srishilan & Shukula, 2017). The effect of H_2 and CH_4 on the reduction of manganese was not taken into account. The remaining gaseous compounds were used in the electricity generation unit.

A comparison of the slag properties for both processes was made in Table A-5.

Table A-5. Typical compositions and properties of the alloy and slag (Ahmed *et al*., 2014; Vignes, 2013).

Alloy			Slag		
Component	**HCFeMn#**	**Ironmaking***	**Component**	**HCFeMn#**	**Ironmaking***
Mn	75	0.2	**MnO**	19	n/a
Fe	17	95	**FeO**	0.85	0.2
C	7	4.6	**SiO_2**	26	35
Si	0.18	0.3	**CaO**	27	42
S	n/a	0.02	**MgO**	9.2	7.5
P	0.18	0.08	**Al_2O_3**	12	10
Slag/metal	0.8	0.3	**Basicity**	0.97	1.1

The quality of the alloy product tapped from each furnace is determined by the slag characteristics. Ironmaking processes typically recover more iron due to it being relatively easy to reduce, unlike manganese. The slag basicity is calculated using equation 30, where the gangue mineral content in the slag is taken into account.

Off-gas produced by each furnace contains energy-generating compounds such as CO and H_2. Table A-6 lists the composition and energy content of the gas that is normally generated by each furnace system. Energy values for combustion-based technologies are generally higher due to two reasons. Higher production of CO_2 to generate heat provides more reactant for the Boudouard reaction where In the COREX®, the volatile matter is cracked at the dome of the melter-gasifier before it leaves the smelting unit with higher amounts of CO leaving as reducing gas for solid-state reduction. CO is generated. Another reason is the high volumes of off-gas generated via the combustion route.

Table A-6: Example of SAF, BF, and COREX off-gas composition (Kumar *et al*., 2008).

Component (vol%)	**SAF**	**BF**	**COREX®**
CO	20	23	45
CO_2	80	21	35
H_2	-	5	18
N_2	-	52	2
Energy value (MJ/Nm^3)	0.22	3.1	8.2
MJ/tHM	180	3784	9840
MWh/tHM	0.05	1.06	2.76

Appendix B: Process Model Data

Raw material compositions listed in Table B-1 to Table B-3 were chosen were based on the quality of data that was provided by the author in published literature and the typical compositions used in the FeMn production process in South Africa. All solid material streams were assumed to be at atmospheric pressure when not inside the furnace, therefore only the temperatures provided for each stream.

Table B-1. Manganese ore composition.

Component	Mamatwan	Gloria	Wessels-50	Wessels-L
MnO_2	23.40	23.60	35.20	39.90
$MnCO_3$	0.00	3.24	0.00	0.00
MnO	29.80	29.30	36.10	28.70
Fe_2O_3	6.60	7.20	14.50	17.40
SiO_2	4.00	5.70	3.60	3.23
Al_2O_3	0.50	0.30	0.40	0.44
$CaMg(CO_3)_2$	16.10	17.48	4.60	1.33
$CaCO_3$	21.14	13.18	0.91	8.13
CaO	2.90	0.00	0.00	0.00
H_2O	1.30	0.40	0.90	1.31
SO_3	0.00	0.00	0.00	0.11
P	0.02	0.02	0.04	0.11
Mn	37.88	39.17	50.22	47.46
Mn/Fe	8.20	7.77	4.95	3.7
Temperature	25 ℃	25 ℃	25 ℃	25 ℃

1 Mamatwan: (Featherstone, 1974)

2 Gloria: (Erwee, 2015)

3 Wessels-50: (S E Olsen *et al*., 2007)

4 Wessel-L: (Featherstone, 1974)

Ores listed in Table B-1 generally have a high manganese content and they can be considered medium- to high-quality. Ores with higher Mn/Fe ratios are the highest quality. The higher manganese content in ore translates to fewer gangue minerals that enter into the process as a result lower slag to metal ratios will be estimated by the model.

Three carbon sources were used, the SAF made use of a blend of coke and coal, the BF made use of only coke, and COREX® only uses coal.

Table B-2. Carbon sources for reductant and combustion.

Component	Coke	Anthracite	Coal
C	85.00	79.68	58.00
VM	1.60	3.84	27.00
Fe_2O_3	1.16	4.12	0.00
SiO_2	6.71	6.31	5.80
Al_2O_3	3.85	3.24	3.10
CaO	0.37	0.36	0.00
MgO	0.04	0.15	0.00
H_2O	0.00	4.00	5.00
P	0.02	0.72	-
S	0.19	0.44	-
Temperature	25 ℃	25 ℃	25 ℃

1 Coke: (Erwee, 2015)

2 Anthracite: (Erwee, 2015)

3 Coal: (Kumar *et al*., 2008)

Two fluxes were used in the model, these are common flux sources used in the South African FeMn processing and are locally sourced. Another fluxing agent used in BF and COREX® is dolomite, however, it was not included in the model.

Table B-3. Flux sources used to alter the basicity of the slag.

Component	Quartzite	Limestone
SiO_2	96.00	4.10
Al_2O_3	0.43	0.53
$CaCO_3$	0.52	75.00
$MgCO_3$	0.53	0.65
H_2O	0.55	0.34
LOI	1.97	19.38
Temperature	25 ℃	25 ℃

1 Quartzite: (Erwee, 2015)

2 Limestone: (Kumar *et al*., 2008)

Based on the raw material compositions chosen, the reactions in each phase were chosen from Table A-4 and the chosen reactions are displayed in Table B-4 and Table B-5. Assumptions about the extent of the consumption of the limiting reagent are provided. The extent of the reaction is crucial for both the mass and energy equations. Elements are distributed between streams and reaction energy consumption/generation can be quantified. Different assumptions were made between furnaces for equations [2], [6], and [9]. The extent of the water-gas shift and Boudouard reaction were assumed to be the same as the SAF and BF 70% of the CO from solid-state reduction reactions.

Boudouard reactions were assumed to not exist in the COREX® solid-state reduction unit. Therefore, the only gas that is exposed to solid carbon is only from combustion and liquid-state reduction.

Table B-4. Solid-state reduction reactions and assumptions

No.	Reaction equation	Assumptions about the extent (x) of the reaction
[1]	$H_2O_{(l)} \leftrightarrow H_2O_{(g)}$	Limiting reagent: $H_2O_{(l)}$ x = 1
[2]	$H_2O_{(g)} + CO_{(g)} \leftrightarrow H_{2(g)} + CO_{2(g)}$	Limiting reagent: $H_2O_{(g)}$ x = 0.6 – 0.7
[3]	$MgCO_3 \rightarrow MgO + CO_{2(g)}$	Limiting reagent: $MgCO_3$ x = 1
[4]	$MnCO_3 \rightarrow MnO + CO_{2(g)}$	Limiting reagent: $MnCO_3$ x = 1
[5]	$CaCO_3 \rightarrow CaO + CO_{2(g)}$	Limiting reagent: $CaCO_3$ x = 1
[6]	$C_{(s)} + CO_{2(g)} \rightarrow 2CO_{(g)}$	Limiting reagent CO_2 x = 0.4 – 0.9 Equation in stage 2 for the COREX model
[7]	$MnO_2 + \frac{1}{2}CO \rightarrow \frac{1}{2}Mn_2O_3 + \frac{1}{2}CO_{2(g)}$	Limiting reagent: MnO_2 x = 1
[8]	$\frac{1}{2}Mn_2O_3 + \frac{1}{6}CO \rightarrow \frac{1}{3}Mn_3O_4 + \frac{1}{6}CO_2$	Limiting reagent: Mn_2O_3 x = 1
[9]	$\frac{1}{3}Mn_3O_4 + \frac{1}{3}CO \rightarrow MnO + \frac{1}{3}CO_2$	Limiting reagent: Mn_3O_4 x = 0.7/0.75
[17]	$\frac{1}{3}Fe_3O_4 + \frac{4}{3}CO \rightarrow Fe + \frac{4}{3}CO_2$	Limiting reagent: Fe_2O_3 x = 1
[18]	$Fe_3O_4 + CO_{(g)} \rightarrow 3FeO + CO_{2(g)}$	Limiting reagent: Fe_3O_4 x = 1

Table B-5. Liquid-state reduction reactions and assumptions

No.	Reaction equation	Assumption about the extent of the reactions
[11]	$Mn_3O_{4(l)} + C \rightarrow 3MnO + CO$	Limiting reagent: $Mn_3O_{4(l)}$ x = 1
[12]	$FeO_{(l)} + C \rightarrow 2Fe_{(l)} + CO_{(g)}$	Limiting reagent: $FeO_{(l)}$ x = 1
[13]	$MnO_{(l)} + C \rightarrow Mn_{(l)} + CO_{(g)}$	Mn produced determined by the fraction in alloy
[14]	$SiO_{2(l)} + 2C \rightarrow Si_{(l)} + 2CO_{(g)}$	Si produced determined by the fraction in alloy
[15]	$C \rightarrow C_{sol}$	C content determined by the fraction in alloy

Published literature on manganese ore smelting was used to inform the gas utilisation in the furnace. For the SAF, 70% of the manganese in the ore is assumed to be converted to MnO, refer to equation 9 (Tangstad and Olsen, 1995; Swamy *et al*., 2001). For the other two furnaces, better gas utilisation is expected due to the physical construct of the furnace. However, no literature provides gas utilisation values for the BF or the COREX®. A value of 75% was used for both furnaces, refer to equation 9. The rest of the reactions were assumed to display the same conversions. The carbonates were assumed to decompose according to equations 3 and 5 and the energy consumption was accounted for. Some Stage 2 reactions in Table B-5 were limited by the alloy quality specifications.

The various compositions of the alloy stream were chosen in such a manner that they adhered to grade B ASTM FeMn alloy standards. Table B-6 lists the assumptions made about the alloy and slag stream.

Table B-6. Assumptions for the alloy and slag streams.

	Alloy	**Slag**
Composition (%)	Mn: 75– 75.15 Fe: 17.85– 18.05 C: 5.8– 6 Si: 1 P: 0.1– 0.15	MnO: 22– 25 FeO: 0– 7
Mass (kg)	1000	Slag to metal ratio: 0.6– 0.8
Temperature (℃)	1500	Thermal equilibrium with the alloy: 1500

Initial assumptions were made about the alloy and some of the slag properties to allow for various estimations to be made about the inlet raw material compositions and mass rates. The final alloy and slag compositions were estimated by distributing elements into their respective streams using the reaction equations provided.

The energy balance requires an estimate of the heat supplied/consumed by each stream flowing in and out of the furnace system. Heat estimations are calculated using unit mass heat capacity value or equation and multiplied by the number of mass units. The general assumption for all solid and gaseous furnace streams is that there are negligible interactions between streams components, except for the slag. Therefore negating the step of calculating the enthalpy of mixing for all streams. Heat capacity equations and data for the compounds identified in the system were obtained from various sources. Information on widely used components in the gas phase and some solids that result from solid-state reduction were accessed from literature from the chemical engineering field. Data were obtained from publications by Green and Perry (2008). Most compounds and reaction enthalpies can be obtained from a variety of reference literature and thermochemical software. The alloy enthalpy was estimated using a specifically designed database for a ferromanganese alloy accessed through FactSage 7.2 (FactSage 7.2, 2018). The slag enthalpy was estimated using a published slag solution model (Bjorkvall *et al*., 2016).

A module is a file containing a group of code in Python 3.6. One module was created to store all the functions that were used across all furnace models. The module was called ‘Process’ and the functions were called similarly to the built-in functions available in Python. Functions were specifically created to execute repetitive calculations on streams to convert mass flow units, estimate enthalpy calculations, and group the type of reactions that occur on a particular stream. Special types of functions were also created to estimate the amount of flux and the blend ratio, choose the ore blend based on the estimated Mn/Fe ratio, and

calculating off-gas temperatures. The calculation sequences shown in Figure 3-4 to Figure 3-6 were implemented in separate files. The required output variables were returned to the Excel file.

Each furnace mass and energy balance model was created in a separate module and made use of the Process module customised equations to estimate stream compositions and masses. In the next paragraphs, a brief description of the functions that were used in the mass and energy model will be provided.

For estimating the mass and quality of the manganese input a list of 41 manganese ores was made in Excel with Mn/Fe ratios varying between 8 and 4 in increments of 0.5. The list was imported into Python to be used by the 'ore_mix' function. The function requires an estimated Mn/Fe ratio based on the Mn and Fe in the slag, alloy, and dust streams. Furthermore, a 'dilution' coefficient is introduced for the SAF and BF due to the coke and anthracite that contain Fe in the ash. The coefficient further increases the Mn/Fe ratio to account for the extra Fe that comes in. This was done to ensure that the effective Mn/Fe ratio entering the furnace system is the same or higher than the alloy product (S.E. Olsen *et al*., 2007). Using the estimated Mn/Fe ratio 'ore_mix' iterates through the 41 mixtures and identifies the closest match and outputs the details of the particular stream. The model then uses the ratio of manganese in the ore mixture to total ore mixture to obtain the mass of the manganese stream.

When estimating the flux requirement 'SAF_flux_estimate' was built. The mass and blend of quartzite to limestone was estimated. The function required a basicity value for the manganese ore mixture as an input. An arbitrary basicity value 'BA_aim' was assumed, higher than the ore basicity value. The 'SAF_flux_estimate' function made use of the 'BA_aim' to decide whether to add 2 kg of quartzite or limestone. If the basicity of the manganese mixture was lower than 'BA_aim' then limestone was added. Conversely, if the manganese basicity was higher, then quartzite was added. The 'BA_aim' value was changed to suit the required slag basicity.

Reaction functions were created for each stream containing the various reactions that occur to the stream components. An example of the COREX® function for the manganese stream in stage one is shown in Figure B-1.

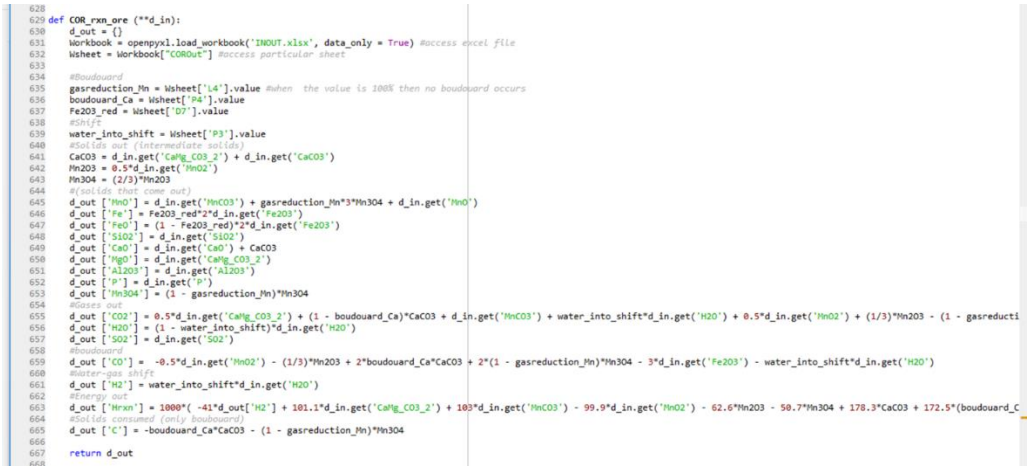

```
def COR_rxn_ore (**d_in):
    d_out = {}
    Workbook = openpyxl.load_workbook('INOUT.xlsx', data_only = True) #access excel file
    Wsheet = Workbook["COROut"] #access particular sheet

    #Boudouard
    gasreduction_Mn = Wsheet['L4'].value #when  the value is 100% then no boudouard occurs
    boudouard_Ca = Wsheet['P4'].value
    Fe2O3_red = Wsheet['D7'].value
    #Shift
    water_into_shift = Wsheet['P3'].value
    #Solids out (intermediate solids)
    CaCO3 = d_in.get('CaMg_CO3_2') + d_in.get('CaCO3')
    Mn2O3 = 0.5*d_in.get('MnO2')
    Mn3O4 = (2/3)*Mn2O3
    #(solids that come out)
    d_out ['MnO'] = d_in.get('MnCO3') + gasreduction_Mn*3*Mn3O4 + d_in.get('MnO')
    d_out ['Fe'] = Fe2O3_red*2*d_in.get('Fe2O3')
    d_out ['FeO'] = (1 - Fe2O3_red)*2*d_in.get('Fe2O3')
    d_out ['SiO2'] = d_in.get('SiO2')
    d_out ['CaO'] = d_in.get('CaO') + CaCO3
    d_out ['MgO'] = d_in.get('CaMg_CO3_2')
    d_out ['Al2O3'] = d_in.get('Al2O3')
    d_out ['P'] = d_in.get('P')
    d_out ['Mn3O4'] = (1 - gasreduction_Mn)*Mn3O4
    #Gases out
    d_out ['CO2'] = 0.5*d_in.get('CaMg_CO3_2') + (1 - boudouard_Ca)*CaCO3 + d_in.get('MnCO3') + water_into_shift*d_in.get('H2O') + 0.5*d_in.get('MnO2') + (1/3)*Mn2O3 - (1 - gasreducti
    d_out ['H2O'] = (1 - water_into_shift)*d_in.get('H2O')
    d_out ['SO2'] = d_in.get('SO2')
    #Boudouard
    d_out ['CO'] =  -0.5*d_in.get('MnO2') - (1/3)*Mn2O3 + 2*boudouard_Ca*CaCO3 + 2*(1 - gasreduction_Mn)*Mn3O4 - 3*d_in.get('Fe2O3') - water_into_shift*d_in.get('H2O')
    #Water-gas shift
    d_out ['H2'] = water_into_shift*d_in.get('H2O')
    #Energy out
    d_out ['Hrxn'] = 1000*( -41*d_out['H2'] + 101.1*d_in.get('CaMg_CO3_2') + 103*d_in.get('MnCO3') - 99.9*d_in.get('MnO2') - 62.6*Mn2O3 - 50.7*Mn3O4 + 178.3*CaCO3 + 172.5*(boudouard_C
    #Solids consumed (only boubouard)
    d_out ['C'] = -boudouard_Ca*CaCO3 - (1 - gasreduction_Mn)*Mn3O4

    return d_out
```

Figure B-1. Manganese ore reaction function for the COREX®.

Detail of the ore stream and the mass are required to execute the calculation. The output consists of the resultant components of the reduced solids, various gaseous compounds such as CO and CO_2 that go into the off-gas, carbon requirements, and net energy requirement for reduction reactions. Water-gas shift and Boudouard reactions were taken into account. The functions were created for input and intermediate streams.

Each stream entering and leaving the furnace had a designated function to calculate the energy it contributes or takes away from the furnace. The energy balance consists of stream enthalpies, reactions, and electricity for the SAF. An example of the slag stream enthalpy calculation is shown in Figure B-2. Component interactions were taken into account in the slag model enthalpy calculation instead of pure components. The pure component method was applied to all other streams of the furnace system.

```
def slag_H (**d_in): #Stream B
#The mole fractions of the slag will be recalculated to include AlO1.5 using a basis of 1
    AlO = 2*d_in.get('Al2O3')/(2*d_in.get('Al2O3') + d_in.get('CaO') + d_in.get('FeO') + d_in.get('MgO') + d_in.get('MnO') + d_in.get('SiO2'))
    CaO = d_in.get('CaO')/(2*d_in.get('Al2O3') + d_in.get('CaO') + d_in.get('FeO') + d_in.get('MgO') + d_in.get('MnO') + d_in.get('SiO2'))
    FeO = d_in.get('FeO')/(2*d_in.get('Al2O3') + d_in.get('CaO') + d_in.get('FeO') + d_in.get('MgO') + d_in.get('MnO') + d_in.get('SiO2'))
    MgO = d_in.get('MgO')/(2*d_in.get('Al2O3') + d_in.get('CaO') + d_in.get('FeO') + d_in.get('MgO') + d_in.get('MnO') + d_in.get('SiO2'))
    MnO = d_in.get('MnO')/(2*d_in.get('Al2O3') + d_in.get('CaO') + d_in.get('FeO') + d_in.get('MgO') + d_in.get('MnO') + d_in.get('SiO2'))
    SiO = d_in.get('SiO2')/(2*d_in.get('Al2O3') + d_in.get('CaO') + d_in.get('FeO') + d_in.get('MgO') + d_in.get('MnO') + d_in.get('SiO2'))

    #Compent interaction = Component1*Component2(constant1 + constant3*(component1 - component2) + constant5*(component1 - component2)**2)
    Al_Ca = AlO*CaO*(-125997 + 6594.66*(AlO - CaO) - 44390*(AlO - CaO)**2)
    Al_Fe = AlO*FeO*(-7091.4 + 0*(AlO - FeO) - 0*(AlO - FeO)**2)
    Al_Mg = AlO*MgO*(-7049.76 - 30313.22*(AlO - MgO) - 0*(AlO - MgO)**2)
    Al_Mn = AlO*MnO*(-22165.1 - 13054.5*(AlO - MnO) + 13408*(AlO - MnO)**2)
    Al_Si = AlO*SiO*(-10256.9 + 27248.2*(AlO - SiO) - 10811.9*(AlO - SiO)**2)
    Ca_Fe = CaO*FeO*(-45175.2 + 10819*(CaO - FeO) + 5804.6*(CaO - FeO)**2)
    Ca_Mg = CaO*MgO*(-80961.3 + 0*(CaO - MgO) - 0*(CaO - MgO)**2)
    Ca_Mn = CaO*MnO*(-45175.2 + 10819*(CaO - MnO) + 5804.6*(CaO - MnO)**2)
    Ca_Si = CaO*SiO*(-42988.5 - 414694*(CaO - SiO) - 37739*(CaO - SiO)**2)
    Fe_Mg = FeO*MgO*(5173.66 + 0*(FeO - MgO) - 0*(FeO - MgO)**2)
    Fe_Mn = FeO*MnO*(0 + 0*(FeO - MnO) - 0*(FeO - MnO)**2)
    Fe_Si = FeO*SiO*(-29830 - 10264*(FeO - SiO) + 26504*(FeO - SiO)**2)
    Mg_Mn = MgO*MnO*(0 + 0*(MgO - MnO) - 0*(MgO - MnO)**2)
    Mg_Si = MgO*SiO*(-126521 - 79099.6*(MgO - SiO) - 28086.2*(MgO - SiO)**2)
    Mn_Si = MnO*SiO*(-89638.2 - 35278.3*(FeO - MgO) + 43013.3*(FeO - MgO)**2)

    #calculation of the heat of mixing
    delta_Hm = 0.9581*(((3*SiO - 1)/2)**3) + Al_Ca + Al_Fe + Al_Mg + Al_Mn + Al_Si + Ca_Fe + Ca_Mg + Ca_Mn + Ca_Si + Fe_Mg + Fe_Mn + Fe_Si + Mg_Mn + Mg_Si + Mn_Si

    #H_component = H(1873) + Cp*(T - 1873)
    T = d_in.get('T')
    H_Al = -683848 + 71.674*(T - 1873)
    H_Ca = -472643.2 + 55.386*(T - 1873)
    H_Fe = -140357.5 + 68.199*(T - 1873)
    H_Mg = -449977.5 + 60.216*(T - 1873)
    H_Mn = -244491.7 + 61.582*(T - 1873)
    H_Si = -799737.2 + 71.63*(T - 1873) + 0.00188/(2*(T**2 - 1873**2)) - 3906000*(1/T - 1/1873) # = H(1873) + A*(T - 1873) + B/(2*(T**2 - 1873**2)) - C*(1/T - 1/18
    #calculation of the entire slag enthalpy
    delta_H = (delta_Hm + AlO*H_Al + CaO*H_Ca + FeO*H_Fe + MgO*H_Mg + MnO*H_Mn + SiO*H_Si)*d_in.get('moleT')

    v_out = delta_H #J/mol
```

Figure B-2. Enthalpy calculation for the slag stream (Bjorkvall *et al*., 2016).

In general, component enthalpy values are calculated at the specified stream temperature in relation to the zero point 273.15 K. The individual values are summed up to yield a value termed ‘delta_H’ which is then used in the system energy balance equation.

For combustion reliant systems the mass balance and energy balance are linked by the carbon source. Any changes made to the energy requirement translate to changes in the mass requirement.

```python

for i in range(8): #the counting starts from zero

    #Secant algorithm: Values for X(i-1) and Y(i-1): i

    #This takes into account all carbon requirements in order to calculate other streams
    Loop_Carbon_mass1 ['mt'] = (elements[5]/1000)*(COR_stage2_carbon + Combustion_mole[i] + (Assume_COR_combustion.get('boudouard')*Combustion_mole[i]))/Loop_Carbon_mass1.get('C')
    Loop_Carbon1              = coal_mole(**Loop_Carbon_mass1)
    Loop_Carbon1_rxn = COR_rxn_coal(**Loop_Carbon1)
    Loop_H_carbon1 = carbon_H (**Loop_Carbon1)

    Loop_Oxygen_mole1_O2 = (Combustion_mole[i]/2) #moles of O2 not O
    Loop_Oxygen_mole1['moleT'] = Loop_Oxygen_mole1_O2/Loop_Oxygen_mole1.get('O2')
    Loop_Oxygen_mole1['T'] = sheet['H2'].value + 273.15
    Loop_H_Oxygen1 = blast_H (**Loop_Oxygen_mole1)

    #Slag
    #In total mass terms
    Loop_Slag1_SiO2 = (COR_Reducedsolid_rxn.get('SiO2') + Loop_Carbon1_rxn.get('SiO2'))*(elements[3] + 2*elements[2])/1000
    Loop_Slag1_Al2O3 = (COR_Reducedsolid_rxn.get('Al2O3') + Loop_Carbon1_rxn.get('Al2O3'))*(2*elements[4] + 3*elements[2])/1000
    Loop_Slag1_CaO = (COR_Reducedsolid_rxn.get('CaO'))*(elements[6] + elements[2])/1000
    Loop_Slag1_MgO = (COR_Reducedsolid_rxn.get('MgO'))*(elements[7] + elements[2])/1000
    Loop_Slag1_MnO = (COR_Reducedsolid_rxn.get('MnO'))*(elements[0] + elements[2])/1000
    if COR_Reducedsolid_rxn.get('FeO') != None:
        Loop_Slag1_FeO = (COR_Reducedsolid_rxn.get('FeO'))*(elements[1]+elements[2])/1000
    else: Loop_Slag1_FeO = (0)*(elements[1]+elements[2])/1000

    Loop_Slag1 ['mt'] = Loop_Slag1_SiO2 + Loop_Slag1_Al2O3 + Loop_Slag1_CaO + Loop_Slag1_MgO + Loop_Slag1_MnO + Loop_Slag1_FeO
    #In mass fraction terms
    Loop_Slag1 ['SiO2'] = Loop_Slag1_SiO2/Loop_Slag1.get('mt')
    Loop_Slag1 ['Al2O3'] = Loop_Slag1_Al2O3/Loop_Slag1.get('mt')
    Loop_Slag1 ['CaO'] = Loop_Slag1_CaO/Loop_Slag1.get('mt')
    Loop_Slag1 ['MgO'] = Loop_Slag1_MgO/Loop_Slag1.get('mt')
    Loop_Slag1 ['MnO'] = Loop_Slag1_MnO/Loop_Slag1.get('mt')
    Loop_Slag1 ['FeO'] = Loop_Slag1_FeO/Loop_Slag1.get('mt')
    Loop_Slag1 ['T']   = COR_Alloy_mass.get('T') #slag and alloy at same temperature
    Loop_Slag_mole1 = slag_mole(**Loop_Slag1)
    Loop_H_slag1 = slag_H(**Loop_Slag_mole1)


    #Reduced gas (leave out VM energy generation term for now)
    Loop_Reducegas1['CO'] = COR_Reducedsolid_rxn.get('CO') + 2*Assume_COR_combustion.get('boudouard')*Combustion_mole[i]
    Loop_Reducegas1['CO2'] = Combustion_mole[i] - Assume_COR_combustion.get('boudouard')*Combustion_mole[i]
    Loop_Reducegas1['H2'] = Loop_Carbon1_rxn.get('H2')
    #Loop_Reducegas1['NOx'] = Loop__rxn.get('NOx')
    #Loop_Reducegas1['SO2'] = Loop__rxn.get('SO2')
    Loop_Reducegas1['T'] = sheet['H6'].value + 273.15
    Loop_H_Reducegas1 = gases_H (**Loop_Reducegas1)


    Temp1_Hrxn_stagetwo = COR_Reducedsolid_rxn.get('Hrxn') + Loop_Carbon1_rxn.get('Hrxn')
    COR_delta_j1 = ((Loop_H_Reducegas1 + Loop_H_slag1 + Temp1_Hrxn_stagetwo + COR_H_alloy + Energy_loss) - (COR_H_Reducedsolid + Loop_H_carbon1 + Loop_H_Oxygen1))
    Loop_Hrxn_combust1 = 393500*Combustion_mole[i] - 172500*Assume_COR_combustion.get('boudouard')*Combustion_mole[i]
    #F(X) = 0
    Y1 = COR_delta_j1 - Loop_Hrxn_combust1

#- - - - - - - - - - - - - - - - - - - - - - - - - - - - - - - - - - - - -
    #Values for X(i) and Y(i): i+1

    #This takes into account all carbon requirements in order to calculate other streams
    Loop_Carbon_mass2 ['mt'] = (elements[5]/1000)*(COR_stage2_carbon + Combustion_mole[i+1] + (Assume_COR_combustion.get('boudouard')*Combustion_mole[i+1]))/Loop_Carbon_mass1.get('C')
    Loop_Carbon2              = coal_mole(**Loop_Carbon_mass2)
    Loop_Carbon2_rxn = COR_rxn_coal(**Loop_Carbon1)
    Loop_H_carbon2 = carbon_H (**Loop_Carbon2)

    Loop_Oxygen_mole2_O2 = (Combustion_mole[i+1]/2) #moles of O2 not O
    Loop_Oxygen_mole2['moleT'] = Loop_Oxygen_mole2_O2/Loop_Oxygen_mole2.get('O2')
    Loop_Oxygen_mole2['T'] = sheet['H2'].value + 273.15
    Loop_H_Oxygen2 = blast_H (**Loop_Oxygen_mole2)

    #Slag
    #In total mass terms
    Loop_Slag2_SiO2 = (COR_Reducedsolid_rxn.get('SiO2') + Loop_Carbon2_rxn.get('SiO2'))*(elements[3] + 2*elements[2])/1000
    Loop_Slag2_Al2O3 = (COR_Reducedsolid_rxn.get('Al2O3') + Loop_Carbon2_rxn.get('Al2O3'))*(2*elements[4] + 3*elements[2])/1000
    Loop_Slag2_CaO = (COR_Reducedsolid_rxn.get('CaO'))*(elements[6] + elements[2])/1000
    Loop_Slag2_MgO = (COR_Reducedsolid_rxn.get('MgO'))*(elements[7] + elements[2])/1000
    Loop_Slag2_MnO = (COR_Reducedsolid_rxn.get('MnO'))*(elements[0] + elements[2])/1000
    if COR_Reducedsolid_rxn.get('FeO') != None:
        Loop_Slag2_FeO = (COR_Reducedsolid_rxn.get('FeO'))*(elements[1]+elements[2])/1000
    else:
        Loop_Slag2_FeO = (0)*(elements[1]+elements[2])/1000

    Loop_Slag2 ['mt'] = Loop_Slag2_SiO2 + Loop_Slag2_Al2O3 + Loop_Slag2_CaO + Loop_Slag2_MgO + Loop_Slag2_MnO + Loop_Slag2_FeO
    #In mass fraction terms
    Loop_Slag2 ['SiO2'] = Loop_Slag2_SiO2/Loop_Slag2.get('mt')
    Loop_Slag2 ['Al2O3'] = Loop_Slag2_Al2O3/Loop_Slag2.get('mt')
    Loop_Slag2 ['CaO'] = Loop_Slag2_CaO/Loop_Slag2.get('mt')
    Loop_Slag2 ['MgO'] = Loop_Slag2_MgO/Loop_Slag2.get('mt')
    Loop_Slag2 ['MnO'] = Loop_Slag2_MnO/Loop_Slag2.get('mt')
    Loop_Slag2 ['FeO'] = Loop_Slag2_FeO/Loop_Slag2.get('mt')
    Loop_Slag2 ['T']   = COR_Alloy_mass.get('T') #slag and alloy at same temperature
    Loop_Slag_mole2 = slag_mole(**Loop_Slag2)
    Loop_H_slag2 = slag_H(**Loop_Slag_mole2)

    #Reduced gas (leave out VM energy generation term for now)
    Loop_Reducegas2['CO'] = COR_Reducedsolid_rxn.get('CO') + 2*Assume_COR_combustion.get('boudouard')*Combustion_mole[i+1]
    Loop_Reducegas2['CO2'] = Combustion_mole[i+1] - Assume_COR_combustion.get('boudouard')*Combustion_mole[i+1]
    Loop_Reducegas2['H2'] = Loop_Carbon2_rxn.get('H2')
    #Loop_Reducegas2['NOx'] = Loop__rxn.get('NOx')
    #Loop_Reducegas2['SO2'] = Loop__rxn.get('SO2')
    Loop_Reducegas2['T'] = sheet['H6'].value + 273.15
    Loop_H_Reducegas2 = gases_H(**Loop_Reducegas2)


    Temp2_Hrxn_stagetwo = COR_Reducedsolid_rxn.get('Hrxn') + Loop_Carbon2_rxn.get('Hrxn')
    COR_delta_j2 = ((Loop_H_Reducegas2 + Loop_H_slag2 + Temp2_Hrxn_stagetwo + COR_H_alloy + Energy_loss) - (COR_H_Reducedsolid + Loop_H_carbon2 + Loop_H_Oxygen2))
    Loop_Hrxn_combust2 = 393500*Combustion_mole[i+1] - 172500*Assume_COR_combustion.get('boudouard')*Combustion_mole[i+1]
    #F(X) = 0
    Y2 = COR_delta_j2 - Loop_Hrxn_combust2

    #Estimate the next value X(i+1)
    Next = Combustion_mole[i+1] - ((Combustion_mole[i+1] - Combustion_mole[i])/(Y2 - Y1))*Y2
    Combustion_mole.append(Next)

    #--------------End of for Loop-----------------------------------------------------

```

Figure B-3. Iteration loop code for the COREX model.

Other streams that are affected by energy generation are the slag and off-gas. In order to estimate the coal/coke, air/oxygen, slag, and off-gas streams an iterative process had to be used. Figure B-3 shows an image of the code used to perform the secant method iterations when calculating the various streams.

A similar method was used in the BF process model due to combustion. The iteration loop begins with the initial estimations of each stream based on the limited information from the carbon consumption from the reactions. The energy balance equation is then used as the function that determines the next value of the carbon requirement. The iteration loop is terminated when the net energy balance of the system under observation is close to zero and the various streams are then determined from the final output.

When the Python calculations are terminated the Excel file that stores all information is automatically opened with updated process calculations if changes were made. Figure B-4 is an image of the Excel input/output page for the SAF.

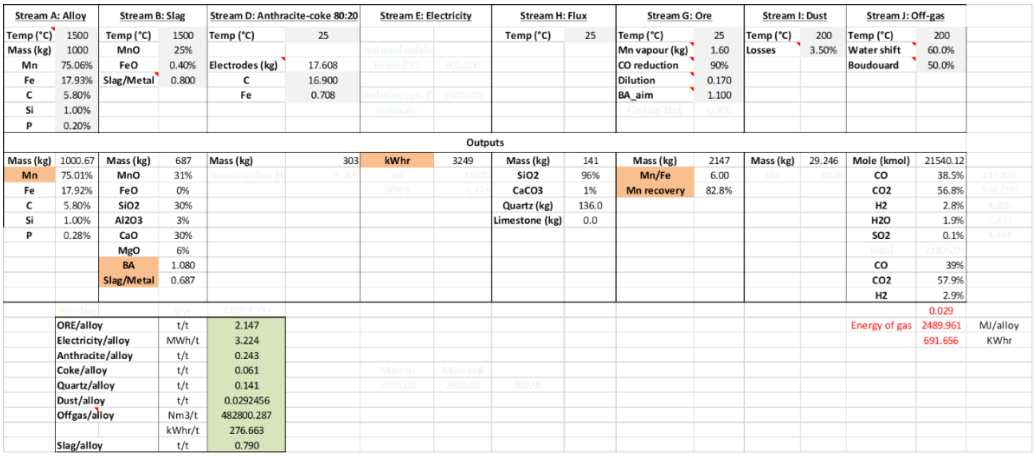

Stream A: Alloy		Stream B: Slag		Stream D: Anthracite-coke 80:20		Stream E: Electricity		Stream H: Flux		Stream G: Ore		Stream I: Dust		Stream J: Off-gas		
Temp (°C)	1500	Temp (°C)	1500	Temp (°C)	25			Temp (°C)	25	Temp (°C)	25	Temp (°C)	200	Temp (°C)	200	
Mass (kg)	1000	MnO	25%							Mn vapour (kg)	1.60	Losses	3.50%	Water shift	60.0%	
Mn	75.06%	FeO	0.40%	Electrodes (kg)	17.608					CO reduction	90%			Boudouard	50.0%	
Fe	17.93%	Slag/Metal	0.800	C	16.900					Dilution	0.170					
C	5.80%			Fe	0.708					BA_aim	1.100					
Si	1.00%															
P	0.20%															
Outputs																
Mass (kg)	1000.67	Mass (kg)	687	Mass (kg)	303	kWhr	3249	Mass (kg)	141	Mass (kg)	2147	Mass (kg)	29.246	Mole (kmol)	21540.12	
Mn	75.01%	MnO	31%					SiO2	96%	Mn/Fe	6.00			CO	38.5%	
Fe	17.92%	FeO	0%					CaCO3	1%	Mn recovery	82.8%			CO2	56.8%	
C	5.80%	SiO2	30%					Quartz (kg)	136.0					H2	2.8%	
Si	1.00%	Al2O3	3%					Limestone (kg)	0.0					H2O	1.9%	
P	0.28%	CaO	30%											SO2	0.1%	
		MgO	6%													
		BA	1.080											CO	39%	
		Slag/Metal	0.687											CO2	57.9%	
														H2	2.9%	
															0.029	
														Energy of gas	2489.961	MJ/alloy
															691.656	KWhr

ORE/alloy	t/t	2.147
Electricity/alloy	MWh/t	3.224
Anthracite/alloy	t/t	0.243
Coke/alloy	t/t	0.061
Quartz/alloy	t/t	0.141
Dust/alloy	t/t	0.0292456
Offgas/alloy	Nm3/t	482800.287
	kWhr/t	276.663
Slag/alloy	t/t	0.790

Figure B-4. Process calculations output page in Excel for the SAF.

The values highlighted in grey are all input values retrieved by Python before calculations can be made. During this process, the Excel file needs to be closed in order for Python to execute the code. The bottom half of the table are all the calculated outputs and they were converted into mass ratios per ton of alloy to be used in the economic model.

Appendix C: Techno-economic Data

The cash flow statement consisted of CAPEX and OPEX items. For the CAPEX a battery limits estimate was conducted on the major equipment in the flowsheet and the rest of the other components were estimated using fractions. Table C-1 lists aspects of the original data used to calculate the equipment costs.

Table C-1. Cost data used to estimate the CAPEX components for each furnace flowsheet.

Equipment list **Currency USD million**	**Original** **Cost | Year | Capacity**	**Required** **Cost | Capacity**	**Reference**
Raw materials			
Sinter plant	51.90 | 1996 | 200 m^2	45.55 | 87 m^2	(Bhattacharya & Vishwakaram, 1998)
Briquetting plant (Ore)	0.10 | 1957-59 | 131.4 kt/y	0.38 | 59 kt/y	(Woods, 2007)
Briquetting plant (Coal)	0.45 | 1971 | 35.04 kt/y	10.31 | 429 kt/y	(Chiang and Clifton, 1971)
Oxygen plant	49.17 | 1996 | 595 kt/y	33.71 | 148 kt/y	(Bhattacharya & Vishwakaram, 1998)
Coking plant	79.21 | 1996 | 467.01 kt/y	121.08 | 445 kt/y	(Gallaher & Depro, 2002)
Furnace			
Submerged arc furnace	7.10 | 2015 | 9 MVA	69.10 | 150 MVA	(Anderson *et al*., 2015)
Transformers	107.60 | 2009 | 305 MVA	79.77 | 206 MVA	(Anderson *et al*., 2015)
Blast furnace	101.07 | 1996 | 2 000 m^3	69.00 | 700 m^3	(Bhattacharya & Vishwakaram, 1998)
COREX® system	184.38 | 1996 | 1 000 kt/y	133.02 | 375 kt/y	(Bhattacharya & Vishwakaram, 1998)
Gas handling			
Power plant Efficiency = 40 %	27.32 | 1996 | 30 MW	19.85 | 11 MW SAF 62.96 | 50 MW BF 98.47 | 90 MW COREX	(Bhattacharya & Vishwakaram, 1998)
Dust catcher	0.14 | 1957-59 | 10 Nm^3/s	2.12 | 38 Nm^3/s	(Woods, 2007)
Venturi scrubber: two-stage	13.20 | 1957-59 | 30 Nm^3/s	27.04 | 5 Nm^3/s	(Woods, 2007)
Wet scrubber, venturi	0.59 | 1957-59 | 10 Nm^3/s	8.11 | 38 Nm^3/s	(Woods, 2007)
Alloy handling plant			
Multi deck screen 1 (x3)	0.24 | 1957-59 | 1.5 m^2	12.70 | 60 m^2	(Woods, 2007)
Jaw crusher	3.13 | 1957-59 | 374.85 kt/y	14.76 | 300.2 kt/y	

Table C-1 Continued. Cost data used to estimate the CAPEX components for each furnace flowsheet.

Equipment list Currency USD million	**Original Cost | Year | Capacity**	**Required Cost | Capacity**	**Reference**
Alloy recovery plant			
Jaw crusher	3.13 | 1957-59 | 374.85 kt/y	11.12 | 237 kt/y	(Woods, 2007)
Screen	0.18 | 1957-59 | 1.5 m^2	4.62 | 20 m^2	(Woods, 2007)
Jig	0.28 | 2015 | 250 kt/y	0.27 | 237 kt/y	(Anderson *et al*., 2015)
Cone crusher	1.03 | 1957-59 | 292 kt/y	5.30 | 237 kt/y	(Woods, 2007)
Electromagnet	0.11 | 1957-59 | 5 kW	0.98 | 10 kW	(Woods, 2007)
Water treatment plant			
Thickener/Sedimentation	0.48 | 1957-59 | 100 m^2	1.88 | 50 m^2	(Woods, 2007)
Anaerobic reactor	0.11 | 1957-59 | 10 000 m^3	0.44 | 5 000 m^3	
Clarifier	0.83 | 1957-59 | 400 m^2	2.6 | 200 m^2	
Aerobic digestion	9.78 | 1957-59 | 0.12 m^3/s	9.56 | 0.007 m^3/s	
Pressure filter	0.11 | 1989 | 26 119 m^3/y	0.65 | 213 875 m^3/y	
Cooling tower	0.06 | 1998 | 9 000 m^3/h	0.03 | 1 487 m^3/h	

Table C-5 lists the costing data used to estimate the battery limits capital cost estimation for each flowsheet. Some of the cost data were obtained for erected structures with all associated costs, however, some unit processes required the use of a method provide by Woods (2007) to estimate the cost of a unit. Table C-2 shows an example of the method provided by Woods (2007) to estimate equipment costs.

Table C-2. Example of the capital cost estimation method provided by Woods (2007).

Equipment	**Data provided**	**Calculation**
Wet scrubber, venturi	FOB = $ 200 000 Instrumentation = 0.01*1.65 (L+M)* = 2 Tax = 0.2 L+M = FOB*(L+M)* + Inst Taxes = Tax*FOB PM = L+M + Taxes Offsite = (0.325)*L+M BM = PM + Offsite	Bare module cost = = FOB*(L+M) + Inst + Tax*FOB + (0.325)*L+M = 2*200 000 + 0.01*1.65 + 0.2*200 000 + 0.325*(2*200 000 + 0.01*1.65) = 591 862.50 USD

Furnace availability was used to estimate the flow rates required to achieve the chosen annual production rate. This value was obtained from publications, it was assumed to be 325 days for the SAF (Anderson *et al*., 2015), and 350 days for the BF and COREX (Pfeifer, 2009). Flow rates required for sizing equipment were calculated based on the assumed availabilities.

Other CAPEX items were estimated based on the total fixed capital cost estimated using the percentages listed in Table C-3.

Table C-3. Other fixed capital cost items (Ruhmer, 1991; Woods, 2007).

Fixed capital cost items	Fraction of battery limit estimate
Contingency	20%
Land	2.5%
Start-up costs	3%
Working capital	20%

Operational costs were estimated using the operational indexes obtained from the mass and energy balance. Commodity prices were obtained from various sources and used to fit linear regression lines. Year 1 was assumed to be in 2019 and prices from year 2 onwards were estimated using the linear regression lines provided in Table C-4. The regression lines were fitted on historical data that dates back to 2002 for all commodities except coke, coking coal, and electricity.

Table C-4. Commodity prices and regression equations used to estimate future prices.

Commodity	Price in year 2019 (R/t)	Regression equation	R^2
Manganese ore[1]	1 217.19	$0.0647x - 0.462x^2 + 54.152x + 57.932$	0.9573
Anthracite[1]	1 314.82	$-0.215x^2 + 57.078x + 249.51$	0.9428
Coke[2]	4 228.26	$305.91x - 1\,429.9$	0.6568
Bituminous coal[1]	430	$56.754e^{0.119x}$	0.9767
Coking coal[3]	1036.85	$280.39e^{0.0842x}$	0.7917
Electricity[4]	70.02	$5.5242x - 26.605$	0.9917
Quartzite[1]	281.92	$0.3246x^2 + 7.642x + 54.791$	0.9664
Lime stone[1]	178.46	$6.7682x + 49.961$	0.9464
Ferromanganese[1]	14 356.85	$4\,380.6e^{0.0678x}$	0.6354

1: (Auchterlonie, 2019)

2: (Investing.com, n.d.)

3: (Index Mundi, 2020)

4: (Motiang, 2018)

The year 2002 is equivalent to year 1 in the linear regression model. Consequently, the year 2020 is equivalent to year 18 when calculating the commodity price using the regression provided. A large variance in some of the data was noticed from the R^2 value, for coke, coking coal, and ferromanganese sharp price changes were observed.

Other operational items not directly estimated from the mass and energy balance are listed in Table C-5. These items were not varied over the project lifetime unless they are estimated using a varying figure such as the Royalties and patents. The estimates are industry averages and were obtained from three publications.

Table C-5. Other OPEX item calculations (Anderson *et al*., 2015; Green & Perry, 2008; Ruhmer, 1991)

OPEX Items	Estimation method
Electrode paste (R/t)	R 8680.38/t (SAF)
Labour (R/day)	R 60 000/day
Maintenance	8 % of Fixed capital
Labour related costs	60 % of labour
Supplies	15 % Maintenance
Indirect costs	50 % (Labour + Maintenance)
Insurance	4 % Fixed capital
Royalties and patents	3.5 % Product Sales

The scenario analysis made use of the percentage changes listed in Table C-6.

Table C-6. Scenario analysis estimations.

Commodity	Best-case estimate	Worst-case estimate
Manganese ore	-0.09	0.16
Anthracite	-0.09	0.08
Coke	-0.26	0.15
Bituminous coal	-0.09	0.08
Coking coal	-0.10	0.23
Electricity	-0.05	0.02
Quartzite	-0.07	0.08
Limestone	-0.05	0.06
Ferromanganese	0.27	-0.14
Fixed capital cost	-0.25	0.30
Working capital	0.15	0.25
Labour related costs	0.42	0.95
Maintenance	0.06	0.08
Supplies	0.10	0.20
Insurance	0.03	0.05
Royalties and patents	0.01	0.05

Tax rate	28.00%																				
Depreciation	40.00%	20.00%	20.00%	20.00%																	
Land acquisition	2.50%																				
Outcomes	**SAF**	**BF**	**COREX**																		
Base case rate	15.00%	15.00%	15.00%																		
NPV	R 7,706.36	R 7,267.29	R 11,430.46																		
DPBP	8	9	7																		
IRR	28.07%	26.89%	33.11%																		
Mill ZAR	2019	2020	2021	2022	2023	2024	2025	2026	2027	2028	2029	2030	2031	2032	2033	2034	2035	2036	2037	2038	2039
Years: Life 20	**0**	**1**	**2**	**3**	**4**	**5**	**6**	**7**	**8**	**9**	**10**	**11**	**12**	**13**	**14**	**15**	**16**	**17**	**18**	**19**	**20**
SAF																					
Land	-138.86																				
Fixed capital expenditure		-5554.57																			
Startup capital expediture			-138.86																		
Working capital expenditure		-1110.91																			
Revenue generated		0.00	1274.96	4093.22	5840.48	6250.20	6688.66	7157.87	7660.01	8197.37	8772.42	9387.82	10046.39	10751.15	11505.36	12312.47	13176.21	14100.54	15089.71	16148.27	17281.09
Production expenditure		0.00	1009.22	2689.45	3404.75	3562.67	3726.75	3897.31	4074.67	4259.17	4451.14	4650.92	4858.86	5075.32	5300.67	5535.27	5779.50	6033.76	6298.43	6573.94	6860.70
Pretax profit		0.00	265.75	1403.77	2435.73	2687.53	2961.91	3260.56	3585.34	3938.20	4321.29	4736.90	5187.52	5675.83	6204.69	6777.20	7396.71	8066.78	8791.27	9574.33	10420.39
Depreciation		0.00	2221.83	3066.99	2774.14	1110.91	0.00	0.00	0.00	0.00	0.00	0.00	0.00	0.00	0.00	0.00	0.00	0.00	0.00	0.00	0.00
Income tax		0.00	0.00	0.00	-94.75	441.45	829.33	912.96	1003.89	1102.70	1209.96	1326.33	1452.51	1589.23	1737.31	1897.62	2071.08	2258.70	2461.56	2680.81	2917.71
Profit after tax		0.00	0.00	0.00	-243.65	1135.16	2132.57	2347.61	2581.44	2835.50	3111.33	3410.57	3735.02	4086.60	4467.38	4879.59	5325.63	5808.08	6329.72	6893.52	7502.68
After tax cashflow	-138.86	-6665.48	126.88	1403.77	2435.73	2246.08	2132.57	2347.61	2581.44	2835.50	3111.33	3410.57	3735.02	4086.60	4467.38	4879.59	5325.63	5808.08	6329.72	6893.52	7502.68
Cummulative cashflow	-138.86	-6804.35	-6677.46	-5273.69	-2837.96	-591.89	1540.69	3888.29	6469.73	9305.24	12416.56	15827.13	19562.15	23648.74	28116.12	32995.71	38321.34	44129.42	50459.14	57352.65	64855.34
NPV	7706.36																				
DPBP	241.742																				
IRR NPV	0.03																				
BF																					
Land	-189.71																				
Fixed capital expenditure		-3794.11	-3794.11																		
Startup capital expediture				-189.71																	
Working capital expenditure			-1517.64																		
Revenue generated		0.00	0.00	5457.62	5840.48	6250.20	6688.66	7157.87	7660.01	8197.37	8772.42	9387.82	10046.39	10751.15	11505.36	12312.47	13176.21	14100.54	15089.71	16148.27	17281.09
Production expenditure		0.00	0.00	3048.04	3114.08	3263.64	3425.83	3601.55	3791.77	3997.51	4219.86	4459.98	4719.13	4998.64	5299.92	5624.52	5974.08	6350.36	6755.25	7190.80	7659.21
Pretax profit		0.00	0.00	2409.58	2726.39	2986.56	3262.83	3556.32	3868.24	4199.86	4552.56	4927.83	5327.25	5752.52	6205.44	6687.95	7202.13	7750.18	8334.46	8957.47	9621.88
Depreciation		0.00	0.00	3035.29	1517.64	1517.64	1517.64	0.00	0.00	0.00	0.00	0.00	0.00	0.00	0.00	0.00	0.00	0.00	0.00	0.00	0.00
Income tax		0.00	0.00	-175.20	338.45	411.30	488.65	995.77	1083.11	1175.96	1274.72	1379.79	1491.63	1610.70	1737.52	1872.63	2016.60	2170.05	2333.65	2508.09	2694.13
Profit after tax		0.00	0.00	-450.51	870.30	1057.62	1256.53	2560.55	2785.13	3023.90	3277.85	3548.04	3835.62	4141.81	4467.91	4815.32	5185.53	5580.13	6000.81	6449.38	6927.76
After tax cashflow	-189.71	-3794.11	-5311.75	2395.08	2387.94	2575.26	2774.18	2560.55	2785.13	3023.90	3277.85	3548.04	3835.62	4141.81	4467.91	4815.32	5185.53	5580.13	6000.81	6449.38	6927.76
Cummulative cashflow	-189.71	-3983.81	-9295.56	-6900.49	-4512.54	-1937.28	836.89	3397.44	6182.57	9206.47	12484.32	16032.36	19867.98	24009.79	28477.70	33293.03	38478.56	44058.69	50059.50	56508.88	63436.63
NPV	7267.29																				
DPBP	647.102																				
IRR NPV	1.25																				
COREX																					
Land	-187.52																				
Fixed capital expenditure		-3750.31	-3750.31																		
Startup capital expediture				-174.92																	
Working capital expenditure			-1500.12																		
Revenue generated		0.00	0.00	5457.62	5840.48	6250.20	6688.66	7157.87	7660.01	8197.37	8772.42	9387.82	10046.39	10751.15	11505.36	12312.47	13176.21	14100.54	15089.71	16148.27	17281.09
Production expenditure		0.00	0.00	2140.93	2149.25	2239.45	2340.68	2453.96	2580.35	2721.06	2877.39	3050.78	3242.83	3455.30	3690.13	3949.50	4235.79	4551.69	4900.15	5284.50	5708.44
Pretax profit		0.00	0.00	3316.69	3691.22	4010.75	4347.97	4703.92	5079.66	5476.31	5895.03	6337.04	6803.55	7295.85	7815.23	8362.98	8940.42	9548.85	10189.56	10863.76	11572.65
Depreciation		0.00	0.00	3000.24	1500.12	1500.12	1500.12	0.00	0.00	0.00	0.00	0.00	0.00	0.00	0.00	0.00	0.00	0.00	0.00	0.00	0.00
Income tax		0.00	0.00	88.61	613.51	702.98	797.40	1317.10	1422.30	1533.37	1650.61	1774.37	1905.00	2042.84	2188.26	2341.63	2503.32	2673.68	2853.08	3041.85	3240.34
Profit after tax		0.00	0.00	227.84	1577.59	1807.65	2050.45	3386.82	3657.35	3942.94	4244.42	4562.67	4898.56	5253.01	5626.96	6021.34	6437.10	6875.17	7336.48	7821.91	8332.31
After tax cashflow	-187.52	-3750.31	-5250.43	3053.17	3077.72	3307.77	3550.57	3386.82	3657.35	3942.94	4244.42	4562.67	4898.56	5253.01	5626.96	6021.34	6437.10	6875.17	7336.48	7821.91	8332.31
Cummulative cashflow	-187.52	-3937.82	-9188.25	-6135.08	-3057.37	250.41	3800.98	7187.80	10845.16	14788.10	19032.52	23595.19	28493.75	33746.76	39373.72	45395.07	51832.17	58707.34	66043.82	73865.73	82198.04
NPV	11430.46																				
DPBP	801.264																				
IRR NPV	-0.48																				

Figure C-1. Cash flow statements for each capital project.

Figure C-1 shows an image of the cash flow statements used to estimate all the financial performance indicators. The capital was distributed over the first three years for the SAF and the first four years for the BF and COREX®.